Interspecific and intraspecific relationships, and biogeography of flap-footed geckos, *Delma* Gray 1831 (Squamata: Pygopodidae)

A Thesis Presented to the Faculty of the
Department of Biology,
Villanova University

In Partial Fulfillment of the Requirements for the Degree of

Master of Science
in Biology

By
Ian G. Brennan

May 2014

Under the Direction of Aaron M. Bauer

Table of Contents

Dedication 3
Acknowledgments 4
Biographical Sketch 5
List of Figures 6
List of Tables 6
Abstract 7
I. Introduction to the Pygopodidae 9
I.i—Historical biogeography of Australia 9
I.ii—An introduction to the Gekkota in Australia 11
I.iii—Pygopodidae Boulenger 1884 13
I.iv—*Delma* Gray 1831 18
I.v—Historical taxonomic position of the Pygopodidae within Squamata 20
II. Materials and methods 21
II.i—Taxon Sampling 21
II.ii—Gene Selection 22
II.iii—Phylogenetic Analyses 24
II.iv—Concatenation 27
II.v—Species Delimitation 28
II.vi—Divergence Dating 29
II.vii—Research Goals 30
III. Mito-nuclear discordance and speciation by aridification in flap-footed geckos, *Delma* Gray 1831 (Gekkota: Pygopodidae) 32
III.i—Abstract 32
III.ii—Introduction 33
III.iii—Molecular Methods and Phylogenetic Analyses 33
III.iv—Results 37
III.v—Discussion 52
IV. Molecular and morphological evaluation of *Delma australis* (Squamata: Pygopodidae) with descriptions of two new species from biogeographically significant areas in Western Australia 66
IV.ii—Introduction 67
IV.iii—Materials and Methods 68
IV.iv—Taxonomy 72
IV.v—*Delma australis* Kluge, 1974 75
IV.vi—*Delma australis* S.WA **sp. nov.** 81
IV.ii—*Delma australis* N.SA **sp. nov.** 89
IV.viii—Results 93
IV.ix—Discussion 98
V. Notes on hemipenial morphology of the Pygopodidae Boulenger 1884: a phylogenetic tool 105
V.i—Abstract 105
V.ii—Introduction: Diversity within a Divergent Lineage 105
V.iii—Monophyly of the Pygopodidae and Previous Phylogenetic Study 106
V.iv—Hemipenial Morphology and Systematics 108
V.v—Methods and Materials: Hemipenial Preparation 110
V.vi—Characters and Hemipenial Descriptions 111
V.vii.—Phylogenetic Discussion of Hemipenes in Pygopodidae 119
V.viii.—Cloacal Spurs and Reproductive Behavior 125
VI.—Literature Cited 129
Appendix 1 140
Appendix 2 141

Dedication

For my Aunt Irene,
who taught me being weird was cool

And to my parents and sister,
for their unwavering support of a child herpetologist

Acknowledgments

Without the unflinching support and guidance of my committee chair and advisor Dr. Aaron Bauer, and committee members, Dr. Todd Jackman and Dr. Adam Langley, this project, and my graduate student career at Villanova would never have been successful. Dr. Bauer's savant-like herpetological knowledge, unparalleled library, and dark sense of humor have been an immense help throughout my career here. Dr. Jackman's patience in helping to grow my understanding of phylogenetics, and eagerness to have a beer and talk systematics has been incredible. I'd like to thank the Bauer-Jackman lab post-docs, Dr. Matt Heinicke, and "Mr. Pinga Loca" Dr. Juan Daza, for their friendship, and help with navigating graduate life. Dr. Paul Doughty, who helped to shape this project—you've become a great mentor and friend—thank you for sharing your experiences, friends, and skull Mondays. Many thanks to my fellow graduate students and friends—and there have been plenty through my three years here—who have helped get me through long days and nights in the lab: Evan Kelemen, Sarah Baillie, Kevin Neal, Ben Karin, Michael Lough-Stevens, Jackie Childers, Katie Allen, Mikhail Chavis, Luke Musser, James Titus-McQuillan. I owe even more thanks to the Fire Island Gibbons: Arianna Kuhn, Andrew Kathriner, Rachel Skinner, and Elyse Freitas, who have made life in lab consistently fun—I hope your artistic skills continue to grow and swell as you erect your academic careers. Kate Freeman, thank you for your unwavering support and positivity as I whinged and moaned my way through writing this thesis. Happy reading.

Biographical Sketch

Ian G. Brennan grew up in Montgomery, New Jersey, a central NJ suburb approximately equidistant from New York City and Philadelphia. Like most herpetologists, his interest in reptiles and amphibians started young, chasing frogs and turtles in backyard ponds, flipping rocks and logs for salamanders, and—like most northeastern kids—dreaming of lizards and snakes. As an undergraduate, Ian attended Union College in Upstate New York, where he split his time as a double-major between the biological sciences and studio arts. Even though he had studied and loved herpetology, the chance to live and breathe it came when he moved to the Wet Tropics of Queensland Australia in 2010. While there, he caught wily monitors, moved venomous snakes away from homes, and fell asleep to the noise of breeding frogs. Coming to Villanova in 2011 meant the chance to return to Australia for field work, and the opportunity to delve into the academic and research-driven side of herpetology. Ian hopes to continue his life-long learning as a herpetologist and evolutionary biologist, contributing to scientific education and literacy.

List of Figures

Figure I.1: Image of hindlimb flap of *Pygopous lepidopodus*
Figure I.2: Phylogenetic relationships among the Pygopodidae (Jennings et al., 2003)
Figure I.3: Phylogenetic relationships among the Pygopodidae (Kluge, 1976)
Figure II.1: Inter- and intraspecific relationships of *Delma australis* group
Figure II.2: Inter- and intraspecific relationships of *Delma inornata* group
Figure II.3: Phylogenetic position of *Delma mitella* and the *Delma fraseri* group
Figure II.4: Interspecific relationships of *Delma plebeia* group
Figure II.5: Interspecific relationships of the Northwest *Delma* group
Figure III.1: Preferred phylogeny of the Pygopodidae as inferred by nDNA
Figure III.2: Phylogeny of the Pygopodidae as inferred by mtDNA
Figure III.3a: Inter- and intraspecific relationships of *Delma* as inferred by ND2 (1 of 3)
Figure III.3b: Inter- and intraspecific relationships of *Delma* as inferred by ND2 (2 of 3)
Figure III.3c: Inter- and intraspecific relationships of *Delma* as inferred by ND2 (3 of 3)
Figure III.4: Comparison of mtDNA vs. nDNA phylogenies of *Delma*
Figure III.5: Bayesian time-tree of divergence dates within Pygopodidae
Figure III.6: Map of arid Australian corridors
Figure IV.1: Images of the *Delma australis* group species
Figure IV.2: Map of *Delma australis* genetic sampling
Figure IV.3: Phylogeny of *Delma australis* group as inferred by ND2
Figure IV.4: Preferred phylogeny of *Delma australis* group as inferred by mito-nuclear dataset
Figure IV.5: Head scalation of *Delma australis* holotype
Figure IV.6: Head scalation of *Delma australis* S.WA holotype
Figure IV.7: Head scalation of *Delma australis* N.SA holotype
Figure IV.8: Map of *Delma australis* group species distributions
Figure IV.9: Map of *Delma australis* group species distributions atop contemporary landcover

List of Tables

Table I.1: Synapomorphies of the Gekkota, Pygopodidae, and *Delma*
Table I.2: Genetic loci and primers used in this study
Table I.3: Partitioning schemes and models of best fit for genetic assessment
Table V.1: Taxa, locality data, and sources of specimens for hemipenial assessment
Table V.2: Summary of hemipenial characters of pygopodid geckos

Interspecific and intraspecific relationships, and biogeography of flap-footed geckos, *Delma* Gray 1831 (Squamata: Pygopodidae)

Ian Brennan

Abstract

The Gekkotan clade is a speciose and cosmopolitan group, with nearly 1500 members and constituents on six continents. Little known however are the pygopodids, the flap-footed geckos of the Family Pygopodidae (Gray, 1845). These gekkotans are limited to Australia (44 species) and New Guinea (2 species), but have diverged extensively into the most ecologically diverse limbless radiation save Serpentes, occupying a broad range of habitats and ecological niches. Current phylogenetic understanding of the family has relied almost exclusively on two works—Kluge (1974) and Jennings et al. (2003)—which have produced and synthesized an immense amount of morphological, geographical, and molecular data. However, current interspecific relationships within the largest genus *Delma* Gray 1831 are based exclusively upon a concatenated molecular dataset provided by two mitochondrial loci (16s, ND2), and a short segment (372 bp) of the nuclear protein-coding gene C-mos. Here, I reevaluate the inter- and intraspecific relationships within the genus *Delma* using two mitochondrial (16s, ND2) and four nuclear loci (Rag1, MXRA5, C-mos, DYNLL1), and identify points of strong conflict between nuclear and mitochondrial genomic data. We address mito-nuclear discordance, and resolve this conflict by recognizing several points of mitochondrial introgression as the result of deep hybridization events. Our results suggest a paraphyletic *Delma australis* group, from which we recognize two new species based upon morphological and molecular data. Additionally, while extensive morphological assessment of the genus has produced morphometric, osteological, and

scutellation data, we add to the paucity of hemipenial descriptions of the family. Accurately assessing and addressing species richness and relationships within this endemic Australian Gekkotan genus is relevant for understanding patterns of squamate speciation across the continent. Identification of cryptic species lineages are vital to informed habitat protection and development, and cataloging local, Australian, and worldwide biodiversity.

I. Introduction to the Pygopodidae

I.i—Historical biogeography of Australia

Australia is a land of superlatives. It is the lowest, flattest, and oldest continent on earth, and second only to Antarctica it is also the driest and most sparsely populated. It is the smallest continent on our planet, but also the only country that constitutes an entire continent. Most notably however, Australia is the world's richest country for squamate diversity and endemism, with more than 900 native species (Cogger, 2014; McDonald, 2014; Wilson and Swan, 2013). Floral and faunal endemism is particularly high in Australia due largely in part to the continent remaining in isolation for more than 35 Mya, when the Australian tectonic plate detached from Antarctica, and headed north towards the Asian plate. Millions of years of isolation of Gondwanan lineages, in addition to over-water colonization and island-hopping events from mainland Asian groups, have resulted in a remarkably rich and unique Australian biota. Prior to the Miocene, the Australian continent was a largely mesic biome, covered by broad swaths in of rain and sclerophyllous forests, grass and shrubland (Byrne et al., 2011; Byrne et al., 2008). Following South America's split from Antarctica in the Late Cenozoic approximately 20 Mya, and initiation of the circumpolar current—which cooled the world's climate—the Australian continent began a path of increasing aridification (McGowran et al., 2004). In it's northward drift, Australia avoided the massive glacial maxima of the Pleistocene, and began a warming trend with gradual desiccation that has helped to shape a massive radiation of arid-adapted biota, and restrict ancestral mesic-adapted relatives (Williams, 2001).

In present day Australia, the primarily xeric interior is surrounded by spinifex shrublands, temperate and tropical grasslands, and coastal forests (Cracraft, 1986). Relictual rainforest lines the northeast coast, a monsoonal band crosses the northern quarter of the country, and temperate forests are confined to the far southwest and southeast corners of the continent and Tasmania.

However, as recently as 20 Mya, the arid zone was a warm, wet center of Australia (Byrne et al., 2008). As aridification extended radially from the center of the continent and the Late Miocene approached 20–10 Mya, drought-tolerant biota proliferated; *Gossipium* (Liu et al. 2001), *Acacia* (Murphy et al., 2003), chenopods (Kadereit et al., 2006), *Santalum* (Harbaugh & Baldwin, 2007), dasyurids (Krajewski et al., 2000), diplodactylids (Oliver et al., 2007; Pepper et al., 2006), pygopodids (Jennings et al., 2003), sphenomorphines (Rabosky et al., 2007), agamids (Hugall et al., 2004). Although geological evidence for the period from 10–6 Mya remains scant, we do know that rainforests continued to shrink, *Eucalyptus* and *Casuarina* woodlands, and dry, open shrublands continued to expand, and arid-adapted plants and animals associated with these biomes continued rapid radiations: Tetratheca (Crayn et al., 2006), Chenopods (Shepherd et al., 2004), *Acacia* (Byrne et al., 2001), Dasyurids (Blacket et al., 2000), Agamids (Melville et al., 2001), *Egernia* (Chapple & Keogh, 2004), gall-inducing *Acacia* thrips (McLeish et al., 2007), diving beetles (Leys et al., 2003), and subterranean amphipods and isopods (Cooper et al., 2007) (Byrne et al., 2008). Despite a brief return to a warm, moist climate and expansion of rainforests during the Pliocene 6–2.5 Mya, the majority of the Australian landscape remained covered by sclerophyllous forest and woodlands, shrublands and grasslands. Following the Pliocene warming, Australia entered a two-step procession towards its current hyper-arid state.

In the Pleistocene, 2.5–0.4 Mya, as Northern Hemisphere glacial ice caps expanded and contracted, sea levels dropped, land expanded, and a cooler sea caused less evaporation, initiating the final stages of Australian desertification and several xeric adapted squamate radiations: *Egernia multiscutata* and *E. ornata* (Chapple et al., 2004), *Heteronotia binoei* (Strasburg & Kearney, 2005), *Tiliqua rugosa* (Cooper, unpublished), and *Menetia greyii* (Adams et al., 2003). Finally, frequency and intensity of drought periods increased until reaching a

crescendo during the last glacial maximum approximately 21,000 years-before-present (ybp), at which point sea level drop, land area, and aridity reached a peak.

Arid biomes cover approximately 70% of Australia's 7.5 million km^2 (Byrne et al., 2008), however, they are relatively depauperate in overall species richness, supporting just 10% of Australian plants (Barker and Greenslade, 1982) and 15% of Australian birds (Schodde and Weatherly, 1982). Australian squamates are however the exception, with 43% of species living in arid zones (Byrne 2008). Continental desertification on a massive scale has no doubt facilitated extremely successful species-rich squamate radiations within Australia; 400 + skinks (family Scincidae), 70 + dragons (Agamidae), 160 + geckos (Carphodactylidae, Diplodactylidae, Gekkonidae, Pygopodidae), 30 monitors (Varanidae), and 200 + snakes (Acrochordidae, Colubridae, Elapidae, Homalopsidae, Hydrophiidae, Pythonidae, Typhlopidae), all across approximately 138 genera (McDonald, 2014). Additionally, in-situ diversification of squamate lizards in expansive arid biomes of central and western Australia such as sandridges, grasslands, and shrublands has resulted in areas which support upwards of 40 sympatric lizard species (Pianka, 1969). The prolific nature of squamate radiations in Australia suggests not success in the face of adverse climatological conditions, but instead xerification-mediated radiations—speciation by aridification.

I.ii—An introduction to the Gekkota in Australia

The infraorder Gekkota represents a remarkably successful, cosmopolitan lineage, composed of more than 1450 species across 118+ genera and seven families (Carphodactylidae, Diplodactylidae, Eublepharidae, Gekkonidae, Phyllodactylidae, Pygopodidae, and Sphaerodactylidae) (Bauer, 2013; Gamble et al., 2008; Han et al., 2004; Uetz and Hošek, 2014). Excluding dibamids—which are generally accepted as the basal squamate lineage—geckos likely

represent the sister group to all other squamates, having diverged from a common ancestor approximately 225–180 Mya (Pyron et al., 2013; Vidal and Hedges, 2009). Of the seven families, representatives of four families inhabit Australia: the Carphodactylidae, Diplodactylidae, Pygopodidae (collectively the Pygopodoidea), and the Gekkonidae. The Pygopodoidea represent a monophyletic group composed of a Carphodactylidae-Pygopodidae clade, sister to the Diplodactylidae [D (C +P)]. Recent molecular and morphological support places the Pygopodoidea as sister group to all remaining gekkotans, from which they split ca. 150 Mya, prior to Australia's severance from Gondwana (Daza & Bauer, 2012; Oliver & Sanders, 2009). These findings refute previous morphological hypotheses that Eublepharidae represented the basal gekkotan lineage (Daza and Bauer, 2012; Estes et al., 1988; Han et al., 2004; Kluge, 1987). As divergence dates for each pygopodoid family predate ca. 60 Mya, it is safe to suggest an East Gondwanan diversification for these groups, intimating their presence on the Australian continent prior to its separation from Antarctica ca. 32 Mya (Byrne et al., 2008). This stands in contrast to nearly all other Australian squamate lineages, which are believed to have arrived in Australia via a number (10–15) of independent vicariant events (Oliver & Sanders, 2009). These vicariant squamate groups include the gekkonids, which are represented in Australia by the native genera *Cyrtodactylus*, *Gehyra*, *Heteronotia*, *Lepidodactylus*, and *Nactus*, and several invasive species of the genus *Hemidactylus*. As *Hemidactylus* and *Lepidodactylus* exist on continental Australia only via human introduction, I will not address their origins on Australian islands (Carranza and Arnold, 2006; Fitzsimons, 2011; Hoskin, 2011). Based upon our current phylogenetic understanding of the Gekkonidae however, each native gekkonid genus is believed to have arrived in Australia via an independent vicariant event (Heinicke et al., 2010, 2011).

Gekkotans have had remarkable success radiating within Australia, totaling nearly 200 native species. The vast majority of these, approximately 153 species or 80.5% are pygopodoid in origin. Oliver & Sanders (2009) rightly acknowledge the origin of pygopodoid radiations in context of the similarly aged but more "distinctly Australian" marsupials (Beck, 2008). Exceeded only by Myobatrachid frogs (Roelants et al., 2007), pygopodids represent one of the oldest Australasian vertebrate radiations. As ancient Gondwanan lineages, the crown split of the Pygopodoidea, i.e. when Diplodactylidae split from their sister group Carphodactylidae-Pygopodiade, ca. 60 Mya, was followed shortly thereafter by the split between Carphodactylidae and Pygopodidae several million years later (Oliver & Sanders, 2009).

I.iii—Pygopodidae Boulenger 1884

While subdigital lamellae—the adaptation which allows geckos to stick to all manner of surfaces—appears to have developed and disappeared several times over the course of Gekkotan history, the Pygopodidae show no history of, or need for scansorial pads (Gamble et al., 2012). Instead, the snakelike pygopodids are characterized by an absence of forelimbs, imbricate body scales, and a severe reduction of hindlimbs—giving them the common name "flap-footed geckos" (Fig. I.1) (Wilson & Swan, 2008). Current taxonomy recognizes 44 species across seven genera; *Aprasia* Gray 1839 (13 spp.), *Delma* Gray 1831 (21 spp.), *Lialis* Gray 1835 (2 spp.), *Ophidiocephalus* Lucas & Frost 1897 (1 sp.), *Paradelma* Kinghorn 1926 (1 sp.), *Pletholax* Cope 1864 (1 sp.), and *Pygopus* Merrem 1820 (6 spp.), however the validity of the genus *Paradelma* remains a point of contention within pygopodid systematics (Jennings et al., 2003; Kluge, 1974).

Substantial morphological divergence from the tetrapodal-squamate body plan, geographic dispersal, and ecological diversification have led to a remarkable radiation of limbless squamates, and a particularly aberrant group of gekkotans. Natural history and ecology

of genera and species vary greatly: fossorial myrmecophiles, *Aprasia*; terrestrial squamate-specialist ambush predators, *Lialis*; shrub-swimmers, *Delma concinna*, *Pletholax*; and arthropod-generalists, *Pygopus,* with nectarivorous habits, *Paradelma* (Tremul, 2000; Wilson and Swan, 2006; etc). Diurnality in the majority of pygopodid species occurs as a secondarily derived trait, and belies their gekkotan morphology, specifically; vertical pupils, the lack of a fovea—the sensitive retinal region found in many diurnal organisms, and absence of oil droplets in the visual cells of the eye (Greer, 1989; Röll, 2000, 2001). These characteristics suggest a nocturnal origin for the pygopodids, an affinity shared with ancestral geckos.

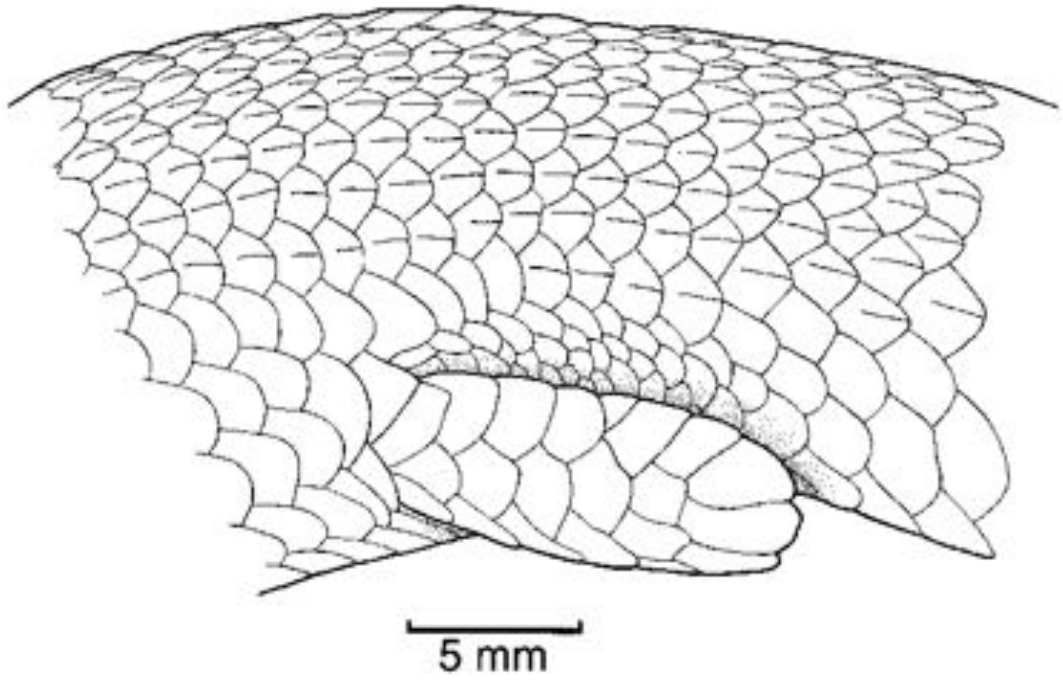

Figure I.1. Hindlimb flap of *Pygopus lepidopodus* adopted from Shea (1993). [B. Jantulik]

Pygopodids are however unique among geckos in being characterized by a distinct sex chromosome arrangement, in which males exhibit three chromosomes X1, X2, and Y. The two pairs of sex chromosomes are reduced to a trio; X1, X2, and their matching chromosomes fused to form a Y (Gorman and Gress 1970; King 1977).

Patchell and Shine (1986) among others (Storr 1964, Shea 1993) have proposed the concept of convergence in behavior, appearance, and morphology between pygopodids and snakes, specifically *Aprasia* to *Ramphotyphlops*, *Lialis* to small elapids (*Furina*, *Cacophis*, and *Demansia*), and the nuchal banding of *Delma* and *Pygopus* to that of *Furina* and *Pseudonaja*. Ontogenetic change associated with growth generally dulls the banding of larger *Delma* species, perhaps at the same rate which *Pseduonaja* spp. also lose nuchal banding. Smaller *Delma* species, such as *D. desmosa, D. elegans, D. tincta*, and *D. torquata* appear to retain this color pattern through adulthood. This apparent example of convergent evolution is accentuated by the congruence of the most accelerated period of pygopodid speciation with the beginning of the elapid radiation in the Miocene, at earliest 23 Mya (Jennings et al., 2003; Sanders et al., 2008). The majority of extant elapids are much younger, with origins within the last 10 MY. However, time-tree calibration for accurate assessment of divergence times within the Pygopodidae remains contentious due to the ambiguous nature of proper taxonomic placement of the only fossil pygopodid (Lee et al., 2009).

Molecular (Jennings et al., 2003; Oliver & Sanders, 2009), morphological (Daza and Bauer, 2012; Kluge, 1974; 1976), and karyotypic (Gorman and Gress, 1970; King and King, 1977) data unequivocally support the monophyly of the Family Pygopodidae, as well as generic lineages within the family. However, conflict arises when interpreting the intergeneric relationships, potentially as the result of a rapid radiation at the base of the pygopodid tree (Jennings et al., 2003; Oliver, 2009). There is high support for *Delma* as the sister group to all remaining pygopodids, and evidence for a close relationship between *Paradelma* and *Pygopus* (Fig. I.2). Proponents of synonymizing *Paradelma* with *Pygopus* (Jennings et al., 2003; Kluge, 1976) cite morphological and molecular results which draw *Paradelma* so closely allied with *Pygopus* as to negate its independence. My results recognize a mitochondrial DNA (mtDNA)

similarity (84.9%) comparable to that between *Delma australis* and *butleri* (84.7%). Despite low molecular divergence, we continue to recognize the validity of *Paradelma* on the grounds of ecological and morphological uniqueness, in accordance with many other sources (Cogger, 2000; Greer, 1989; Oliver, 2009; Wilson & Swan, 2008).

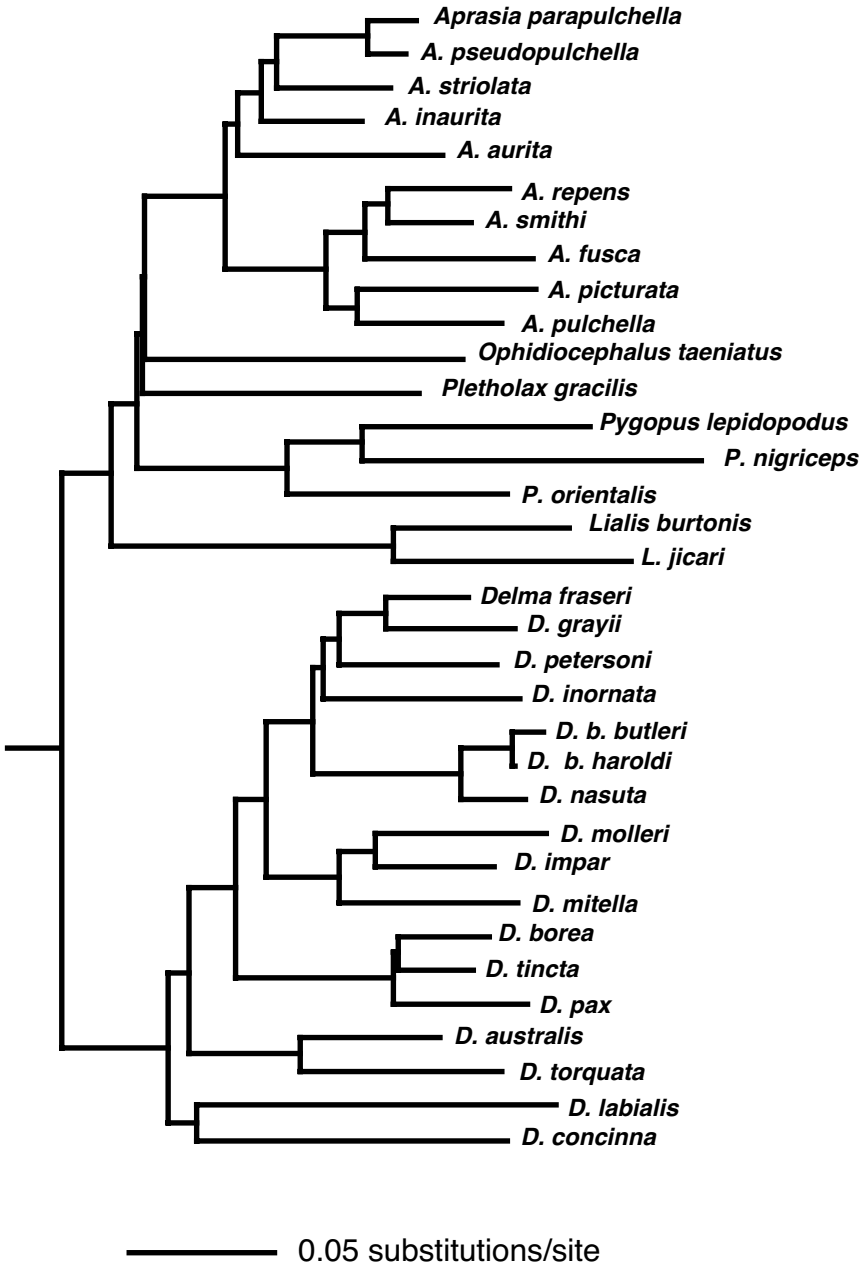

Figure I.2. Phylogenetic relationships among the Pygopodidae as inferred by combined morphology and DNA data by Jennings et al. (2003).

Morphological assessments (Jennings et al., 2003; Kluge, 1976; Wells, 2007) of the Pygopodidae have suggested a close relationship between *Aprasia* and *Ophidiocephalus* (Fig. I.3), however fossoriality may lead to homoplasy (e.g. attenuate tail, reduction of dentition, fusion and loss of cranial elements) confusing accurate phylogenetic assessment (Daza and Bauer, In press). In contrast, our results suggest a sister group relationship between the monotypic *Ophidiocephalus* and shrub-swimming *Pletholax*, both small, thin pygopodids restricted in range and habitat type. There is high support for the position of *Aprasia* as sister genus to a similarly well supported *Lialis-Paradelma/Pygopus* group. This historical reconstruction suggests the evolution of fossorial body-plans and habits in pygopodids (*Aprasia* and *Ophidiocephalus*) may have occurred twice independently, and the comparatively larger, longer, stouter bodies of *Lialis*, *Paradelma*, and *Pygopus* occurred ancestrally. Conversely, the ancestral body plan of pygopodids exclusive of *Delma* could have been thin and semi-fossorial, and the *Paradelma-Lialis* group represents a single large-bodied lineage. Until accurate intergeneric relationships are resolved or additional pygopodid fossils surface, the plesiomorphic pygopodid body plan and ecology remains enigmatic.

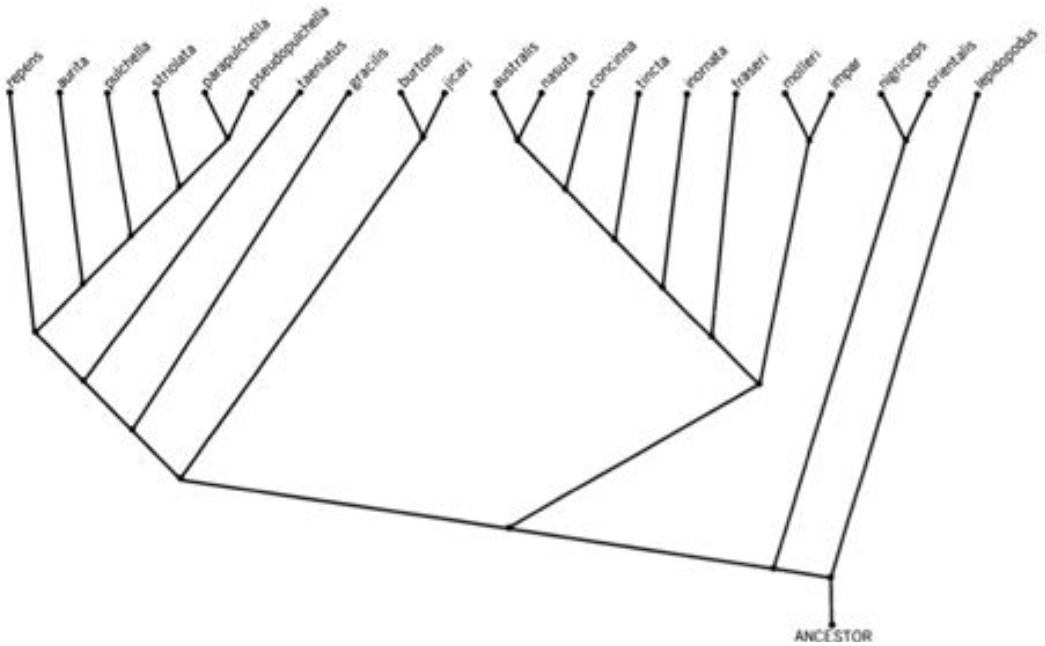

Figure I.3. Phylogenetic relationships among the Pygopodidae as inferred by morphology by Kluge (1976).

I.iv—*Delma* Gray 1831

Type species: *Delma fraseri* Gray 1831

Content: *Delma australis* Kluge, 1974; *Delma 'australis'* sp. nov. Maryan, Brennan, Adams & Oliver, 2014; *Delma borea* Kluge, 1974; *Delma butleri* Storr, 1987; *Delma* (*Aclys*) *concinna* Kluge 1974; *Delma desmosa* Maryan, Aplin & Adams, 2007; *Delma elegans* Kluge, 1974; *Delma fraseri* Gray, 1831; *Delma grayii* Smith, 1849; *Delma haroldi* Storr, 1987; *Delma* (*Pseudodelma*) *impar* Fischer, 1882; *Delma inornata* Kluge, 1974; *Delma labialis* Shea, 1987; *Delma mitella* Shea, 1987; *Delma molleri* Lütken, 1863; *Delma nasuta* Kluge, 1974; *Delma pax* Kluge, 1974; *Delma petersoni* Shea, 1991; *Delma plebeia* De Vis, 1888; *Delma tealei* Maryan, Aplin & Adams, 2007; *Delma tincta* De Vis, 1888; *Delma torquata* Kluge, 1974.

Delma represents a perplexing radiation within the Pygopodidae; despite a continent-wide distribution, moderate species richness (22 spp.), several deep molecular divergences, and adaptation to a variety of habitat types, the genus remains remarkably conservative in morphology, appearance, and diet (Jennings et al. 2003; Kluge, 1974, 1976; Oliver, 2009). *Delma* are distinguished from all other pygopodids by the combination of several characters: head scales (including parietals) enlarged and symmetrical, anterior nasal scales nearly always in contact, nostril bordered by more than two scales (except in *D. impar*), external ear opening large, usually fewer than 18 midbody scale rows, dorsal and ventral scales smooth, paired ventral scales, preanal pores absent, tail 2–4 times snout-vent length (SVL). Large hindlimb remnants—relative to other pygopodids—along with conspicuous ear openings, and generalist crushing dentition, support the basal position of *Delma* in the pygopodid radiation (Patchell and Shine, 1986).

Behaviorally, little is known of this genus, however; delmas often live in dense low vegetation, preferably tussock grasses and spinifex, in which they are able to disperse quickly in a serpentine fashion (Wilson & Swan 2008). We collected *Delma* both day and night, from a variety of cover types, including beneath spoils heaps, beneath stones, logs, and dry grass clippings. Over open ground and in response to attempted predation, *Delma*, like other pygopodids—*Ophidiocephalus* (Ehmann, 1981)—may saltate, using the tail as a spring,

adjusting the body into a sine wave configuration as it propels the body vertically or forward (Bauer, 1986; Gans, 1974; Kluge, 1974). Although other limb-reduced squamates appear to have converged on this behavior—trogonophid amphisbaenians (Gans, 1974), the viperid *Bitis caudalis* (Gans and Mendelssohn, 1972), and *Ophiosaurus* anguids (Cliburn, 1957)—the mechanics and outcome of the saltation event differ substantially (Bauer, 1986).

Delma appear to be active arthropod generalist hunters, with their diets almost exclusively insectivorous. *Delma butleri, fraseri*, *grayii*, *inornata*, *nasuta*, and *petersoni*—and presumably others—are both diurnal and nocturnal predators, dependent upon temperature (Patchell and Shine, 1986; Pianka, 2010). Preliminary study intimates the potential for prey specialization between species of *Delma* (Pianka, 2010), however historical data suggests otherwise (Jennings et al., 2003; Patchell and Shine, 1986). Although Patchell and Shine (1986) proposed a convergence in morphology and ecology between pygopodids and elapids, *Delma* lack an equivalent in the Australian snake fauna in behavior and as insectivores. In other parts of the world, insectivorous snakes are not uncommon—*Chionactis*, *Opheodrys,* and *Tantilla* of North America; *Aparallactus* of Southern Africa; *Typhlopidae* found globally; *Oligodon* and *Eirenis* of Asia—and the absence of terrestrial insectivorous snakes in Australia may be attributable to the presence of *Delma* as serpentine arthropod generalists (Patchell and Shine, 1986; Savitzky, 1983). As current estimates of divergence dates suggest, more likely, the success and species richness of *Delma* is attributable to filling the available niche prior to the diversification of insectivorous snakes in Australia.

Hutchinson (1997) addressed mandibular and dentition variation in *Delma* in reference to the description of *Pygopus hortulanus* from a single mandible. *Delma* retain the bicuspid crown condition of Pygopodoid geckos, suggesting an unspecialized dentition, indicative of a generalized diet of arthropods, and supporting the position of *Delma* basally in the pygopodid

tree. The splenial is slightly reduced with a moderately slender dentary, and posterior surangular foramina are narrowly separated. *D. concinna* poses the most divergent mandible within the genus *Delma*, as it is substantially elongated, however it remains recognizable and attributable to the genus.

I.v—Historical taxonomic position of the Pygopodidae within Squamata

Despite our current confidence in allying the Pygopodidae with Gekkota (Shea, 1989; Conrad, 2008; Daza & Bauer, 2012; Jennings et al., 2003; Kluge, 1974; Kluge, 1976; Vitt & Caldwell, 2009; Oliver, 2009; Oliver & Bauer, 2011), older classifications often left their position ambiguous (Boulenger, 1884; Gadow, 1901) or attributed the Pygopodidae to the Diploglossa (Cope, 1900; Camp, 1923). A publication as recently as 1996 (Jamieson et al.) even suggested consideration of a common ancestry between pygopodids and snakes. And although pygopodids have indeed become serpentine in appearance, and often in behavior (see *Lialis*), they have retained morphological and behavioral characteristics which ally them with other gekkotans. For example, pygopodids share large eyes covered by an immovable spectacle, caudal autotomy, amphicoelous vertebrae, broad dorso-ventrally flattened skulls, oviparity yielding paired eggs, the ability to vocalize, and pleurodont dentition among other characters which in combination describe the Gekkota uniquely (see Table I.1 in Appendix 1 for complete list of synapomorphies) (King and Horner, 1993; Romer, 1956). Prior studies (Daza and Bauer, 2012; Daza and Bauer, In press; Jennings et al., 2003; Lee et al., 2009; Oliver, 2009; Oliver and Bauer, 2011; Oliver and Sanders, 2009) hypothesize a divergence between the Pygopodidae and their pygopodoid sister taxon the Carphodactylidae, approximately 37 million years ago (Mya).

Despite the obvious morphological schism between pygopodids and other gekkotans, evidence for the close relationship between these groups has been recognized and supported for a

considerable period of time (Boulenger, 1885; Greer, 1989; McDowell and Bogert, 1954; Miller, 1966; Shute and Bellairs, 1953; Underwood, 1957; Wever, 1974). Recent molecular studies have supported the position of pygopodids within the Pygopodoidea as well as within the Gekkota, but intergeneric relationships within the Pygopodidae have varied greatly, with no single topology receiving overwhelming support (Daza and Bauer, 2012; Jackman et al., 2008; Jennings et al., 2003; Oliver and Bauer, 2011; Oliver and Sanders, 2009). Phylogenetic assessments using morphological data have also failed to create a single, favored tree, and have conflicted strongly with molecular trees. *Aprasia* has on a number of occasions been deemed distinctive enough to warrant its own family: Aprasiadae (Gray, 1845); Ophiopsisepsidae, as *Ophiposiseps* (Jensen, 1901); and most recently Wells (2007) resurrected Aprasiadae to encompass *Aprasia* and *Ophidiocephalus*. Molecular results refute monophyletic Aprasiadae and Pygopodidae Wells 2007, as well as monophyletic Pygopodinae and Lialisinae Kluge, 1976.

II. Materials and methods

II.i—Taxon Sampling

Specimens, tissues, and extractions were kindly provided by several institutions and researchers across Australia and the United States; the Western Australian Museum (WAM), Australian Museum—Sydney (AMS), South Australian Museum (SAM), Queensland Museum (QM), Museum of Comparative Zoology at Harvard (MCZ), Museum of Vertebrate Zoology at UC Berkeley (MVZ), Dr. W. Bryan Jennings (WBJ), Dr. Paul M. Oliver, and Dr. Aaron Bauer. To contribute to our dataset, over two months in Western Australia we collected a number of additional tissues for several species. Our molecular sampling covers all currently recognized *Delma* species, as well as considerable in-group intraspecific sampling, and a number of outgroup pygopodids (Appendix 2). While a number of species—*pax*, *plebeia, tealei, mitella,*

labialis, grayii, molleri, impar, desmosa, torquata, concinna, petersoni, elegans—exhibit relatively regional distributions with little geographic variation, we investigated several species—*australis, borea, butleri, fraseri, nasuta, tintca*—with extremely broad ranges, phenotypic variation, or disjunct populations, for instances of deep genetic divergences or cryptic speciation. These species with wide geographic distributions were sampled broadly across their ranges, allowing for more accurate estimates of diversity within species.

II.ii—Gene Selection

Molecular datasets have become indispensable in quickly and accurately resolving organismal relationships. Molecular phylogenetic success requires choosing and applying markers which are relevant as well as informative for the study taxa. Although relatively uninformative in comparison to more contemporary loci, some markers provide a considerable existing dataset, which may be added to. In contrast, identifying loci which are particularly informative to the study group and provide necessary insight to phylogenetic relationships, may not be applicable to a broader taxa. Increasing the number of genetic markers generally increases resolution in phylogenetic study (Maddison, 1997; McGuire et al., 2007; Portik et al., 2011; Pyron et al., 2013; Stanley et al., 2011), however, additional, novel markers may also increase discordance and weaken phylogenetic assessments (O'Neill et al., 2013). While the use of known informative loci gleaned from previous studies is particularly useful as a safe and confident way of resolving phylogenetic problems, it is also important in supporting continuously expanding squamate datasets such as Pyron et al. (2013) and Gamble et al. (2012). In contrast, identification and use of novel or recently recognized genetic markers provide the ability to choose an appropriate loci given the historical parameters of the study group; age, similarity, rate of diversification.

Here, we have used a multi-locus dataset composed of two mitochondrial (16s, ND2) and four nuclear markers (RAG1, MXRA5, C-mos, DYNLL1). Mito-nuclear molecular datasets have been shown to increase resolution and support over each used singly (Fisher-Reid and Wiens, 2011). Owing to the biology of the mitochondria as maternally inherited genomic material, and in contrast to the biparental nature of nuclear material, mitochondrial DNA (mtDNA) and nuclear DNA (nDNA) are useful in answering different questions (Fisher-Reid and Wiens, 2011; Kubatko et al., 2011; Leaché, 2009; Leaché and McGuire, 2006). Due to the uniparental inheritance of mtDNA, the effective population size is roughly one-quarter that of nDNA. As the rate of lineage sorting is inversely proportional to the effective population size, mtDNA should sort relationships at approximately four-times the rate of nDNA (Brown et al., 1979). Because of this mtDNA/nDNA disparity, and because mutational rates between loci vary, synonymous substitution rates of mtDNA may exceed 4.5–9.0 times that of average nuclear genes, and 1.7–3.4 times higher than the fastest nuclear genes (Ballard and Whitlock, 2004; Moriyama and Powell, 1997). Accelerated evolutionary rates prove mtDNA markers successful in elucidating inter- and intraspecific phylogenetic and phylogeographic questions (Igea et al., 2010). In comparison, deeper divergences are more accurately addressed via nDNA loci (Fisher-Reid and Wiens, 2011).

Used singly, mtDNA can occasionally provide misleading results, suffering from incomplete lineage sorting (coalescence), introgression, and long arm attraction (Jackman et al., 2008; Leaché and McGuire, 2006). Several deep branches, with relatively young divergence dates within species groups as hypothesized by Jennings et al. (2003) and Oliver (2009) suggest relationships within *Delma* necessitated both mitochondrial and nuclear loci for proper evaluation of interspecific relationships. The mitochondrial genes 16s rRNA (16s) and NADH dehydrogenase subunit 2 (ND2) are well established, and have been effective in various studies

of squamates, including an existing dataset from Jennings et al. (2003). The nuclear marker recombination activation gene 1 (RAG1) is another heavily-used loci, prized for its informativeness at both deep and shallow points within a phylogenetic tree (Donnellan et al., 1999; Fenwick et al., 2009; Fisher-Reid and Wiens, 2011; Jennings et al., 2003; Oliver et al., 2010; Oliver and Sanders, 2009; Sanders et al., 2008; Shea, 1993). Additionally, I have employed the use of oocyte maturation factor (C-mos) (Saint et al., 1998) based on the content of a preexisting dataset, as well as matrix-remodelling associated 5 (MXRA5) (Portik et al., 2012) and dynein light chain LC8-type 1 (DYNLL1) (Fujita et al., 2010) based on their utility in recent studies.

II.iii—Phylogenetic Analyses

Phylogenetic trees may be built under a number of methods, including character- and model-based analyses. Despite their potential pitfalls—and arguments that character- or model-based methods exhibit weaknesses when used individually—when used together, these methods strongly corroborate one another, rarely exhibiting strong incongruence (Cunningham et al., 1998; Felsenstein, 1978; Huelsenbeck et al., 2002; Rindal and Brower, 2011). Combination of these methods are well established in squamate phylogenetics, showing the methodology to be successful (Fenwick et al., 2009; Jackman et al., 2008; Jennings et al., 2003; Leaché and McGuire, 2006; Sanders et al., 2008). We incorporated maximum parsimony (MP), maximum likelihood (ML), and Bayesian inference (BI) analyses to address phylogenetic questions within *Delma*.

As a character-based analytical method, maximum parsimony uses discrete characters such as morphological states, as well as less conspicuous characters such as molecular sequences to establish a tree of best fit through the least evolutionary steps. Maximum parsimony

methodology revolves around the concept that the tree with the fewest assumptions, and therefore fewest steps will provide the most accurate reconstruction. The philosophy that a tree with fewer assumptions and therefore evolutionary steps is preferred over a phylogeny with more steps, is at the heart of the methodology of maximum parsimony. We used the computer program PAUP (Swofford, 2003) to carry out our MP analysis. This program uses a heuristic search method, assuming each molecular base is an unordered character with four potential alternative states (A, T, G, C), among other techniques such as branch swapping and weighting of character states and transitions. Bootstrapping and Bremer support are methods of establishing topological robustness through testing the resiliency of your most preferred parsimonious tree(s). By re-sampling and replacing existing data with randomized results (bootstrapping), or comparison between the most parsimonious tree(s) and other suboptimal trees (Bremer support), we reevaluate our results with the intention of understanding the strength of the most parsimonious trees returned by PAUP. The MP method is not without its dangers however, MP trees are subject to the ills of long-branch attraction, in which parsimony analysis inaccurately recognizes deeply divergent long branches as sister taxa (Felsenstein, 1978). The relatively young age and shallow branches, and robust taxon sampling helped to reduce the risk of long branch attraction (Wiens, 2005).

Model-based methods require a priori assumptions regarding the rate of evolution of the genetic material being used (Huelsenbeck et al., 2001). We used the JModelTest and the Akaike's information criterion (AIC) method to establish the appropriate model for mutation/substitution rate for this group. Molecular data was partitioned by gene and codon position (Table I.2). Both ML and BI require this a priori model selection, a process derided by cladists for its inclusion of addition assumptions, but supported by phylogeneticists for its ability to create more accurate, well supported trees (Cunningham et al., 1998; Huelsenbeck et al.,

2002). Despite this conflict, model-based methods allow for the creation of branch lengths, which provide an estimation of divergence between an ancestral node and its crown taxa representatively through length.

Table I.2. Primers used for PCR amplification and sequencing.

Gene	Primer name	Sequence	Primer reference
ND2	MetF1 L4437	5'- AAGCTTTCGGGCCCATACC -3'	Macey *et al*., 1997
	ND2F17	5'-TGACAAAAAATTGCNCC-3'	Macey *et al*., 2000
	TRPR3 H5540	5'-TTTAGGGCTTTGAAGGC-3'	Macey *et al*., 1997
	CO1R1	5'-AGRGTGCCAATGTCTTTGTGRTT-3'	Macey *et al*., 1997
16S	16ScL2189	5'-GTMGGCCTAAAAGCAGCCAC-3'	Reeder, 1995
	16SbH2920	5'-GCGCTGTTATCCCTAGGGTAACTTG-3'	Reeder, 1995
RAG1	RAG1 396	5'-TCTGAATGGAAATTCAAGCTGTT-3'	Groth & Barrowclough, 1999
	RAG1 F700	5'-GGAGACATGGACACAATCCATCCTAC-3'	Bauer *et al*., 2007
	RAG1 R700	5'-TTTGTACTGAGATGGATCTTTTTGCA-3'	Bauer *et al*., 2007
	RAG1 397	5'-GATGCTGCCTCGGTCGGCCACCTTT-3'	Groth & Barrowclough, 1999
MXRA5	MXRA5 PF2	5'-AAYATTTTGGCAAAAGTCCGWGGRA-3'	This study
	MXRA5 PR2	5'-GCTTKGGTCTYYTGAACCTATTTGG-3'	This study
DYNLL1	DYNLL1 ex1.F	5'-TGATCAAGAATGCGGATATGTCTGAG-3'	Fujita *et al.*, 2010
	DYNLL1 F312	5'-CCCATGAGYGACTGAAGCAAC-3'	This study
	DYNLL1 R1224	5'-TCAAACCACCTCAGTAACTTGCT-3'	This study
	DYNLL1 ex2 R	5'-TCTTCCCACAATACAGTGCCAAGTAG-3'	Fujita *et al.*, 2010
C-mos	Cmos G73	5'-GCGGTAAAGCAGGTGAAGAAA-3'	Saint *et al*., 1998
	Cmos G74	5'-GTMGGCCTAAAAGCAGCCAC-3'	Saint *et al*., 1998

Despite similarities, ML and BI work to establish phylogenetic trees in equal but opposite directions. Bayesian inference works to produce the most fitting tree based upon the given model of evolution and sequence data supplied to the program (Huelsenbeck et al., 2001). Alternatively, maximum likelihood estimates the degree of fit between a given tree and the sequence data provided, to establish a tree with the greatest fit—methodologically a reversal of Bayesian inference. Regardless, both methods allow for a measure of tree support; like MP, ML uses bootstrap values, while BI measures support through posterior probabilities. The posterior probability of a given tree is measured as a combination of the prior probability of the tree and the likelihood of the tree, as a test of its accuracy (Huelsenbeck et al., 2001). We ran ML trees using RaxML for 5,000 bootstrap replicates. BI trees were run via MrBayes (Huelsenbeck and Ronquist, 2001a), and set to run for 200 million generations with sampling each 1,000 trees, with

2 runs across 4 chains, resulting in 400,000 trees, and a burn-in of the first 5,000 trees. Both runs converged on an identical topology with near-identical BPP values.

Phylogenetic problems often arise when there is gene-tree species-tree discordance. These incongruences—deep coalescence, incomplete lineage sorting—may be the result of several complications which cannot be resolved or understood through analysis of a single gene. Inclusion of multiple genes may result in its own complications, such as incongruence between gene trees of different genes. While a simple comparison of support values often ameliorates these conflicts, coalescent based methods such as *BEAST and BEST may provide the best way to alleviate individual gene conflict. These methods are time and resource intensive, and require significant prior knowledge of population size and extinction rate estimates. Instead, we opt to use a fossil calibrated Bayesian time tree method to estimate divergence dates within *Delma*.

Conveniently, fossil pygopodid remains exist. Both ancient (Hutchinson, 1997)and more recent (Mead et al., 2008) *Pygopus* fossils have been identified and described from deposits and caves. Accurate phylogenetic placement and dating of the *Pygopus hortulanus* mandible allowed us to use BEAST (Bayesian evolutionary analysis by sampling trees) to create a time-tree of pygopodid divergences (Drummond and Rambaut, 2007). BEAST uses mutational rate estimates similar to that of MrBayes, in addition to flexible molecular clock and fossil calibrations to recreate the most likely divergence estimates.

II.iv—Concatenation

Multilocus datasets, and the potential for differing evolutionary histories and mutational rates, can prove problematic when it comes time to analyze data. Conflicting theories exist when utilizing multi-marker datasets. The first, concatenation, aligns data from mutliple loci into a single string of data. When genes are concordant with one another, this allows for improved

resolution as the result of an increase in informative sites. The pitfall however, comes as we recognize not all genes have the same evolutionary history. Concatenation can mask gene conflict as the result of incomplete lineage sorting, introgression, or rate heterogeneity (Maddison, 1997). While the former two causes can result in strongly supported discordant topologies, and should not be concatenated into a agreeable dataset, difficulties arising from rate heterogeneity causing fuzzy trees or unsupported branches may be assuaged by proper gene partitioning. Unlinking substitution rate, clock rate, and tree topology of individual loci in a concatenated dataset such as in BEAST, allows a considerable amount of freedom for the evolutionary history of each locus. Unlinked tree topologies are the primary function of the second methodology, consensus trees. Consensus methods build trees from each gene provided, and comparing them to ultimately build a single species tree. Unfortunately, consensus methods as used in programs such as *BEAST and BEST are time and computationaly intensive, and so we instead used maximum likelihood and Bayesian inference methods.

II.v—Species Delimitation

Irrespective of the static nature of taxonomy and systematics, speciation remains a continuous process (de Queiroz 1998), often with ambiguous higher level designations. Additionally, there is consistent disagreement over which criteria to use, and how to identify a population as a species (Wiens, 2004; Leache & Fujita, 2010). While allopatry may encourage speciation, it may also make delimitation by the biological species concept difficult (Mayr, 1942; Dobzhansky, 1950). Conversely, sympatry generally works against speciation events, unless niche partitioning is available, or novel characters arise. Accurate identification and recognition of individual species is fundamental to proper understanding of ecology, biodiversity, and biogeography, as well as providing a vital framework for informed habitat management, development and conservation (Sites Jr and Marshall, 2004). Species units allow for estimations

of biological richness, endemism, and conservational value, among other criteria, allowing a basis for proper evaluation.

However, species boundaries are often ambiguous, and methods of species delimitation are varied, with no single strategy without fault (Frost and Hillis, 1990; Sites Jr and Marshall, 2003, 2004; Strutzenberger et al., 2011). Species delimitation methods using an arbitrary threshold of genetic distance or morphological divergence inevitably encounter exceptions, and so, qualitative judgments must be made ad hoc per the sampled taxa, and in light of higher level relationships within the study group (Frost and Hillis, 1990; Sites Jr and Marshall, 2004). Recognizing species in a morphologically conservative group such as *Delma* causes its own problems. However, a focal group which is morphologically conserved, with broad geographic ranges, and ecological differentiation suggests a prime candidate for studying cryptic speciation. Recent molecular study has identified several cryptic species within pygopodids (Maryan et al., 2013b; Oliver et al., 2010) and even within *Delma* (Jennings et al., 2003; this study). Simultaneously however, species recognized by morphology alone have been secondarily synonymized due to insufficient molecular divergence (Jennings et al., 2003; Maryan et al., 2007). Species divergence and radiation may proceed ecologically, morphologically, or genetically; ultimately providing the necessary criteria for species delimitation (Leaché et al., 2009). I take a coalescent approach to determining valid species units within *Delma*, using age and depth of recognized divergences, in concert with morphological assessment to address independently evolving lineages.

II.vi—Divergence Dating

Estimating divergence dates within the Pygopodidae is aided by the presence of a fossil pygopodid, discovered in the Riversleigh deposits of northwest Queensland. Since its discovery

and description, this fossil mandible has been a topic of contentious debate surrounding its phylogenetic placement and age, and its impact on fossil-calibrated time-trees. Conservative placement of *Pygopus hortulanus* fossil may prove disruptive to accurate dating within the family. By conservatively placing the fossil deeper in the tree than necessary (between *Pygopus* and *Lialis* or between *Pygopus* and *Delma*, as has been used in other literature (Heinicke et al., 2013; Lee et al., 2009) we may artificially force divergence dates to be estimated significantly younger than they actually are. In contrast, liberally placing this fossil within *Pygopus*, as recommended by Hutchinson (1997) in naming the species, may inadvertently overestimate the depth of divergence events within the Pygopodidae. This topic has been addressed extensively by Lee et al. (2009). Hutchinson's (1997) placement of this dentary fossil is also contingent upon Kluge's (1974, 1976) assumption that *Pygopus nigriceps* is more closely related to *Paradelma orientalis* than it is *P. lepidopodus*. While the most accurate conservative placement of this fossil would be to place it between *Pygopus*/*Paradelma* and their sister group, intergeneric relationships have not been confidently established. For phylogenetic analysis purposes, we place this fossil at the base of the *Pygopus*-*Paradelma* split, and retain Hutchinson's (1997) estimate of 20–22 Mya. We used BEAST to estimate divergence dates and tree topology simultaneously under Bayesian theory.

II.vii—Research Goals

The Family Pygopodidae represents an incredibly unique and divergent gekkotan lineage, particularly valuable to Australian biogeography because of high endemism (>95%), moderate species richness (>44 species), and remarkable ecological diversity. The genus *Delma* is just one representative of the family as a whole, however, with 21 species across a variety of habitat types

ranging continental Australia, *Delma* is a prime tool for understanding squamate diversity in Australia. In order to best understand *Delma*, we aimed to address the following:

1. Compose a comprehensive multilocus molecular phylogeny for the genus *Delma*, in order to investigate questions of biogeography and speciation within this genus.
2. Assess intraspecific variation, and the validity and current status of *Delma australis* through molecular and morphological methods.
3. Observe and describe the hemipenial morphology of pygopodids, with a focus on phylogenetic utility in *Delma*.

III. Mito-nuclear discordance and speciation by aridification in flap-footed geckos, *Delma* Gray 1831 (Gekkota: Pygopodidae)

Ian G. Brennan, Aaron M. Bauer, Paul Doughty, Paul M. Oliver, Todd R. Jackman

III.i—Abstract

The gekkotan clade is a speciose and cosmopolitan group, with upwards of 1500 members and constituents on six continents. Little known however are the pygopodids, the flap-footed geckos of the Family Pygopodidae (Gray, 1845). These Gekkotans are limited to Australia (44 species) and New Guinea (2 species), but have diverged extensively into the most ecologically limbless radiation save Serpentes, occupying a broad range of habitats and ecological niches. Current phylogenetic understanding of the family has relied almost exclusively on two works—Kluge (1974) and Jennings et al. (2003)—which have produced and synthesized an immense amount of morphological, geographical, and molecular data. However, current interspecific relationships within the largest genus *Delma* Gray 1831 are based exclusively upon a concatenated molecular dataset provided by two mitochondrial loci (16s, ND2), and a short segment (372 bp) of the nuclear protein-coding gene C-mos. Here, we reevaluate the inter- and intraspecific relationships within the genus *Delma* using two mitochondrial (16s, ND2) and four nuclear loci (Rag1, MXRA5, C-mos, DYNLL1), and identify points of strong conflict between nuclear and mitochondrial genomic data. We address mito-nuclear discordance, and remedy this conflict by recognizing several points of mitochondrial introgression as the result of deep hybridization events. We show *Delma australis* comprises a species group, from which we recognize two new species based upon morphological and molecular data. Results additionally indicate paraphyly in the widely distributed and disjunct species *D. butleri* and *D. tincta*, and we suggest a more careful review of the northwest clade of *D. borea, tincta, pax, desmosa, tealei*, and *elegans*. Accurately assessing and addressing species

richness and relationships within this endemic Australian Gekkotan genus is relevant for understanding patterns of squamate speciation across the continent. Identification of cryptic species lineages are vital to informed habitat protection and development, and cataloging local, Australian, and worldwide biodiversity.

III.ii—Introduction

Phylogenetic relationships within the Pygopodidae have been assessed in-depth on two occasions (Jennings et al., 2003; Kluge, 1976). Despite a massive revision of the family in 1974, Kluge's (1976) preliminary phylogenetic assessment was limited in scope to morphological characters. Adding to this existing dataset, Jennings et al. (2003) used mtDNA (16S, ND2) and nDNA (C-mos) markers in concert with morphology to propose what is currently deemed our phylogenetic understanding of pygopodids. Jennings et al.'s (2003) seminal paper on the Pygopodidae and the phylogeny and data produced, have been used extensively because of remarkably complete intergeneric and interspecific sampling (Garcia‐Porta and Ord, 2013; Lee et al., 2009; Maryan et al., 2013b; Oliver, 2009; Oliver et al., 2010). Based on our contemporary understanding of the importance of strong mitochondrial *and* nuclear datasets, the 372 bp fragment of C-mos used is woefully unequipped to properly reconstruct the nuclear evolutionary history within the Pygopodidae. Here, we expanded upon Jennings et al.'s dataset, with increased intraspecific sampling, including three additional nuclear markers (RAG1—1071 bp, MXRA5—793 bp, DYNLL1—1056 bp), and propose a new phylogeny of interspecific relationships within the genus *Delma*.

III.iii—Molecular Methods and Phylogenetic Analyses

Genomic DNA was isolated—via Qiagen DNeasy Tissue kits (Qiagen)—from liver, heart, or tail tissue kindly provided by several institutions and researchers: the Western

Australian Museum (WAM), Australian Museum (AMS), South Australian Museum (SAM), Queensland Museum (QM), Museum of Comparative Zoology at Harvard (MCZ), Museum of Vertebrate Zoology at UC Berkeley (MVZ), Dr. W. Bryan Jennings (WBJ), Dr. Paul M. Oliver, and Dr. Aaron Bauer. Mitochondrial (mtDNA) and nuclear (nDNA) loci were amplified by polymerase chain reaction (PCR). To take advantage of increased resolution as a result of multi-locus mito-nuclear datasets, we employed both mitochondrial (16s, ND2) and nuclear markers (DYNLL1, RAG1, MXRA5, C-mos) (Fisher-Reid and Wiens, 2011). Primers used for PCR amplification and sequencing are listed in Table I.2. Standard 25 μL PCR reactions utilized; dH_2O, 5x Taqmaster PCR enhancer, 10x PCR Buffer, dNTPs, forward and reverse primers, Taq polymerase, and genomic DNA, and were carried out on an Eppendorf Nexus gradient thermocycler. Thermocycler amplification programs followed a standard protocol with varying annealing temperatures, relative to the loci and primers; initial denaturation period (95°C, 2 min) followed by 34 cycles at 95°C (30 s), 48°C (35 s) annealing, and 72°C (150 s) extension. Amplified PCR products were visualized using 1.5% agarose electrophoresis, purified via Agencourt AMPure magnetic bead system (Agencourt Bioscience), and stored in a refrigerator at 4°C until sequenced. We performed cycle sequencing via BigDye Terminator v3.1 Cycle Sequencing kit using purified PCR product as a template, and sequencing product was purified using Agencourt CleanSeq magnetic bead system (Agencourt Bioscience). Amplified product was sequenced in both forward and reverse directions using an ABI 3730 XL sequencer, to allow for identification of heterozygous sites.

All sequences were aligned by eye, and protein-coding loci were translated to amino acid sequence to maintain proper reading frame and avoid premature stop codons. tRNA secondary structure was addressed and aligned by eye for consistency. Mitochondrial genes were analyzed together because of shared evolutionary history as the result of physical linkage. Nuclear loci

gave varied in degrees of support and rarely in topology, but did not exhibit strong conflict, and so were concatenated into a single dataset which produced a well supported evolutionary scenario. Final aligned mitochondrial and nuclear sequences were 2276 bp (16s–796, ND2–1480) and 3298 bp (DYNLL1–1056, MXRA5–793, RAG1–1071, Cmos–378) respectively, and the concatenated mito-nuclear dataset stretched 4500 bp. We used maximum likelihood (ML) and Bayesian inference (BI) methods to test for conflict between topologies and support values between analytical programs. ML and BI results returned largely concordant topologies, with comparable Bayesian posterior probability (BPP) and bootstrap support (BSS) values across all datasets. We used the Akaike Information Criterion in jModeltest 2 (Darriba et al., 2012; Guindon and Gascuel, 2003) and PartitionFinder (Lanfear et al., 2012) to identify the most accurate models of evolution for each gene and codon position (see Table I.3).

I used RAxML 8.0 (Stamatakis, 2014) for ML analyses, and divided the mitochondrial dataset into three partitions; ND2, tRNA, and 16S; the nuclear dataset into three partitions; MXRA5, RAG1, C-mos; and employed the GTR+I+Γ model of evolution. When analyzed independently, individual loci were not partitioned by codon position because of RAxML's limits on evolutionary models, and were instead analyzed under GTR+I+Γ. Topology estimates used 100 independent tree searches, and 5000 bootstrap replicates to retrieve support values. One vs. three partitions for mtDNA and nDNA did not disrupt topology or change BSS support values substantially.

Table I.3. Models of best-fit for data partitioning as determined by AIC and PartitionFinder

Gene	Model applied
ND2	
1st position	GTR+I+Γ
2nd position	GTR+I+Γ
3rd position	GTR+Γ
16S	GTR+I+Γ
RAG1	
1st position	HKY+Γ
2nd position	GTR+I+Γ
3rd position	GTR+Γ
MXRA5	
1st position	GTR+I+Γ
2nd position	GTR+Γ
3rd position	GTR+Γ
DYNLL1	GTR+Γ
C-mos	
1st position	GTR+Γ
2nd position	GTR+Γ
3rd position	GTR+Γ

BI analyses were performed using MrBayes 3.2 (Huelsenbeck and Ronquist, 2001a; Ronquist et al., 2012). The mitochondrial dataset was divided into six partitions; ND2, ND2 codons (1st, 2nd, 3rd), tRNA, and 16S; and the nuclear dataset into 13 partitions—each gene receiving 4 partitions (whole locus, three codon positions), with the exception of the nuclear intron DYNLL1. Three vs. six partitions for mtDNA and four vs. thirteen partitions for nDNA returned identical topologies and did not significantly disrupt BSS support values. We executed two parallel (two heated and two cold chain) runs for 200 million generations sampled every 1000 generations, with sampling from the first 20 million generations discarded as burn-in.

I used BEAST 1.8.0 (Drummond and Rambaut, 2007) to estimate divergence times within the Pygopodidae as well as *Delma*. I did not enforce a topology for this analysis, but did identify ingroup (*Delma*) and outgroups (*Aprasia, Lialis, Ophidiocephalus, Paradelma, Pygopus*) as monophyletic. I used only nuclear data for our chronogram due to inconsistency between mtDNA and nDNA datasets. Data was partitioned according to gene and codon position, and substitution rates were unlinked. I implemented Yule tree priors and uncorrelated relaxed lognormal clocks for all loci. The analysis was run for 100,000,000 generations, sampled each 1000 generations, and TreeStat v1.8.0 was used to identify and discard appropriate burn-in (10%). The remaining 90,001 trees were inspected and combined using TreeAnnotator v1.8.0, to provide the most informative and preferred topology. Following Lee et al. (2009) I applied a

floating calibration (exponential prior, mean = 10, offset = 20) for the *Pygopus hortulanus* fossil as a result of uncertain phylogenetic placement. As a result I retrieved far wider credibility intervals than a Jennings et al. (2003) who used a fixed calibration point for this fossil, however, I are more comfortable in this assessment than the alternative.

III.iv—Results

The programs jModeltest (Darriba et al., 2012; Guindon and Gascuel, 2003) and PartitionFinder (Lanfear et al., 2012) assigned varying nucleotide substitution models based on nuclear loci and codon positions (Table I.3). Both mtDNA and nDNA datasets unequivocally support (BSS and BPP = 100) the monophyly of all currently recognized genera, as well as the sister-genus relationship between *Paradelma* and *Pygopus*, and the basal split between *Delma* and all remaining pygopodid genera. Remaining intergeneric relationships are generally poorly supported by our mtDNA dataset, with the exception of moderate-to-strong support (BSS = 78, BPP = 94) for recognizing *Aprasia* as the sister taxon to all other pygopodids (exclusive of *Delma*). Our nDNA dataset produces a well supported hypothesis of intergeneric relationships which will be addressed below.

The monophyly of *Delma* remains highly supported (BSS and BPP = 100) across the two datasets, as is the monophyly of most currently recognized species. To date, Jennings et al.'s (2003) mitochondrial tree has been widely accepted as the accurate representation of interspecific relationships within *Delma*. This topology as interpreted by mtDNA reflects these relationships with strong support, however, our concatenated nDNA dataset provides a strongly supported incongruent topology.

Phylogenetic analyses of nuclear data

Bayesian and maximum likelihood analyses of four nuclear loci analyzed independently and as a single concatenated nuclear dataset, are congruent in returning strong support for monophyly of *Delma*, as well as the basal split between the *australis* group and all other delmas. The concatenated data provides high support for most species groups and currently recognized species, however, deeper relationships between species groups receive relatively low support. All nuclear loci, analyzed independently, return largely unresolved or poorly supported interspecific topologies. RAG-1 provided the most well resolved phylogeny, exclusive of the concatenated data, with most interspecific relationships echoed in other nuclear locus genealogies—albeit with low support. I believe the concatenated nuclear dataset provides the most accurate representation of the evolutionary history of *Delma*—fracturing the genus into discrete species groups. The basal split of *australis* and *concinna* (Fig. II.1, III.1—C) from the rest of the genus also finds *australis* paraphyletic with regards to *torquata*. Intraspecific variation, geographic affinities, and species delimitation within the *australis* group will be covered in a subsequent chapter. Exclusive of the *australis* group, *mitella* is identified as the sister taxon to the remaining delmas (Fig. II.3, III.1—D). There is high support for a broadly distributed group comprising *inornata, grayii, nasuta, butleri*, and *haroldi* (Fig. II.2, III.1—E). Similarly, there is strong support for two groups of large, morphologically similar species in *petersoni* and *fraseri* (Fig. II.3, III.1—F), and *molleri*, *impar*, and *plebeia* (Fig. II.4, III.1—G), which stretch across southern and western Australia. Nuclear data also supports the monophyly of a largely northwestern Australian group composed of *borea, desmosa, elegans, pax*, *tealei*, and *tincta*, and their association with the much larger *labialis*, (Fig. II.5, III.1—H) as well as the monophyly of the species within this group. Interspecific relationships within the northwest clade mostly receive poor support, and are not well addressed in this group. This matter is complicated by considerable morphological

similarity, resulting in the potential for misidentification of species, particularly juvenile specimens.

Phylogenetic analyses of mitochondrial data

Although mtDNA data also provide high support for the monophyly of *Delma,* as well as the basal split between the *australis* group and remaining delmas, the mtDNA topology (Fig. III.2, III.3a/b/c) is largely discordant with nDNA data. Species groups are well supported, as well as intra- and interspecific relationships, with moderate support for the positions of the range-limited species *concinna* and *labialis*, basal to other delmas (Fig III.2, III.3b). *Delma australis* is again rendered paraphyletic with respect to the east coast species *torquata*, with substantial substructuring within the *australis* sensu stricto group. There is strong support for a clade of *borea, desmosa, elegans, pax*, *tealei*, and *tincta* (Fig. III.2, III.3b)—a group largely restricted to the northwest corner of the continent, but with two broad-ranging, and paraphyletic species groups in *borea* and *tincta*. An east and southeastern group composed of *impar, mitella, molleri*, and *plebeia* (Fig. III.2, III.3b) are returned as a monophyletic group with strong support for interspecific relationships. As in the nDNA results, *Delma butleri, haroldi*, and *nasuta* form a well supported clade (Fig. III.2, III.3c), however, poor support makes it difficult to distinguish between the currently recognized species *haroldi* and *butleri*. Additionally, a clade comprising *inornata, petersoni, fraseri*, and *grayii* (Fig. III.2, III.3c) stretches along the southern coast of Australia from extreme southern QLD hugging the coast south and west up to Shark Bay, WA. High support unites *fraseri* and *grayii* as sister taxa, with moderate support for *petersoni* as sister species to this pair.

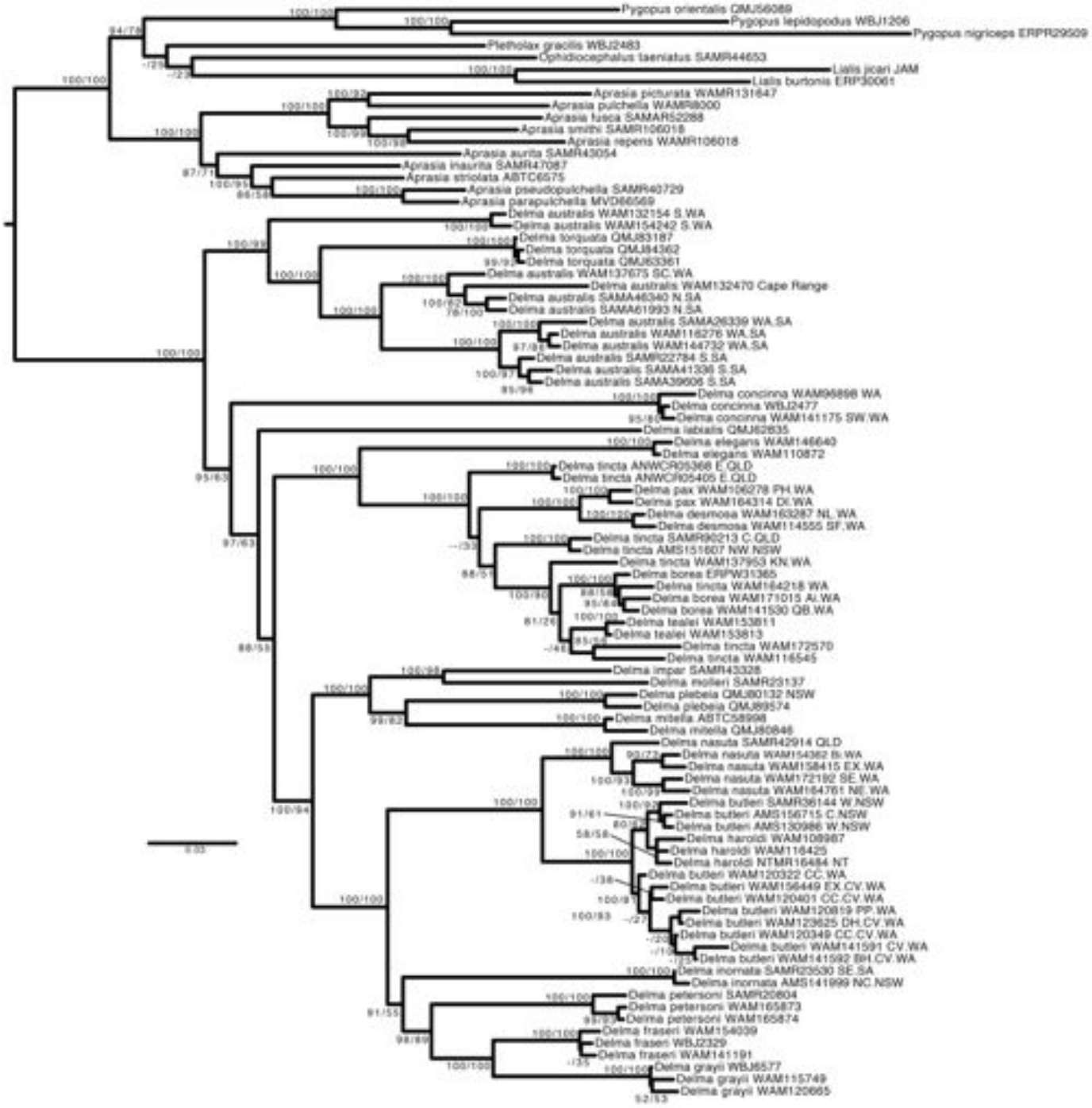

Figure III.2. Maximum likelihood (RaxML) phylogeny of Pygopodidae based on a combined (16S, ND2) mitochondrial dataset. Maximum likelihood bootstrap (BSS) and Bayesian posterior probabilities (BPP) support values are indicated at each node (BPP/BSS).

Figure III.3a. Top third of Maximum likelihood (RaxML) tree of relationships among *Delma* based on the mitochondrial gene ND2. Enlarged numbers indicated maximum likelihood bootstrap support values for key nodes.

Figure III.3b. Middle third of Maximum likelihood (RaxML) tree of relationships among *Delma* based on the mitochondrial gene ND2. Enlarged numbers indicated maximum likelihood bootstrap support values for key nodes.

Figure III.3c. Final third of Maximum likelihood (RaxML) tree of relationships among *Delma* based on the mitochondrial gene ND2. Enlarged numbers indicated maximum likelihood bootstrap support values for key nodes.

Comparison of relationships between mtDNA and nDNA

When analyzed independently, mitochondrial and nuclear datasets provided strongly supported, conflicting topologies, suggesting largely discordant evolutionary histories for speciation with *Delma*. Disagreement between trees is not isolated to weakly supported or unresolved nodes, extending to well supported relationships in both trees (e.g. mtDNA—*fraseri-grayii*; nDNA—*fraseri-petersoni*). Instances of conflict extend beyond individuals within a single species group (fig. III.4), including deeper divergences, such as the position of *concinna* as sister to the *australis* group (nDNA), or to all other delmas (mtDNA).

In all cases, mtDNA allows for the best assessment of intraspecific variation and geographic patterns within species. Although there are apparent instances of paraphyly within currently recognized species, only instances within *australis* and *butleri* remain consistent across mtDNA and nDNA genealogies. The *australis* group is paraphyletic with regards to *torquata*, and exhibits substantial divergences within the remaining group. Interpretation of our mtDNA dataset recognizes northern WA records of *borea* as a unique group, separate from the greater *borea-tealei-tincta* clade, however samples of far western *borea* (WAMR112725, WAMR114391, WAMR157937, WAMR157938) were unavailable for nuclear assessment. Eastern and western populations of *butleri* are split with respect to *haroldi*, which is alternately associated as sister taxon to the eastern *butleri* by mtDNA, and to western clade *butleri* by nDNA. Additionally, *tincta* appears to represent a complex species group, with populations from eastern QLD, central QLD and NSW, and WA appearing as independent monophyletic groups in various places within this northwestern clade. The potential for taxonomic confusion within *tincta* is not surprising given the species broad geographic distribution and conserved morphology. Mito-nuclear discordance accentuated by syntopy (*fraseri, grayii*) within a

morphologically conservative genus such as *Delma* intimates the potential for past introgression events.

Divergence Dates Assessed by BEAST

I used the concatenated nuclear dataset to build a Bayesian time-tree (fig. III.5) using the program BEAST (Drummond and Rambaut, 2007). The resulting topology is largely concordant with our mixed method (ML, BI) concatenated nDNA trees, but provides higher support at a number of previously weakly or moderately supported clades. Confidence intervals are large, as the result of phylogenetic uncertainty in fossil calibration. Monophyly of the northwestern Australia (NWA) group (*labialis*, *elegans, desmosa, pax, borea, tincta, tealei*) (BPP = 98) and its sister group relationship with the monophyletic *plebeia* group (*moller, plebeia, impar*) (BPP = 100) are returned with high support (BPP = 91). *Delma concinna* is again allied with the *australis* group, this time however, with greater support (BPP = 100). The broadly distributed group composed of *inornata, grayii, nasuta, butleri,* and *haroldi* remains well supported (BPP = 100), and paraphyly of *butleri* is consistent with previous nuclear analysis. Despite monophyly of the NWA group, interspecific relationships remain poorly resolved. *Delma tincta* is paraphyletic with regards to *tealei*, and relationships between *desmosa* and *pax* appear confused.

The crown group split within Pygopodidae appears to have occurred approximately 55 Mya, closely following the basal Carphodactylidae—Pygopodidae split ca. 60 Mya. The basal split between the *australis* group+*concinna*, and all other *Delma* appears to have occurred ca. 38 Mya (25–55 Mya), and is mirrored by several hypothesized splits within outgroup pygopodids: *Pletholax—Ophidiocephalus* (36 Mya), *Lialis—Paradelma/Pygopus* (36 Mya), *Aprasia—Lialis* group (39 Mya). A substantial number (n=10) of species group and interspecies divergences occur between 10–20 Mya, while nearly all intraspecific divergence—with the exception of *australis*—are less the 5 Mya old.

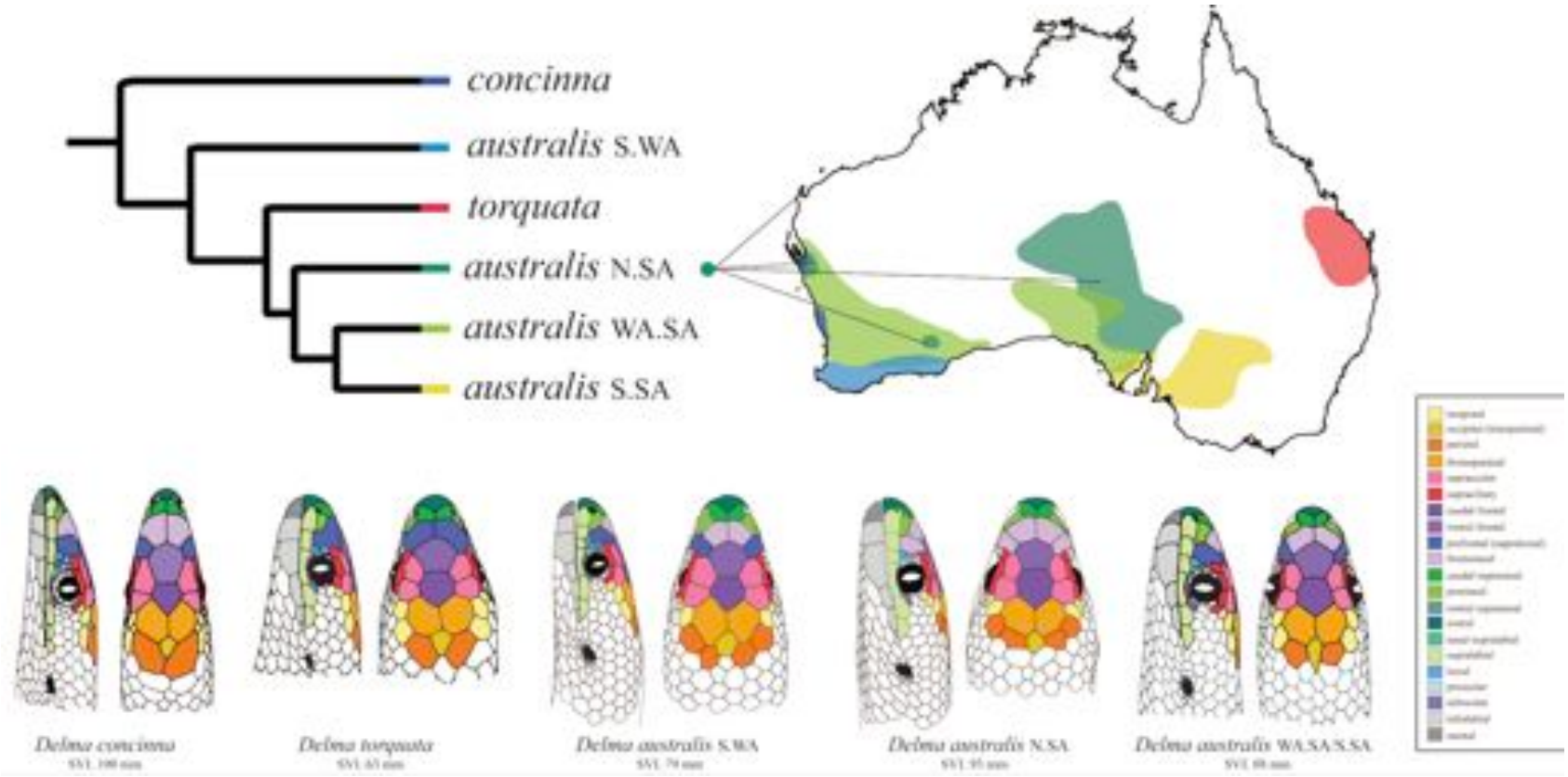

Fig. II.1. Simplified inter- and intraspecific relationships within the *Delma australis* group (III.1C) as inferred by Bayesian/Maximum Likelihood topology of mito-nuclear results, clade distributions, and lateral and dorsal head figures to show general scalation, head trends in shape, and maximum snout-vent length (SVL).

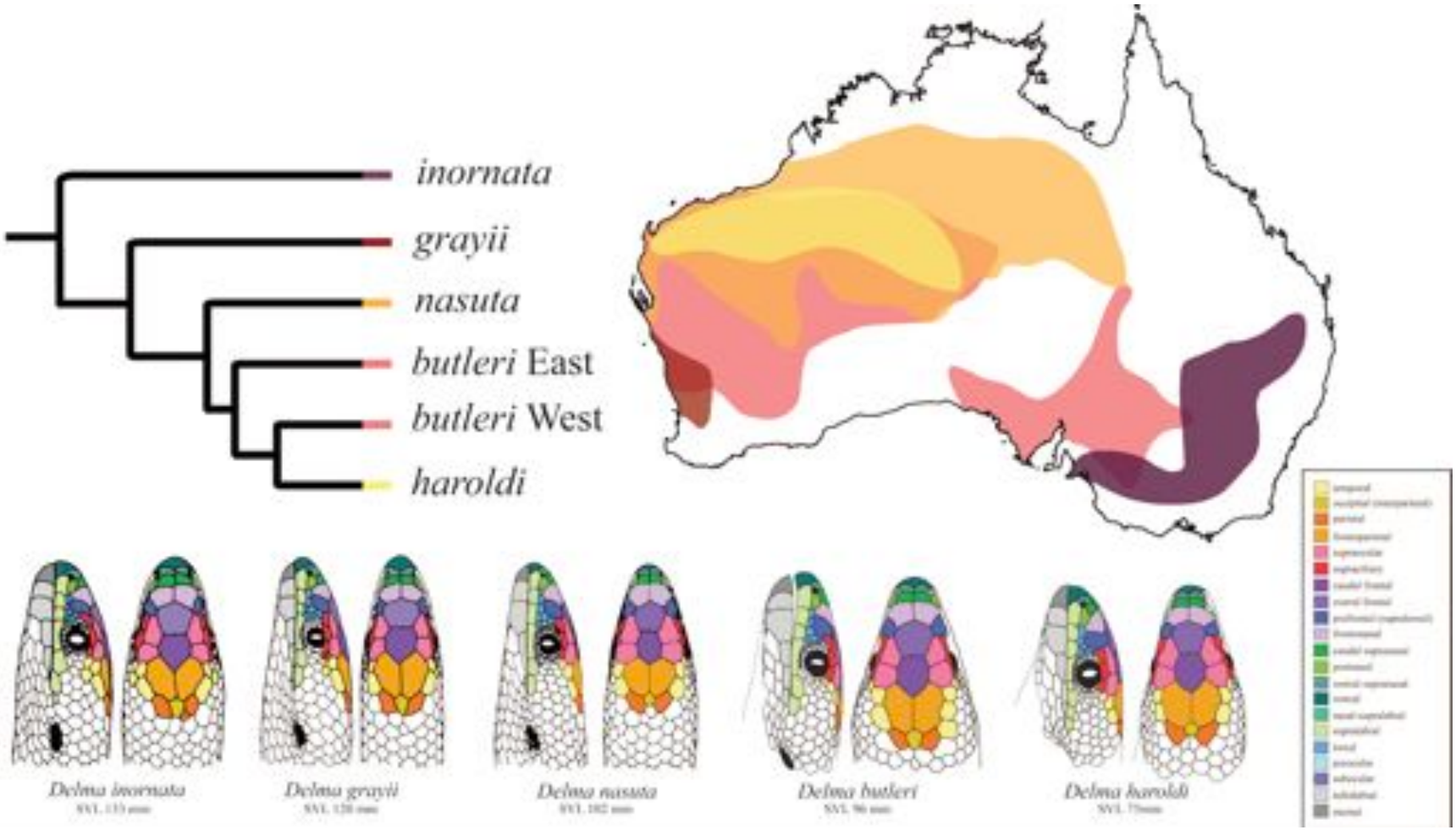

Fig. II.2. Simplified inter- and intraspecific relationships within the *Delma inornata* group (III.1E) as inferred from Bayesian topology of nDNA results, clade distributions, and lateral and dorsal head figures to show general scalation, head trends in shape, and maximum snout-vent length (SVL).

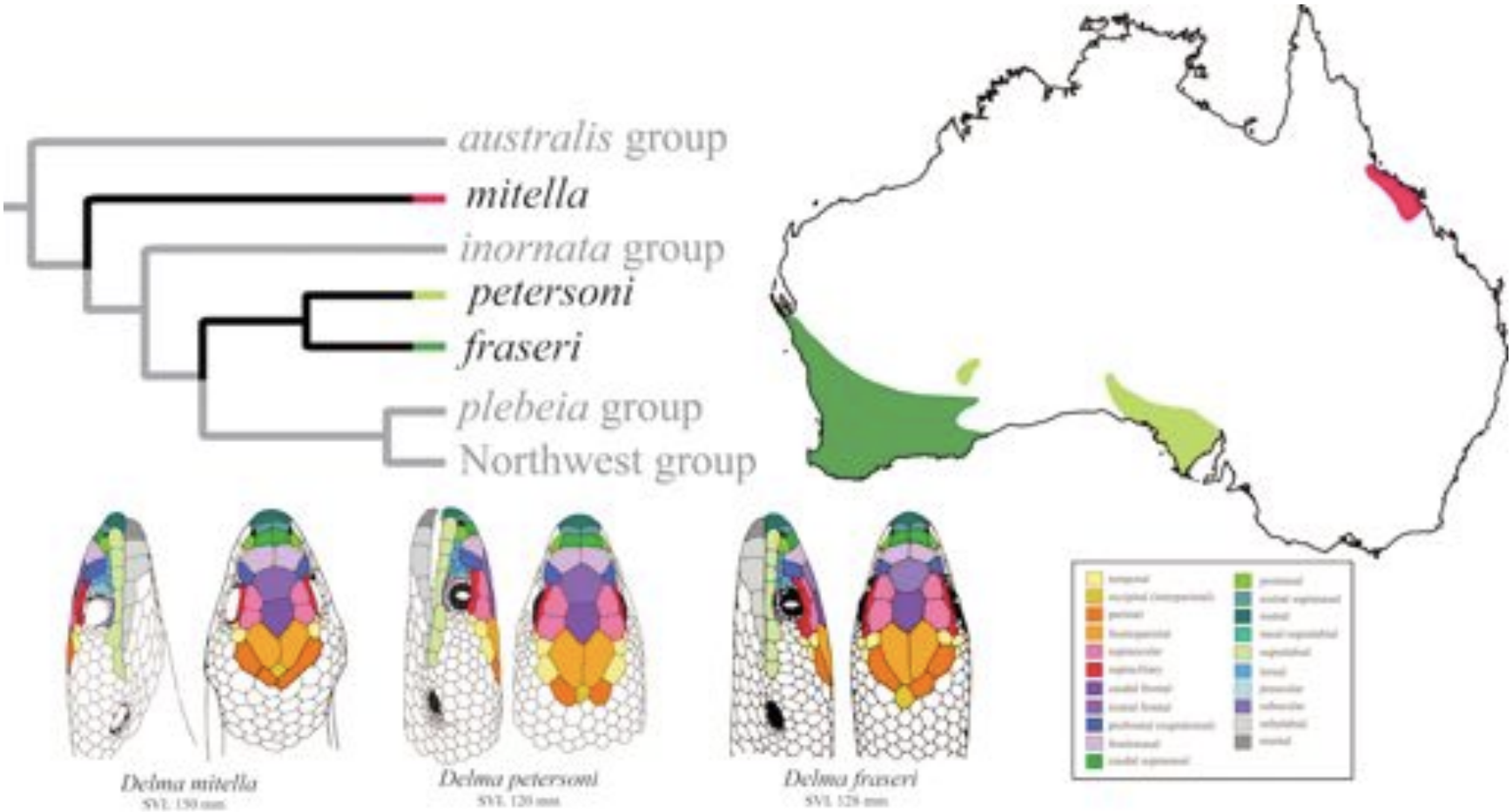

Fig. II.3. Simplified interspecific relationships within *Delma* highlighting the position of *mitella* (III.1D) and the *Delma fraseri* group (III.1F) as inferred from Bayesian topology of nDNA results, clade distributions, and lateral and dorsal head figures to show general scalation, head trends in shape, and maximum snout-vent length (SVL).

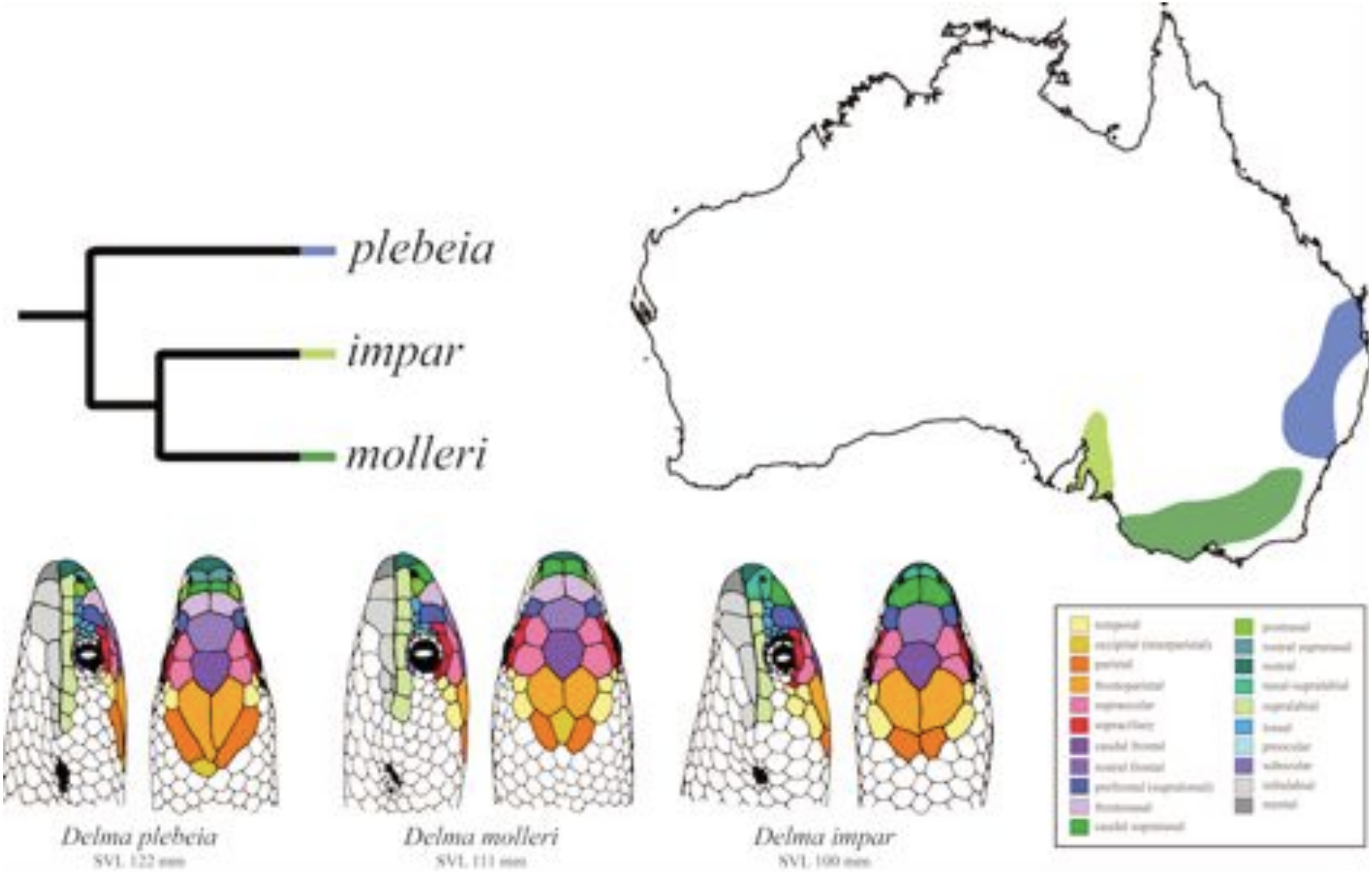

Fig. II.4. Simplified interspecific relationships within the *plebeian* group (III.1G) as inferred from Bayesian/Maximum likelihood topology of nDNA results, clade distributions, and lateral and dorsal head figures to show general scalation, head trends in shape, and maximum snout-vent length (SVL).

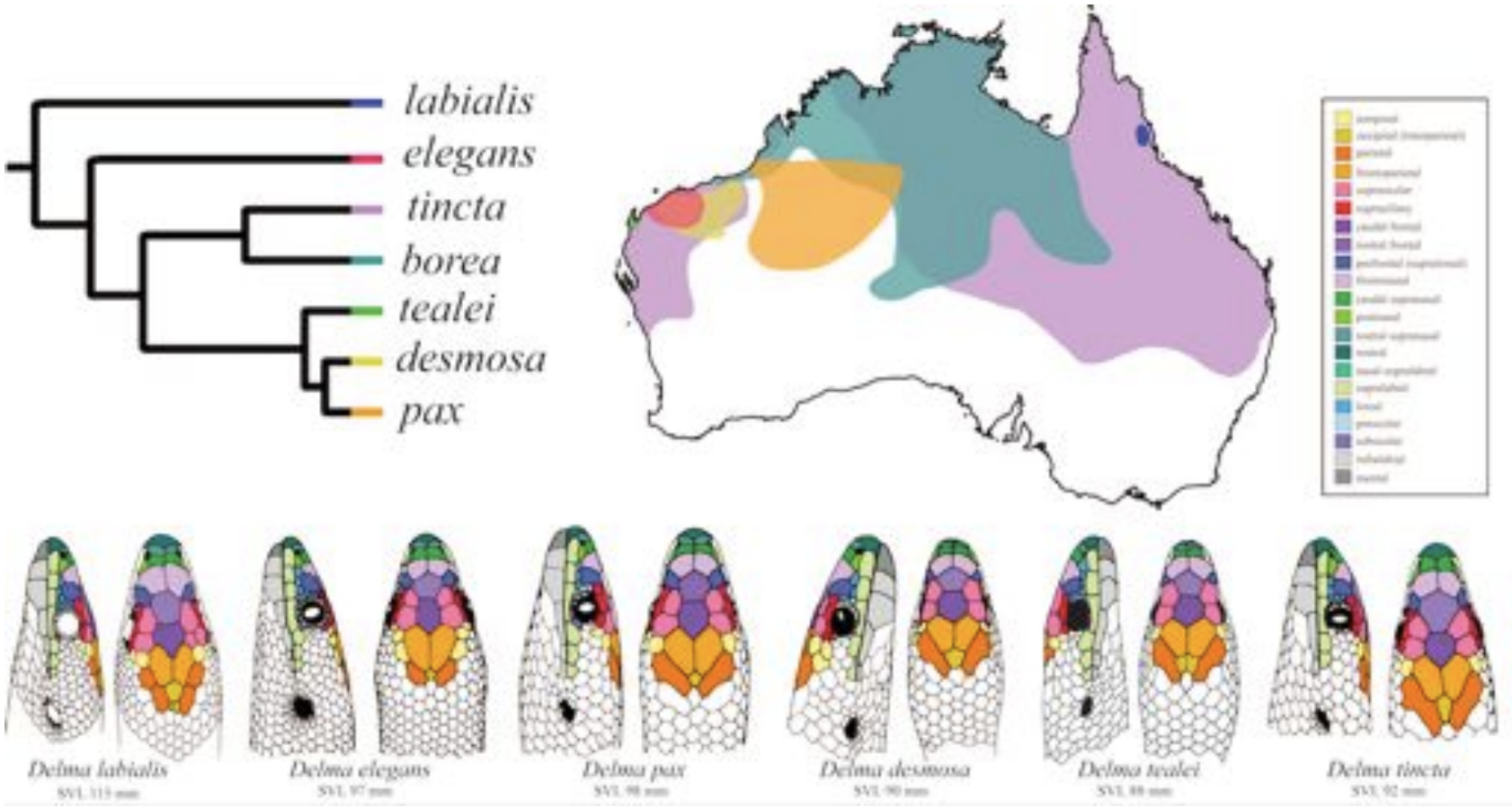

Fig. II.5. Simplified interspecific relationships within the Northwest group (III.1H) as inferred from Bayesian/Maximum likelihood topology of nDNA results, clade distributions, and lateral and dorsal head figures to show general scalation, head trends in shape, and maximum snout-vent length (SVL).

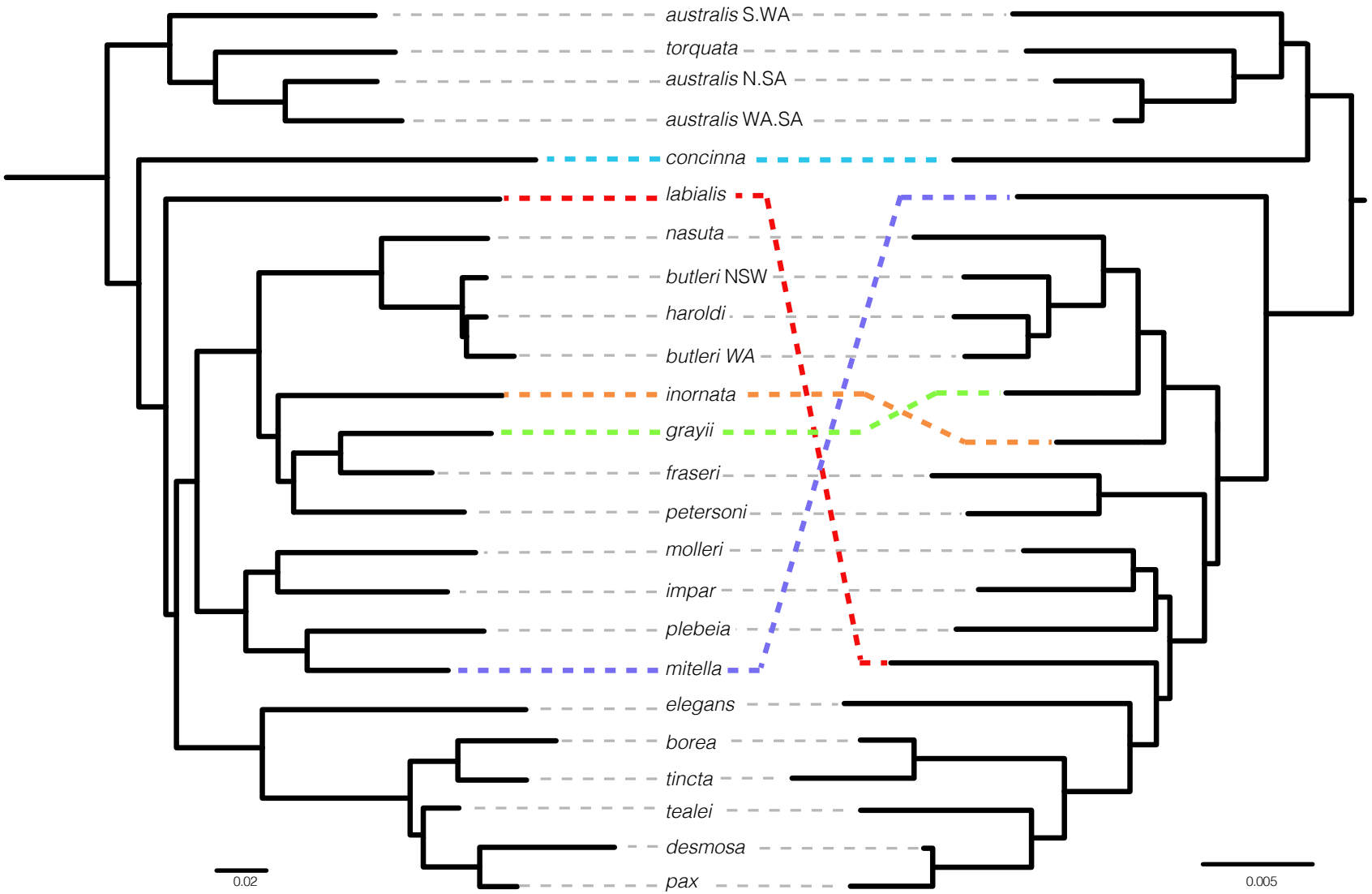

Fig. III.4. Comparison of phylogenetic relationships between mtDNA (L) and nDNA (R) datasets. Grey dotted lines indicate interspecific relationships maintained across both datasets, colored dotted lines indicate interspecific relationships which differ between datasetsm potentially as the result of mtDNA introgression events.

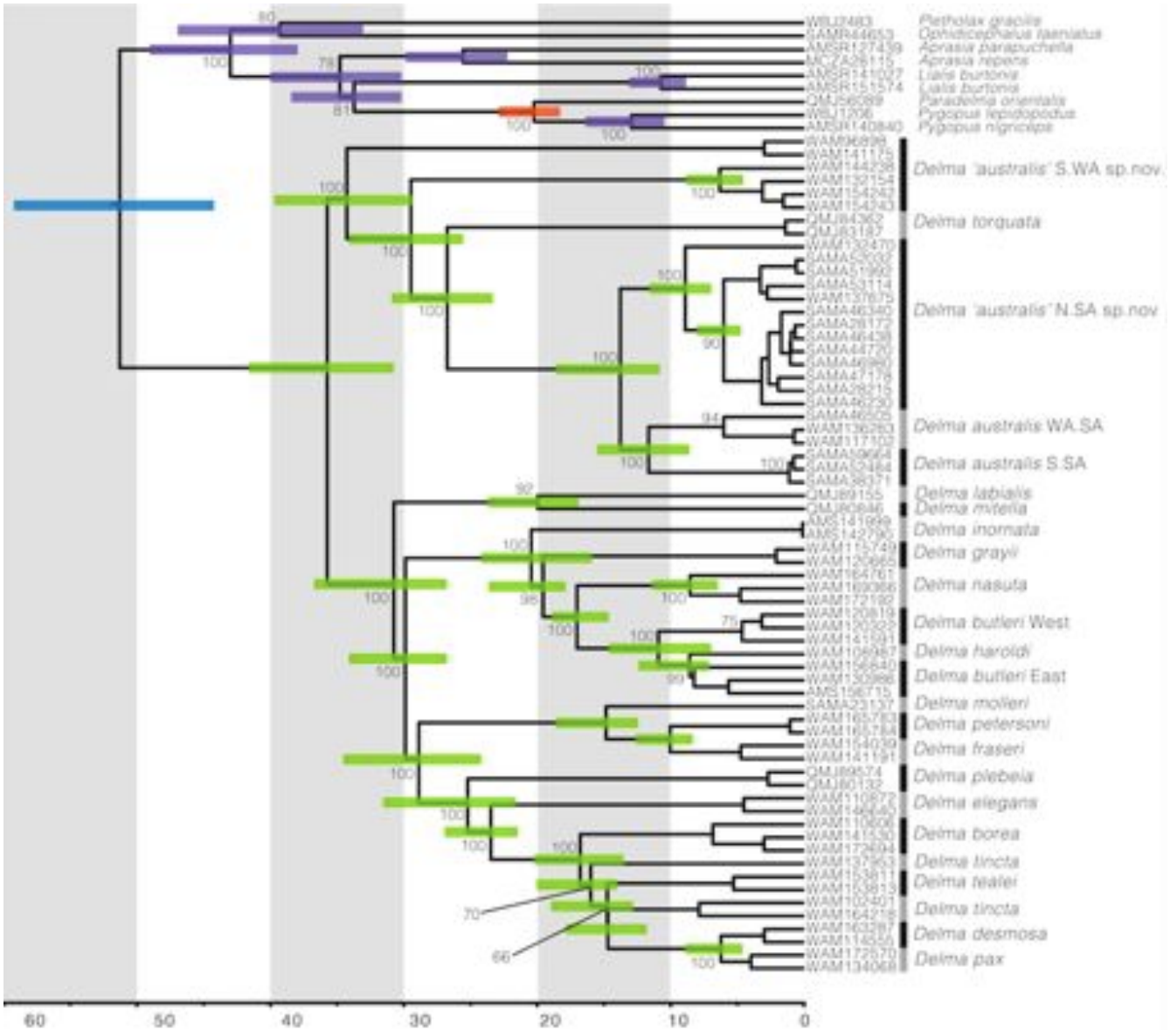

Figure III.5. Bayesian time-tree of divergence dates among Pygopodidae, inferred from the concatenated nuclear dataset (DYNLL1, MXRA5, RAG1, C-mos). Node bars represent 95% credibility intervals, green bars designating the ingroup taxa *Delma*, purple representing outgroup Pygopodids, blue—the crown split of Pygopodids, and orange bar indicating confidence interval for the split between *Paradelma* and *Pygopus*, where we placed the *Pygopus hortulanus* fossil calibration point. Intraspecific confidence intervals have been removed except from deeply divergent lineages .

III.v—Discussion

While current theory suggests an understanding of individual gene-tree discordance generally as the result of: incomplete lineage sorting (ILS), horizontal gene transfer (including hybridization), and gene duplication and extinction (Maddison, 1997; McGuire et al., 2007);

rectifying incongruence between mitochondrial and nuclear information remains difficult. Instances of mito-nuclear discordance are most often recognized in events of recent conflict and are commonly attributed to sex-biased dispersal, and selection (Toews and Brelsford, 2012). Male-biased dispersal is evident via a restriction in mtDNA gene flow between populations relative to nDNA, due to natal philopatry. Conversely, female-biased dispersal results in broad, shallow mtDNA divergences relative to nDNA—neither of which are apparent in the *Delma* results. Discord may also arise as a result of selection

Instead, we find similar to other groups such as *Sceloporus* (Leaché, 2009, 2010), Cordylidae (Stanley et al., 2011), *Thomomys* (Belfiore et al., 2008), and Neoaves (Poe and Chubb, 2004), difficulty associated with resolving some interspecific relationships among *Delma* may be the result of rapid radiation, and subsequent introgression events. Our BEAST analysis of pygopodids—consistent within *Delma*—corroborate Jennings et al.'s (2003) findings of two bursts in speciation rates between 27–30 MYA, and again 10–23 MYA. Rapid molecular diversification as the result of movement bias via sex-based dispersal, or directional selection such as a selective sweep (Rato et al., 2011; Rato et al., 2010) or sexual selection (Panhuis et al., 2001) can confound results when ancestral polymorphism is conserved by independent and conflicting gene trees (Belfiore et al., 2008; Maddison, 1997). These problems are exacerbated when branches are short and wide, suggesting short generations with relatively large effective population size (Maddison, 1997). While increased sampling across and within species may help to assuage the issues associated with rapid increases in speciation rates by providing greater phylogenetic resolution via a broader picture of genetic diversity, a basic violation of the molecular clock remains. Clock-like evolutionary rates may speed up (directional selection) or slow down (stabilizing selection) depending upon external pressures, requiring careful investigation and application of appropriate evolutionary models (Lemmon and Moriarty, 2004).

Concordant phylogenetic relationships

Despite broadly distributed incongruence between mtDNA and nDNA topologies, several areas of strong agreement remain across these datasets. Relationships within the *australis* group (exclusive of *concinna*) are retained with high support, further necessitating a comprehensive assessment of the genus. Not only do we recognize a cryptic south WA group found paraphyletic to the true *australis—torquata* group, but we identify a significant divergence between northern SA and WA/southern SA forms of *australis*, with populational substructuring within the SA/WA group. nDNA and mtDNA agree on monophyly of the species-rich, morphologically similar NWA group, which also exhibit instances of para- and polyphyly in at least two recognized taxa—*borea* and *tincta*. The monophyly of the *butleri, haroldi, nasuta* group remains supported, however, further study may elucidate the apparently complex *butleri—haroldi* relationship.

Discordant phylogenetic relationships

Our molecular sampling comprises all currently recognized species of *Delma*, as well as broad intraspecific sampling across known geographic ranges of most species. Whereas discordance between trees of explosive radiations often results in a number of poorly supported branches—a phylogenetic comb, bush, or polytomy (Kelly et al., 2009; Poe and Chubb, 2004; Stanley et al., 2011)—ours encompasses clades which receive strong, conflicting support across mitochondrial and nuclear datasets, à la Leaché (2010). A quick glance through the literature would suggest that conflict between mitochondrial and nuclear signal (mito-nuclear discordance) is relatively rare. A recent review (Toews and Brelsford, 2012) however, compiled 126 recent cases in animal systems in which there is strong discordance between the two datasets. When these situations arise, it can be difficult to tease apart the specific cause of such incongruity. So, if provided two strongly supported, yet conflicting phylogenies, trouble comes when we are

forced to decide which is the most accurate representation of the true evolutionary history of the group.

Selecting the tree which best exemplifies the accurate historical relationships first requires identifying and assessing the underlying cause of mito-nuclear discordance. Introgression at a fine scale should result in an observable biogeographic pattern—recognizable as distinct nDNA haplotypes at farthest points of the geographic range, with a cline working towards a hybrid contact zone in between. In contrast, ILS could be visualized as a random distribution of common haplotypes across geographic ranges of both species. Although it is easier to positively identify introgression, ILS is less conspicuous—and more difficult to discount.

Differences in the biology and evolution of mitochondrial and nuclear markers make them useful for different studies (Fisher-Reid and Wiens, 2011; Kubatko et al., 2011; Leaché, 2009; Leaché and McGuire, 2006). Brown et al. (1979) intimate the rapid mutation rate of the mitochondrial genome may accelerate the evolutionary rate of mitochondrial DNA to up to ten times that of nuclear DNA, and suggest mtDNA may be useful for determining fine-scale evolutionary relationships. Ballard and Whitlock (2004) and Moriyama and Powell (1997) suggest a more modest evaluation that mitochondrial genes have synonymous substitution rates 4.5–9.0 time higher than average nuclear genes, and 1.7–3.4 times higher than the fastest nuclear genes. Faster evolutionary rates make mitochondrial genes particularly useful for inferring species-level relationships. Conversely, because of slower evolutionary rates, nuclear genes are often more informative for deeper divergences, because they avoid mutational saturation. The circular nature, linked genes, lack of recombination and maternal inheritance of mitochondrial DNA limits the utility mtDNA in answering questions regarding population genetics. The dual ancestry of nNDA makes it exceedingly useful in questions of phylogeography and intraspecific

variation (Portik et al., 2011; Wood Jr et al., 2012). Leaché (2010) among others, electively devalues the informativeness of mtDNA in his study of *Sceloporus* largely because of the origin of mitochondrial markers as a single locus. They argue the benefit of numerous unlinked nuclear loci with differing evolutionary rates and histories—which all support a single species-tree—is a more favorable hypothesis.

As an exercise in identifying mitochondrial introgression at a fine scale, we picked the previously hypothesized sister-species *fraseri* and *grayii*—which are sympatric across the entirety of the range of *grayii*—and the *australis* species complex (including *torquata*). We sequenced all tissues of *fraseri* and *grayii* (n=63 *fraseri*, n=12 *grayii*, total n=75 individuals) available from the Western Australian Museum (WAM), as well as the hypothesized closest sister species *petersoni* (n=3)—which was previously treated as a subspecies of *fraseri*. We also sequenced 69 individuals of the *australis* group (including *torquata* n=3). Despite sympatry over substantial geographic distance, and documented syntopy (Jennings et al., 2003), *fraseri*, *grayii*, and *petersoni* all remained reciprocally monophyletic with no shared haplotypes between species, suggesting no recent introgression events. However, incongruity with the nuclear dataset, and well supported sister relationships between *fraseri* and *petersoni* instead suggest an older hybridization event between *fraseri* and *grayii*, which succeeded the split of *fraseri* and *petersoni*, and is not visible on the phylogeographic level. Mitochondrial introgression between these two sympatric species has subsequently been obfuscated by the rapid mitochondrial mutation rate and divergent evolutionary lineages, all the while remaining similar enough to retain phylogenetic signal. Conversely, the slower nDNA evolutionary rate has preserved the accurate historical relationships between these species. Additionally, relationships within this group are obscured further by another potential hybridization event between *molleri* and *impar*, which are currently separated by a narrow distance in SA—and may recently have been

sympatric. Results of our investigation into hybridization events and gene flow within the *australis* group are presented in the subsequent chapter *Molecular and morphological evaluation of* Delma australis *(Squamata: Pygopodidae) with descriptions of two new species from biogeographically significant areas in Western Australia*.

The nail in the coffin for most studies dealing with mito-nuclear discordance however, is non-monophyly of species in the mtDNA tree. Shared mitochondrial haplotypes (see: *Sceloporus clarkii* and *S. maculata* in Barrow et al. 2014, *Crotaphytus reticulatus* and *C. bicinctores* in McGuire et al. 2007) highlight instances of recent hybridization between these species, potentially as the result of recent range expansions. However, owing to the rapid mutational rate of the mitochondrial genome, ancient hybridization events—deep introgression—are far more difficult to address. In this case, instances of introgression may be embedded deep in the tree, and made inconspicuous by millions of years of mtDNA evolution and strong support of reciprocal monophyly of a given taxa, apparent only as strong mito-nuclear discordance. Stanley et al. (2011) represents a strong example of this conflict, as seven of the nine cordylid lineages are the result of a rapid, poorly supported radiation. The reciprocal monophyly of species or, at minimum populations, in both mtDNA and nDNA genealogies within *Delma* suggests the hybridization events which caused these instances of mitochondrial introgression were not recent.

Speciation in an Aridifying Landscape

The decision to accept the relationships within *Delma* as resolved by nDNA is validated by morphological and biogeographic evidence. Several phylogenetic similarities (*australis—concinna*, *molleri—fraseri*) exist between our nDNA topology and Kluge's (1976) morphological assessment. Acceptance of the mtDNA topology for *Delma* is largely the result of a previously uninformative nuclear dataset. However, interspecific relationships as inferred by

nDNA are unsurprising when viewed in light of general morphology. Species of the *fraseri* clade are large, thick-bodied delmas, with long tails, and considerable facial and nuchal banding which decreases in intensity with age. The sister group relationship between the *plebeia* and NWA clades is similarly appealing. Despite substantially smaller size, NWA species exhibit varying degrees of head, nuchal, labial, and mental banding, similar in appearance to juveniles of the *plebeia* and *fraseri* groups. Considerably smaller adult size, yet retention of juvenile coloration, suggests the possibility of some degree of paedomorphism within the NWA clade—however this hypothesis would require substantial morphological and osteological assessment to validate. In contrast, members of the *inornata* clade (*inornata, grayii, nasuta, butleri, haroldi*—Fig. II.2) are larger and have longer, sharper snouts, and as a rule, lack the broad prominent banding of the previous group—as suggested by the common names patternless delma (*inornata*), unbanded delma *butleri,* and sharp-snouted delma (*nasuta*).

In addition to morphological cues, repeated support for the provided nDNA topology by multiple independent nuclear loci lends high credibility to instances of mitochondrial introgression within *Delma*. Supporting this belief, hypothesized instances of mitochondrial introgression as the result of hybridization appear in sympatric or contemporaneously geographically near species, and not in geographically separated species as might imply ILS. Speciation patterns and divergence dates within *Delma* as inferred by nDNA are highly concordant with the proliferation of other arid biota as Australia dried out in the Late Miocene 20–6 Mya (Byrne et al., 2008).

The absence of pygopodids from closed-forest systems and abundance in arid and semi-arid regions across Australia suggest a distinct drought tolerance similarly found across a number of native Australian lineages. The rapid uptick in species divergence events apparent between 20–6 Mya coincides with increased aridification and expanding xeric habitat across the

continent. Although it is difficult to assess if aridification caused allopatry of populations associated with suitable habitat, resulting in speciation, *or* if the expanse of arid biomes opened new ranges and niches for pygopodids, causing speciation events; current distributions throughout xeric habitat suggests *Delma* were able to rapidly adapt to the changing landscape as mesic environments shrank. Despite a strong association with drought-tolerance, *Delma* have habitat requirements which do not agree with the extremely arid dunefields and deserts of Australia. *Delma* species appear to be strongly associated with *Triodia* spinifex, tussock grass, and related dense, low vegetation. The the paucity of *Delma* records from hyper-arid regions such as Channel Country, Gibson Desert, Little Simpson Desert, Nullarbor Plain, and the Simpson Strzelecki Dunefields coincides with the lack of suitable habitat and groundcover (Pianka, 1969, 2010; Wilson and Swan, 2013). As an effect of desertification, important corridors between more optimal habitat may have mediated dispersal events, particularly in species with broadly distributed, disjunct ranges—e.g. *butleri*, *tincta* (Cracraft, 1986) (fig. III.6). These events have been documented in fairy-wrens (Driskell et al., 2003; Ford, 1987; Schodde and Weatherly, 1982) as well as in the squamates *Ctenophorous scutulatus, Egernia depressa, Ctenotus leonhardii*, and *Eremiascincus richardsonii* (Pianka, 1972). Additionally, speciation as a result of isolation by distance and allopatry, via corridor-mediated dispersal has been suggested as the most likely scenario for another Australian squamate group *Tympanocryptis* (Shoo et al., 2008). As these corridors were largely temporally restricted, they served as a collapsing bridge to suitable habitat, however remain difficult to accurately date.

Because of the generalist habits—both dietary and habitat preferences—of most delmas, identifying direct causes of speciation events is difficult. The rapid radiation of species richness within this group is most likely the result of considerable expansion of xeric biomes, but may also be attributable to rapid growth and subsequent shrink of mesic and rainforest habitats 6–2.5

Mya. Proliferation of temperate biomes and closed forest systems in this period may have reduced or fractured available habitat, resulting in allopatric divergence events. Upon succeeding reduction of this mesic Pleistocene expansion, the potential for secondary contact between previously separated species may have caused the mitochondrial reticulations we see in *Delma* today.

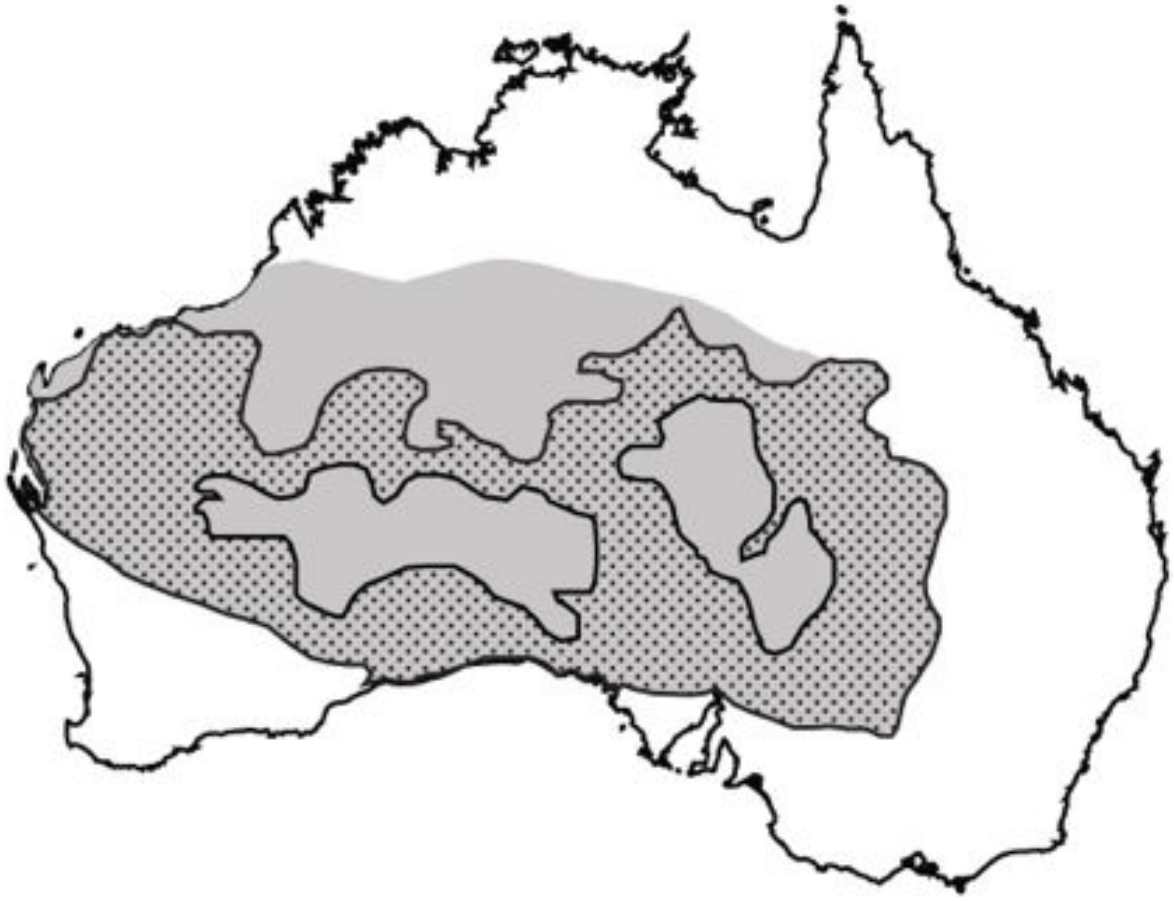

Figure III.6. Map of Australia showing the current extent of the arid zone in grey, and potential historical corridors (dotted area) between more favorable habitat. The northern connection is the Giles Corridor, which connected eastern Mulga scrub to the Pilbara region. The southern stretch is the Nullarbor Plain Corridor which linked east and west Mulga scrub habitats.

Although this paper represents the most comprehensive sampling of *Delma* to date, my findings illicit a number of questions which should be further addressed for greater understanding of pygopodids, as well as more broadly for Australian biogeography. The broad geographical distributions of a number of *Delma* species require greater sampling to better

answer questions of phylo- and biogeographic patterns. Additionally, species with large ranges and recognizable geographic phenotypic variation may hide cryptic species awaiting discovery. Similarly, these questions should also be applied to other pygopodids, particularly the genus *Aprasia*—another moderately species rich, morphologically conserved genus—to investigate instances of mitochondrial introgression and hybridization.

Revising intergeneric relationships within Pygopodidae

Despite morphological (Hutchinson, 1997; Jennings et al., 2003; Kluge, 1976; Wells, 2007) and molecular (Jennings et al., 2003; Oliver, 2009) assessments of relationships within the Pygopodidae, no single, well supported relationship has been suggested. Based on generalist habits, dentition, and osteology some suggested both *Delma* and *Pygopous* to fill the ancestral pygopodid state (Hutchinson, 1997; Kluge, 1976; Shea, 1990). Similarly, fossorial pygopodid genera have been lumped together (Kluge, 1976; Wells, 2007), however, we now commonly recognize homoplasy of morphological characters of fossorial squamates (Daza and Bauer, In press). Although the mtDNA dataset is prone to saturation as such deep divergences, and does little to resolve these intergeneric relationships, nuclear DNA provides a well supported evolutionary history of pygopodids. Across both mtDNA and nDNA phylogenies however, *Delma* is unequivocally returned as the sister group to all other pygopodids. nDNA results suggest a sister group relationship between the monotypic shrub-swimming *Pletholax* and the fossorial *Ophidiocephalus*—both small, thin pygopodids restricted in range and habitat type. The sister genera relationship between *Paradelma* and *Pygopus* is well supported, as is their relationship to *Lialis*, suggesting the evolution of the large-bodied, short-tailed pygopodid occurred singly. These large-bodied pygopodids are next-closely related to the minute *Aprasia*, and distantly to the *Ophidiocephalus—Pletholax* group. Although this assessment of the

relationships between genera within Pygopodidae appears well supported, I acknowledge this remains a work-in-progress, and requires more data to confidently defend these relationships.

Revising interspecific relationships within Delma

This study represents the only investigation of pygopodid relationships to date to include a multilocus nuclear dataset in attempt to resolve the phylogenetic affinities of the genus *Delma*. Our results show strong mito-nuclear discordance, suggesting a number of deep hybridization events within this genus. However, we are able to identify a number of deeply divergent species groups, as well as resolve the status of most interspecific relationships. The broadly distributed *D. australis* group (Fig. II.1, III.1–C) is unequivocally supported as the sister group to all other *Delma* species (Fig. III.1). Deep, geographically associated divergences within this group are discussed in the following chapter. The *inornata* clade (Fig. II.2, III.1–E) represents another widely geographically distributed group, which are characterized by comparatively elongate, narrow head and snout, and small parietal scales. The *inornata* group lack the wide, strong head and nuchal banding which characterizes the *plebeia* and Northwest groups. The widely separated basal members *grayii* and *inornata* suggest a once wider distribution for ancestral members of this group. Additionally, disjunct populations of *butleri* are broadly separated by the hyperarid center of Australia across the Simpson Strzelecki Dunefields, Stony Plains, Great Victoria Desert, Finke, MacDonnell Ranges, and Nullarbor bioregions—most likely due to recent (<10 Mya) aridification. The relatively young age of this split is reflected in the inability of nDNA to accurately resolve relationships between East and West populations of *butleri*, and *haroldi*. The range of *Delma nasuta* extends from Shark Bay in Western Australia, across the northern portion of the continent and into western Queensland, exhibits a substantial amount of variation across

its distribution in WA. Further investigation of genetic diversity of individuals from across the broad range of *D. nasuta* may provide interesting results.

In contrast to the narrow-snouted largely patternless individuals of the *inornata* clade, members of the *fraseri* (Fig. II.3, III.1–F), *plebeia* (Fig. II.4, III.1–G) and Northwest (Fig. II.5, III.1–H) clades generally exhibit strong nuchal, head, and labial banding, similar to that of juvenile *Pseudonaja* spp. While banding diminishes with ontogenetic changes in some species, smaller species (*desmosa, borea, elegans*) retain this patterning into adulthood. Members of the *fraseri* (F) *plebeia* clades (G) occur across the southern and western portions of the continent, stretching from eastern SA to Shark Bay in WA. Relationships within clades F and G intimate an East to West dispersal of these species groups. A relictual population of *petersoni* in WA suggests isolation as a result of aridification in the Nullarbor and Hampton bioregions. The similarly patterned, however smaller individuals of the Northwest (H) clade represent a monophyletic group with largely unresolved intraspecific relationships. Basal-most members of this clade, *elegans* and *labialis* are widely separated geographically, suggesting a broad ancestral distribution for this group. Species richness within the Northwest group peaks in the Pilbara and western Kimberley regions, with a number of sympatric species overlapping in ranges. Morphological similarity within the Northwest group is highlighted by strong nuchal and head banding, particularly in juveniles, long, shield-like parietal scales, and small adult size. Members of group G, superficially resemble members of the *fraseri* clade in large adult size, stoutness of body, and head and labial banding. Based on current distributions of basal members of clades F and G in eastern and southern Australia, and a general East-West pattern of diversification, we hypothesize an eastern origin for the crown of clades F, G, and H. This most recent common ancestor of these groups most likely shared the relatively large, stout body, and strongly patterned head found among basal members of these groups.

Beyond the positions of *D. labialis* and *elegans* at the base of clade H, remaining interspecific relationships within the Northwest group remain difficult to resolve. There is strong support (BPP/BSS 100) for the monophyly of the species *plebeia, elegans, borea, tealei,* and *pax*. The monophyly of a group comprising *D. tincta*, *borea, tealei, desmosa*, and *pax* is also highly supported (BPP/BSS 100) however, with the exception of the sister-taxon relationship between *D. desmosa* and *pax* (BPP/BSS 100), relationships within this group are mostly unsupported. Further investigation is necessary to accurately resolve interspecific relationships within the Northwest group, as well as intraspecific divergence within the broadly distributed species *D. tincta* and *borea*.

The Queensland endemic species *D. mitella* forms a distinct lineage, sister taxon to all remaining delmas save the *australis* group. As the largest member of the genus, *mitella* may represent the ancestral condition for the clade of delmas which represent the sister group to the *australis* group—larger, stouter bodies, with moderate banding and longer snouts.

Not only does this study represent the first multilocus nuclear assessment of interspecific relationships with the genus *Delma*, perhaps more importantly, it highlights the necessity of recognizing the potential for independent evolutionary histories of mtDNA and nDNA data. The strongly discordant mitochondrial and nuclear topologies we present for *Delma* underscore the substantial morphological conservatism of this genus, and acknowledge instances of hybridization between divergent species. Pygopodids represent a uniquely Australian lineage of limbless squamates, rich in ecological diversity. Further investigation of broadly distributed *Delma* species, as well as other pygopodids, may continue to yield insight into patterns of speciation within Australian squamates, and extend our understanding of Australian fauna as a whole.

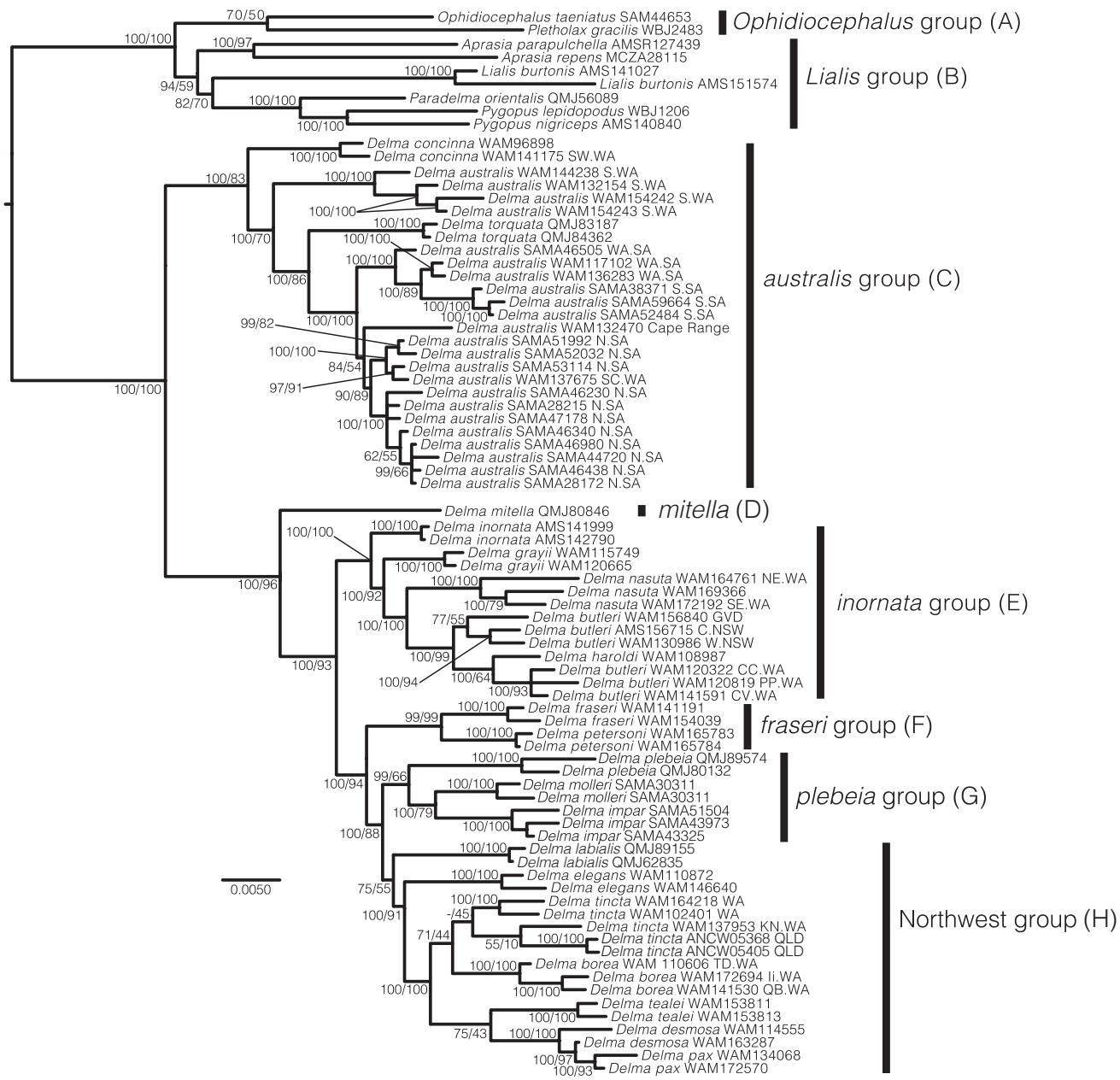

Figure III.1. Preferred phylogeny of relationships within Pygopodidae based on Bayesian inference as inferred by a concatenated nuclear dataset (DYNLL1, MXRA5, RAG1, C-mos). Maximum likelihood bootstrap (BSS) and Bayesian posterior probabilities (BPP) support values are indicated at each node (BPP/BSS).

IV. Molecular and morphological evaluation of *Delma australis* (Squamata: Pygopodidae) with descriptions of two new species from biogeographically significant areas in Western Australia

Brad Maryan, Ian G. Brennan, Paul M. Oliver, Mark Adams, Aaron M. Bauer

IV.i—Abstract

The Australian pygopodid genus *Delma* is characterized by morphologically conservative but genetically divergent lineages and species. Recent analysis of morphological and molecular variation has revealed that two undescribed species presently classified under *Delma australis* Kluge, 1974. *Delma australis* as redescribed is monophyletic across its broad southern Australian distribution, with deep genetic divergence between geographic clades, and considerable intraspecific geographic variation in aspects of head pattern. A closely related, morphologically similar, new species—*Delma australis* S.WA sp. nov.—is described from proteaceous scrub and mallee heaths on sandplain of southern Western Australia. A second new species—*Delma australis* N.SA sp. nov., known from its central and northern South Australia range as well as a single specimen from the dissected limestone plateau of Cape Range on the North West Cape Peninsula, an isolated southern Western Australia population, and a Shark Bay population. Both new species are diagnosed from all other described *Delma* species including regional populations of *D. australis* from WA, SA, and NSW, by a combination of molecular topology, morphometric attributes, scalation, and subtle details of pattern and coloration. Based on phylogenetic affinities and shared morphologies, a *D. australis* species group is proposed to accommodate *D. australis*, *D. concinna* and the two new species described herein. The addition of another two new vertebrate species from these biogeographically significant areas, and especially the southwestern Australian biodiversity hotspot, underlines our paucity of understanding of regional endemism and evolutionary histories in Australian squamates.

IV.ii—Introduction

There are currently 44 described species of pygopodid gecko known from Australia and New Guinea (Cogger, 2014; Uetz and Hošek, 2014; Wilson and Swan, 2013). Of these, *Delma* Gray, 1831 is the most diverse with 21 species, eight of which—including *D. australis*—were described in a comprehensive taxonomic revision by Kluge (1974). Since this revision, several additional species and subspecies have been described (Jennings et al., 2003; Maryan et al., 2007; Shea 1987, 1991; Storr 1987) and a phylogenetic study of pygopodid geckos has also made significant changes (Jennings et al. 2003). However, as indicated by Shea (1987) and Aplin and Smith (2001), our knowledge of the taxonomy of the morphologically conservative genus *Delma* is far from complete.

One species, *D. australis*, is widespread throughout southern Australia inhabiting a variety of habitats (Kluge 1974; Ehmann 1992; Wilson and Swan 2013). Geographic variation in intensity of head patterning represents the most apparent morphological diversity within *australis* (Aplin and Smith, 2001; Kluge, 1974; Shea, 1991). In comparison to other *Delma* species, *australis* is morphologically unique in possessing; small maximum adult size (88 mm SVL), robust build, blunt snout and short tail (Wilson and Knowles 1988; Wilson and Swan 2013). *Delma torquata* of southeastern Queensland shares a similar morphology and has been allied with *australis* in a previous molecular phylogenetic study (Jennings et al., 2003). *Delma (Aclys) concinna* is a small, particularly slender delma, with a distinctive long pointed head and rostrum, found only in Western Australia, north of Perth as far as Shark Bay. Given considerable geographic variation in *D. australis*, and suggestions it may represent a complex of species (Kluge, 1974; Wilson and Swan, 2013), a taxonomic assessment of this species is warranted.

This paper presents the results of a combined molecular and morphological assessment of *D. australis* throughout its range. We validate previous suspicions and provisional recognition

(Aplin and Smith, 2001; Kluge, 1974; Storr et al., 1990) of a southwest Western Australian *australis*-morph, and a cryptic northern South Australia form, as undescribed species, which herein we diagnose and name.

IV.iii—Materials and Methods

Morphological analysis

We examined all specimens of *D. australis* from Western Australia and South Australia held in the Western Australian Museum, Perth (WAM) and South Australian Museum, Adelaide (SAM). We collected general morphology and morphometric data from a subset of these, which were chosen based on specimen preservation quality, and genetic and geographic coverage. Seventy-nine *australis* specimens were assessed from across the species range (Fig. IV.2). Sex of individuals was determined by visual inspection of everted hemipenes in males, presence of eggs in heavily gravid females, or internal examination of gonads. Juveniles (SVL < 50 mm) were not sexed. Head scale terminology, linear measurements and meristic counts largely follow Storr *et al.* (1990) and Maryan *et al.* (2007), in contrast to Kluge (1974).

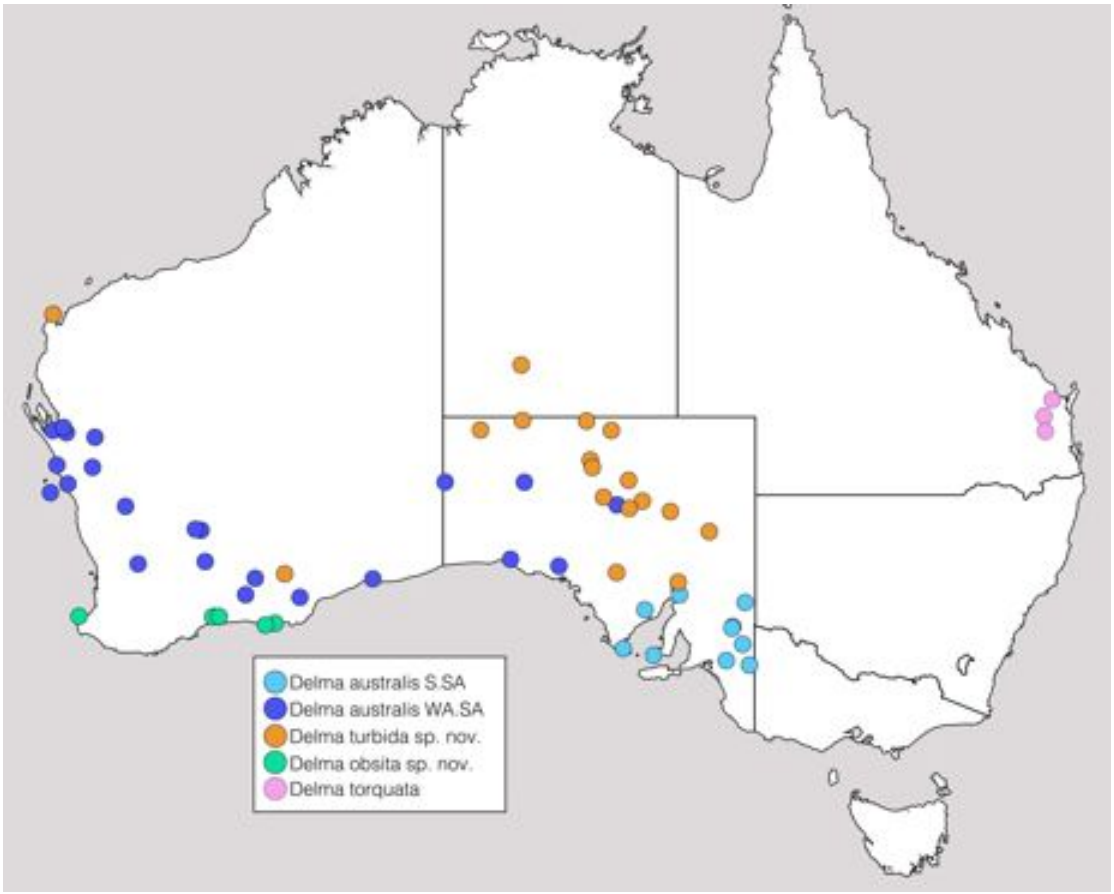

Figure IV.2. Sampling and geographic distributions of *Delma australis* group specimens present in this paper.

For morphological assessment, the following linear measurements were taken in millimeters (mm) using digital calipers; snout-vent length (SVL) measured from tip of snout to vent; tail length (TL) measured only on original tails—from vent to tip of original tail; head depth (HD) measured from a point immediately behind eye; head length (HL) measured from tip of snout to posterior margin of ear; head width (HW) measured from the widest point between ear; hindlimb length (HLL) measured from junction of limb flap with body to distal tip of flap; mouth length (ML) measured from tip of snout to oral rictus; rostral length (RL) measured from anterior to posterior point of rostral scale; rostral width (RW) measured from lateral extremes of rostral scale; snout length (SL) measured from tip of snout to anterior margin of eye and eye width (EW) measured from anterior to posterior extremes of transparent brille. Four meristic

counts were recorded; number of loreal scales (LS) counted between postnasal and circumocular granules; number of hindlimb scales (HLS) counted from distal extreme and origin with body; number of midbody scale rows (MSR) counted completely midway around body, and number of ventrals (VE) counted from immediately behind mental scale to vent.

Specimens preserved in a circular or twisted position were straightened on a flat surface when measured for snout-vent and tail length. Tails were not measured if they were recently broken or obviously regenerated, as suggested by a clear break in coloration. Accordingly, tail length is not used in any taxonomic sense and statistical information is provided for descriptive purposes only.

Molecular Methods and Phylogenetic Analyses

Genomic DNA was isolated from ethanol-preserved liver samples stored at -70ºC from the WAM and SAM, via Qiagen DNeasy Tissue Kit (Qiagen) following standard manufacturer's protocol . Mitochondrial (mtDNA) and nuclear (nDNA) loci were amplified by Polymerase chain reaction (PCR). Our molecular dataset consisted of two mitochondrial (16s, ND2) and four nuclear markers (RAG1, MXRA5, DYNLL1, C-mos), owing to increased resolution as a result multi-locus mito-nuclear datasets (Fisher-Reid and Wiens, 2011). Primers used for PCR amplification and sequencing are listed in Table I.2. Standard 25 µL PCR reactions utilized; dH_2O, 5x Taqmaster PCR enhancer, 10x PCR Buffer, dNTPs, forward and reverse primers, Taq polymerase, and genomic DNA, and were carried out on an Eppendorf Nexus gradient thermocycler. Thermocycler amplification programs followed a standard protocol with varying annealing temperatures, relative to the loci and primers; initial denaturation period (95°C, 2 min) followed by 34 cycles at 95°C (30 s), 48°C (35 s) annealing, and 72°C (150 s) extension. Amplified PCR products were visualized using 1.5% agarose electrophoresis, purified via Agencourt AMPure magnetic bead system (Agencourt Bioscience), and stored in a refrigerator at

4°C until sequenced. We preformed cycle sequencing via BigDye Terminator v3.1 Cycle Sequencing kit using purified PCR product as a template, and sequencing product was purified using Agencourt CleanSeq magnetic bead system (Agencourt Bioscience). Amplified product was sequenced in both forward and reverse directions using an ABI 3730 XL sequencer, to allow for identification of polymorphic sites.

All sequences were aligned by eye, and protein-coding loci were translated to amino acid sequence to maintain proper reading frame and avoid premature stop codons. tRNA secondary structure was addressed and aligned by eye for consistency. Mitochondrial genes were analyzed together because of shared evolutionary history as the result of physical linkage. Nuclear loci gave varied in degrees of support and rarely in topology, but did not exhibit strong conflict, and so were concatenated into a single dataset which produced a well supported evolutionary scenario. Final aligned mitochondrial and nuclear sequences were 2276 bp (16s–796, ND2–1480) and 3298 bp (DYNLL1–1056, MXRA5–793, RAG1–1071, Cmos–378) respectively. Congruence between mitochondrial and nuclear topologies allowed us to concatenate all molecular loci into a single mito-nuclear dataset which stretched 5574 bp. We used maximum likelihood (ML) and Bayesian inference (BI) methods to test for conflict between topologies and support values between analytical programs. ML and BI results returned largely concordant topologies, with comparable Bayesian posterior probability (BPP) and bootstrap support (BSS) values across all datasets. We used the Akaike Information Criterion in jModeltest 2 (Darriba et al., 2012; Guindon and Gascuel, 2003) to identify the most accurate models of evolution for each gene and codon position (see Table I.3).

We used RAxML 8.0 (Stamatakis, 2014) for ML analyses, and divided the mitochondrial dataset into three partitions; ND2, tRNA, and 16S; the nuclear dataset into four partitions; DYNLL1, MXRA5, RAG1, C-mos; and employed the GTR+I+Γ model of evolution. When

analyzed independently, individual loci were not partitioned by codon position because of RAxML's limits on evolutionary models, and were instead analyzed under GTR+I+Γ. Topology estimates used 100 independent tree searches, and 5000 bootstrap replicates to retrieve support values. Partitioning each locus by codon position (one vs. three partitions per) for mtDNA and nDNA did not disrupt topology nor change BSS support values.

BI analyses were performed using MrBayes 3.2 (Huelsenbeck and Ronquist, 2001b; Ronquist et al., 2012). The mitochondrial dataset was divided into six partitions; ND2, ND2 codons (1^{st}, 2^{nd}, 3^{rd}), tRNA, and 16S; and the nuclear dataset into 12 partitions—each gene receiving 4 partitions (whole locus, three codon positions). Three vs. six partitions for mtDNA and three vs. twelve partitions for nDNA returned identical topologies and did not significantly disrupt BSS support values. We executed two parallel (two heated and two cold chain) runs for 200 million generations sampled every 1000 generations, with sampling from the first 20 million generations discarded as burn-in.

IV.iv—Taxonomy

Delma Gray, 1831

Type Species

Delma fraseri Gray, 1831, by monotypy.

Diagnosis

Delma differs from all other pygopodid genera in possessing the following combination of characters: head scales, including the parietals, enlarged and symmetrical; anterior nasal scales nearly always in contact; nostril bordered by more than two scales (except in some *D. impar*); external ear opening large; usually fewer than 18 midbody scale rows; dorsal and ventral scales smooth; preanal pores absent; tail about three times as long as body.

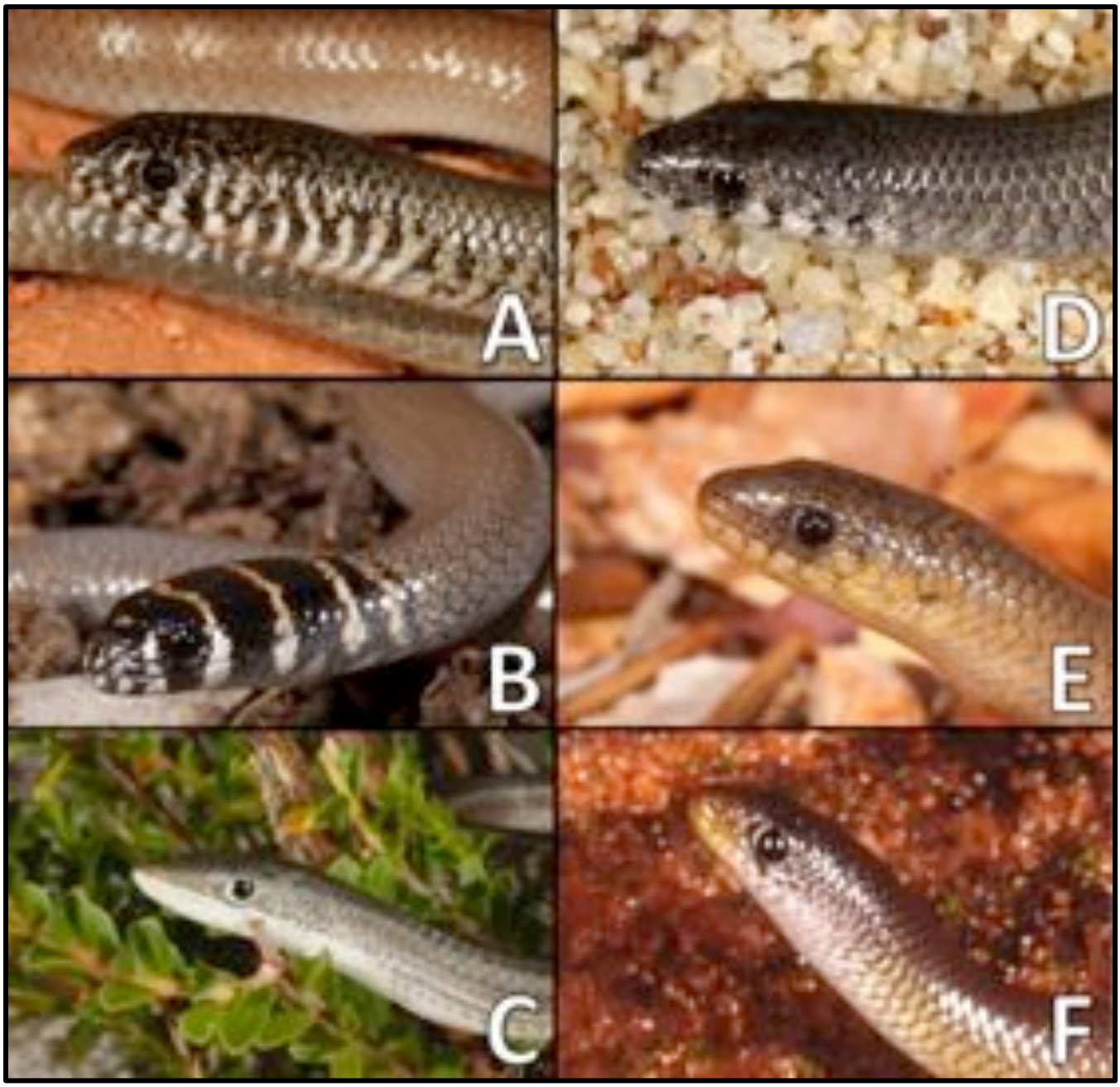

Figure IV.1. Photographs of *Delma australis* group species in life: A. *Delma australis,* South Australia. B. *Delma torquata*, Queenlsand. C. *Delma concinna*, Western Australia. D. *Delma australis* S.WA, Western Australia. E. *Delma australis* N.SA, South Australia. F. *Delma australis* N.SA, Shark Bay, Western Australia.

Content:

D. australis Kluge, 1974; *D. borea* Kluge, 1974; *D. butleri* Storr, 1987; *D. (Aclys) concinna* (2 subspecies) (Kluge, 1974; Storr, 1987); *D. desmosa* Maryan, Aplin and Adams, 2007; *D. elegans* Kluge, 1974; *D. fraseri* Gray, 1831; *D. grayii* Smith, 1849; *D. haroldi* Storr,

1987; *D. (Pseudodelma) impar* Fischer, 1882; *D. inornata* Kluge, 1974; *D. labialis* Shea, 1987; *D. mitella* Shea, 1987; *D. molleri* Lütken 1863; *D. nasuta* Kluge, 1974; *D. australis* S.WA sp. nov.; *D. pax* Kluge, 1974; *D. petersoni* Shea, 1991; *D. plebeia* De Vis, 1888; *D. australis* N.SA sp. nov.; *D. tealei* Maryan, Aplin and Adams, 2007; *D. tincta* De Vis, 1888; *D. torquata* Kluge, 1974.

Delma australis Species Group

Diagnosis

Based on the morphological and molecular analysis of Jennings et al. (2003) and this study we propose a *D. australis* species group, currently composed of *D. australis*, *D. australis* S.WA sp. nov., *D. australis* N.SA sp. nov. and *D. concinna*. Substantial morphological divergence of *concinna*, and its sister-taxon relationship to the rest of the group makes it difficult to diagnose this species group as a whole. Instead, the *australis* complex and *torquata* are diagnosable by the following characters in combination: small maximum adult size, relatively robust build, blunter snout, usually four loreal scales, four frontal scales, fourth supralabial almost always below orbit, 16–20 midbody scale rows, ventral body scales only marginally larger than adjacent lateral body scales, usually three preanal scales, and differs from *torquata* in separation of the frontonasal and prefrontal scales, and position of the occipital scale deeply situated between the parietals and frontoparietals. To date, all described hemipenes of pygopodids have been bi-lobed, we recognize a single-lobe hemipenial condition as a synapomorphy of the *australis* complex.

IV.v—*Delma australis* Kluge, 1974
Marble-faced Delma (Fig. IV.1A, IV.5)

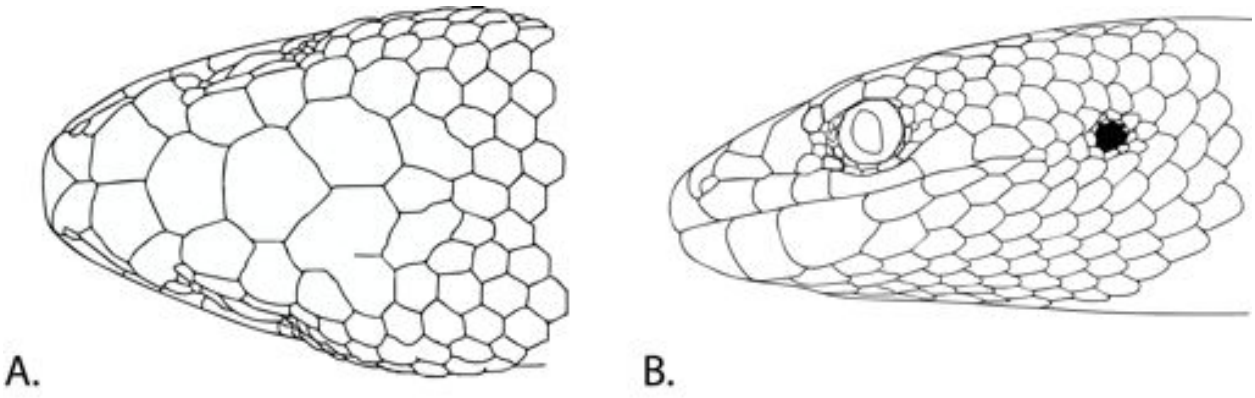

Figure IV.5. Head region of *Delma australis* holotype (WAM 27359). A. Dorsal view. B. Left Lateral view.

Material Examined

Holotype

Australia: *South Australia*: SAMR27359—male, Port Lincoln (34º44'S, 135º52'E) on 19 October 1966 by G.M. Storr.

Paratype

Australia: *South Australia*: SAMR24528—1 female, 37 km ENE of Wirrula (32º22'S, 134º54'E), (24528).

Additional Material

Australia: *Western Australia:* WAM: 12604 (male), Wagin (33º19'S, 117º21'E); 30706, 30749 (males), 12 km E of Fraser Range (32º02'S, 122º55'E); 36229 (female), Pine Hill (33º18'S, 123º23'E); 53461 (female), Newman Rock (32º07'S, 123º11'E); 57909 (male), 11.5 km NE of Charlina Rock (32º33'S, 123º26'E); 58045 (female), Clear Streak Well (32º29'S, 122º24'E); 59745 (female), 20 km ESE of Mount Newmont (32º59'S, 123º18'E); 66844 (female), Coragina Rock (32º55'S, 123º30'E); 66999, 67000 (males), 13 km W of Eyre Homestead (32º15'S, 126º10'E); 67369 (male) 14 km E of Hyden (32º27'S, 119º00'E); 72505 (male), 11.5 km NE of Buningonia Spring (31º20'30"S, 123º37'00"E); *77765 (female), Toolina Rockhole (32º45'05"S, 124º58'50"E); 94091 (male), 25 km NW of Toolina Rockhole (32º35'S, 124º48'E); 94092 (male), 7 km NW of Toolina Rockhole (32º42'30"S, 124º55'00"E); 112665 (female), 11.5 km NE of Buningonia Spring (31º20'30"S, 123º37'00"E); *112666, *112667 (female, male), Ponier Rock (32º56'S, 123º30'E); *116276 , *116277 (males), 22 km S of Kalbarri (27º51'S, 114º10'E); *116744 (male), 5 km W of Overlander Roadhouse (26º24'S, 114º25'E); *117102 (male), 23 km ESE of Overlander Roadhouse (26º36'S, 114º32'E); *117389 (male), Toomey Hills (31º33'26"S, 119º51'38"E); *122450 (juvenile), 24 km WSW of Hamelin Homestead (26º31'21"S, 114º00'09"E); *126345 (female), Aurora Range (30º21'16"S, 119º42'09"E); *131015 (male), 22 km WSW of Hamelin Homestead (26º31'S, 114º00'E); *131778 (female), 12 km WNW of Wandina Homestead (27º56'S, 115º32'E); *135196 (female), Camel Soak (29º26'S, 116º48'E); *136283 (female), Muggon Station (26º46'44"S, 115º37'40"E); *136406, *136407 (females), Norseman area (32º12'S, 121º47'E); *137675 (male), 74 km NW of Balladonia Roadhouse (32º02'S, 122º55'E); 137676 (female), 74 km NW of Balladonia Roadhouse (32º02'S, 122º55'E); *144087

(female), 5 km E of Cunderdin (31º39'S, 117º17'E); *144732 (male), Bungalbin Hill area (30º19'S, 119º29'E); *151125 (juvenile), Eyre Bird Observatory (32º13'28"S, 126º18'10"E); 151210 (female), Salmon Gums area (32º49'12"S, 121º24'36"E); *151218, *151219 (females), Salmon Gums area (32º49'59"S, 121º24'50"E); *152638 (female), Middle Island, Houtman Abrolhos Islands (28º54'35"S, 113º54'53"E); *166866 (female), Oakajee (28º34'25"S, 114º35'04"E).
*denotes individuals included in molecular analyses.

Diagnosis

A small species of *Delma* (SVL up to 93 mm) with moderately robust body and relatively short tail (less than 2.5 times length of body), modally 18 midbody scales, 68–85 ventral scales, one pair of supranasals, six upper labials with usually fourth below eye, supraloreal usually in contact with upper labials and ventral scales not markedly larger than adjacent lateral scales, and simple, plain coloration on body with typically strong dark variegations or narrow bars on head, nape and forebody.

Description of Holotype

Head short and blunt, narrowing very gradually forward of eyes, of equal width as body posteriorly; obvious tympanic aperture, indicated by round opening directly posterior to corner of mouth; snout very blunt and rounded in dorsal profile, rounded in lateral profile; eye positioned above fourth upper labial; nostril positioned on posterior junction of supranasal with first upper labial and postnasal; body moderately robust of equal width and round in cross-section; no vestiges of forelimbs externally; hindlimbs visible as well-developed elongate, rounded flaps adpressed to body at lateral extremes of vent; tail relatively short, tapering very gradually distally at pointed tip.

Head scales smooth, non-imbricate and heterogeneous; large rostral blunt anteriorly, wider than long, with obtuse apex penetrating supranasals; 1 pair of supranasals in broad contact, angled backwards behind rostral and in short contact with first upper labial forward of nostril; 1 postnasal, much wider than high and narrower posteriorly, slightly angled downwards and in

broad contact with second upper labial; prefrontals of equal size in broad contact; 1 supraloreal, much higher than wide and in broad contact with second upper labial; 1 loreal in broad contact with third upper labial and in short contact with second upper labial; 5 supraciliaries, second much larger and first and fifth of equal size, the fourth the smallest; 2 supraoculars, first slightly larger and wider than second; 2 frontals, the posterior most slightly larger; 2 frontoparietals of equal size; 2 parietals of equal size and 1 interparietal penetrating frontoparietals posteriorly; 6 upper labials, fourth elongate and positioned below eye, third the smallest and fifth the highest; 5 lower labials, first in contact behind mental, second the widest and fifth the smallest; mental wider than long with suture posterior to rostral and first upper labial. General form of head and details of scalation illustrated in Figure IV.6. Body scales smooth, non-imbricate, homogeneous, and arranged in parallel longitudinal rows; ventral scales only very marginally wider than the adjacent lateral body scales; 3 preanal scales.

Coloration

After more than 40 years in preservative, the holotype is light brown on the dorsal surface with a slightly darker head densely variegated with black on sides and on dorsal aspect. Lower labials whitish with distinct black bars, centered within (not on sutures) first to third lower labial scales, corner of mouth, than narrow bars around ear opening and on the lateral scales of forebody. A faint dark bar is also present within mental scale. The ventral extension of black bars on to chin and throat is distinct and connective. Ventral surface under head and along body is whitish.

Details of holotype

Measurements in mm (this study). SVL—65, TL—146 (224% of SVL), HD—3.5, HL—7.5, HW—5.0, HLL—3.2, ML—4.7, RL—1.0, RW—1.7, SL—2.8, EW—1.3, LS—1 on both sides, HLS—10, MSR—19, VE —71.

Variation

Scalation: Kluge (1974) examined 76 *D. australis* and recorded minimal individual variation apart from approximately 25% of specimens having a row of small scales between the large dorsolateral plates of the snout and the upper labials, and three specimens with the third upper labial below the eye.

Coloration and pattern: Shea (1991) remarked upon the noticeable geographic variation in the intensity of the head pattern in this species in South Australia, accordingly mapping the patterned form from the southern half and northwest of the state—WA.SA and S.SA and the unpatterned form— *australis* N.SA sp. nov. from the western Lake Eyre drainage (figure IV.2). The holotype of *D. australis* from Port Lincoln, Eyre Peninsula in South Australia is considered representative of Shea's (1991) patterned form in having strong dark variegations on the head, although the pattern is reduced, particularly laterally, in a few specimens. The patterned form—*australis* sensu stricto—is contiguous and similar in populations from northwestern Victoria and southwestern New South Wales.

In Western Australia, WA.SA *australis* display a consistent trend with the WA.SA from SA and S.SA *australis*, with strongly pigmented dark variegations and narrow bars on the lateral scales of forebody in the eastern Coolgardie Goldfields and Mallee bioregions. The degree of intensity on the head is variously accentuated by the amount of pale spots or streaks and is shown throughout the remainder of the species range. In many individuals the dark pattern on the head is very dense, including the insular populations on the Houtman Abrolhos Islands. In overall body appearance the coloration of *D. australis* has been described as brown, pale yellowish brown, reddish brown, rich brown and greyish brown with dorsal scales occasionally flecked or edged with black, and whitish or greyish ventral surfaces usually marked with obscure variegations or reticulations (Cogger, 2014; Kluge, 1974; Wilson and Swan, 2008).

Etymology

australis is derived from the Latin adjective, meaning southern, alluding to the widespread geographic distribution of this species (Kluge, 1974).

Distribution and Sympatry

Delma australis is widespread throughout subhumid to arid areas of southern Australia; from northwestern Victoria, and southwestern New South Wales, in South Australia south of the Spencer Gulf and west of the Eyre drainage, and central and west Western Australia (Cogger, 2014; Shea 1991; Wilson and Swan 2013). In Western Australia, extending north to Shark Bay (base of Peron Peninsula), Meedo Station, Weld Range, Paynes Find, Windarling Hill and Buningonia Spring, south through the Avon Wheatbelt, Mallee and Coolgardie Goldfields bioregions and east to Cocklebiddy. Known from Walyering Hill, Oakajee and near Kalbarri in the far western mainland where it appears to be patchily distributed. Insular populations occur on Rat and Middle Islands in the Houtman Abrolhos Islands (Figure 4).

Recorded instances of sympatry involving *D. australis* include *D. butleri*, *D. fraseri*, *D. grayii* and *D. petersoni* (Chapman and Dell, 1985; How et al., 1987; Shea, 1991) (B. Maryan, personal observation). In the vicinity of Poochera in South Australia, *D. australis*, *D. butleri* and *D. petersoni* have all been recorded (Shea, 1991). Kluge (1974) also mentions probable sympatry with both *D. inornata* and *D. molleri* due to their overlapping distributions.

Habitat

Delma australis mainly occupies mallee habitats with *Triodia* spinifex understory in northwestern Victoria and southwestern New South Wales (Shea, 1991). This habitat association is repeated in South Australia where the majority of the southern and western populations are from *Triodia* or mallee habitats, or combination of both (Shea 1991). In Western Australia, *D. australis* occupies a variety of habitats on different soils that include mallee and/or other

Eucalyptus woodlands and *Acacia* with a spinifex (*Triodia* and *Plectrachne*) or shrubland understory (Shea, 1991). These diverse vegetation communities provide ample cover for *D. australis*, where most specimens have been pit-trapped, found in and under spinifex and sedge tussocks, raked (using a 3-prong cultivator) from leaf litter, spoil-heaps, mats of dead vegetation and found under logs, mallee roots, rocks (including coral slabs on the Houtman Abrolhos Islands) and rubbish, especially pieces of corrugated iron in disturbed areas adjacent to uncleared vegetation. In areas of sympatry with other *Delma* species, *D. australis* tends to seek moister microhabitats (Shea, 1991; Wilson and Swan, 2008). Interestingly, nocturnal observations of *D. australis* on sealed roads or tracks are rare, unlike other larger species of *Delma.*

Comparison with Other Species

Delma australis sensu stricto is here compared with all regionally sympatric and nearest geographical congeners throughout its broad southern Australian distribution.

Delma australis is morphologically most similar to *D. butleri*. However, *D. australis* differs from *D. butleri* in having one pair of supranasals (v. two pairs) and typically 18 midbody scale rows (v. 16). The known distribution of *D. australis* overlaps broadly with *D. fraseri*, *D. grayii, D. molleri*, *D. petersoni* and *D. tincta*. *Delma australis* is easily distinguished from all five by a combination of lackingbroad, dark bands on head and neck, ventral scales markedly larger than adjacent lateral scales and a yellow ventral surface.

All nearest geographical congeners: *D. borea*, *D. concinna*, *D. desmosa*, *D. haroldi*, *D. impar*, *D. inornata* and *D. nasuta* differ from *D. australis* by having a combination of two pairs of supranasals (v. one pair), broad dark bands on head and neck (v. dark variegations or narrow bars on head, nape and forebody), ventral scales markedly larger than adjacent lateral scales (v. ventral scales not markedly larger than adjacent lateral scales) and typically 14□16 or 20 midbody scale rows (v. 18) (Storr et al. 1990; Wilson and Swan 2013).

Delma australis differs from the closely related *D. torquata* from southeastern Queensland in having a larger adult size (SVL up to 93 mm v. up to 63 mm), three preanal scales (v. two), typically the fourth upper labial below the eye (v. typically the third), typically 18 midbody scale rows (v. 16) and dark variegations or narrow bars (when present) on head, neck and forebody (v. broad dark bands) (Wilson, 2005).

Remarks

Kluge (1974) and Storr et al. (1990)illustrate the general form of the head and details of scalation of *D. australis*. Kluge (1974: 78) also illustrated a preserved adult male specimen of the patterned form from near Kokatha in South Australia (SAM R10375). Apart from those already mentioned above, the patterned form of *Delma australis* has also been illustrated in other publications (e.g. Ehmann 1992: 87; Henkel 2010: 141).

IV.vi—*Delma australis* S.WA **sp. nov.**
Southern Heath Delma (Fig. IV.1D, IV.6)

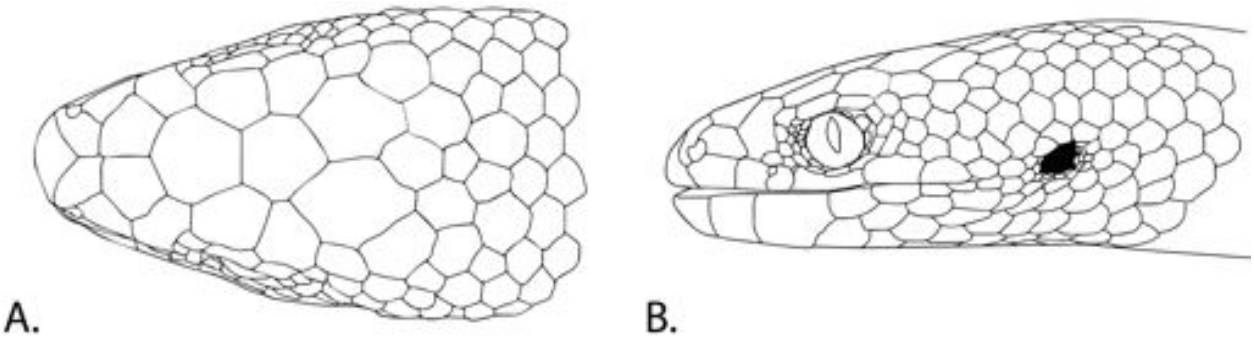

Figure IV.6. Head region of *Delma australis* S.WA holotype (WAM 144237). A. Dorsal view. B. Left lateral view.

Material Examined
Holotype

Australia: *Western Australia*: WAMR144237—male, Bandalup Hill, Ravensthorpe Range (33º40'29"S, 120º23'54"E), on 14 October 2000 by R. Teale and G. Harold.

Paratypes

Australia: *Western Australia*: 1 male, 3.8 km W of Kundip (33º41'S, 120º09'E), (129674); 1 female, Hellfire Bay, Cape Le Grand National Park (34º00'15"S, 122º10'20"E), (131902); 1 female, Duke of Orleans Bay, Wharton Beach (33º56'S,

122º33'E), (132154); 1 male, as for holotype, (144238); 1 male, Kundip (33º40'26"S, 120º11'45"E), (154234); 1 male, Canal Rocks (33º39'46"S, 115º00'45"E), (156978).

Additional Material

Australia: ***Western Australia*** (WAMR)***:*** 42637 (male), 9.6 km SE of Ongerup (34º02'S, 118º03'E); 43858 (male), Duke of Orleans Bay (33º54'S, 122º40'E); 43859–60 (females), 1.6 km W of Duke of Orleans Bay (33º55'S, 122º34'); 46262, 46268 (female, male), Mississippi Bay, Cape Le Grand National Park (33º59'S, 122º16'E); 51769, 51772 (females), Bluff Knoll, Stirling Range National Park (34º23'S, 118º15'E); 57742 (male), Thomas River (33º49'S, 123º02'E); 75620 (male), 6 km ENE of Manypeaks (34º49'S, 118º13'E); 86666, 86669, 86671, 86672 (female, female, male, female), Lort River Station (33º45'S, 121º15'E); 86988 (female), Gordon Inlet (34º17'S, 119º28'E); 89358 (male), East Mount Barren, Fitzgerald River National Park (33º54'S, 119º58'E); 91089 (male), 4 km W of Mount Trio, Stirling Range National Park (34º21'S, 118º04'E); 91740 (male), NE of Cape Arid (33º59'S, 123º12'E); 91742 (male), East Mount Barren, Fitzgerald River National Park (33º55'S, 120º01'E); 95434 (female), Albany (35º02'S, 117º53'E); 96253 (male), Lort River Station (33º27'S, 121º21'E); 129003 (female), Shannon Basin (34º34'20"S, 116º19'19"E); 129674 (?), Kundip (33°41`00"S, 120°09`00"E); 129682 (female), Quagi Beach (33º50'S, 121º17'E); 131899 (female), Mount Merivale (33º48'45"S, 122º06'15"E); 131902 (?), Hellfire Bay (34°00`15"S122°10`20"E); 132154 (?), Duke of Orleans Bay (33°56`00"S, 122°33`00"E); 137203 (male), Stirling Range National Park (34º51'S, 118º25'E); 144236 (male), Bandalup Hill, Ravensthorpe Range (33º40'29"S, 120º23'54"E); 144237 (?), Bandalup Hill (33°40`29"S, 120°23`54"E); 144238 (?), Bandalup Hill (33°40`29"S, 120°23`54"E); 154243 (male), Kundip (33º40'01"S, 120º12'03"E); 156978 (?), Canal Rocks (33°39`46"S, 115°00`45"E).

Diagnosis

A small species of *Delma* (SVL up to 79 mm) with moderately robust body and relatively short tail (less than 2.5 times length of body), modally 18 midbody scales, 73–92 ventral scales, one pair of supranasals, six upper labials with usually fourth below eye, supraloreal usually in contact with upper labials and ventral scales not markedly larger than adjacent lateral scales, and simple, plain colouration on head and body, apart from dark bars on lower labials and lateral scales on forebody.

Description of Holotype

Head short and narrowing gradually forward of eyes, of equal width as body posteriorly; obvious tympanic aperture, indicated by round, slightly-angled opening posterior to corner of mouth, opening is more narrow on right side; snout moderately long and rounded in dorsal profile, flat and rounded in lateral profile; eyes noticeably large on head, positioned above fourth

upper labial; nostril positioned on posterior junction of supranasal with first upper labial and postnasal; body moderately robust of equal width and round in cross-section; no vestiges of forelimbs externally; hindlimbs visible as well-developed elongate, rounded flaps adpressed to body at lateral extremes of vent; tail relatively short, tapering very gradually distally at pointed tip.

Head scales smooth, non-imbricate and heterogeneous; rostral rounded anteriorly, wider than long, with obtuse apex penetrating supranasals; 1 pair of supranasals in broad contact, angled backwards behind rostral and in short contact with first upper labial; 1 postnasal, wider than high, angled downwards and in short contact with second upper labial; prefrontals of equal size and in broad contact; supraloreal much higher than wide, and in broad contact with second upper labial; 4 loreals, the anterior most much larger and others subequal; 5 supraciliaries, second much larger and first and fourth the smallest of roughly equal size; 2 supraoculars, first slightly larger and wider than second; 2 frontals, the anterior most much larger; 2 frontoparietals of roughly equal size; 2 parietals and 1 interparietal penetrating frontoparietals posteriorly; 6 upper labials, fourth elongate and positioned below eye, third the smallest, a small scale intersects suture between second and third upper labial on left side; 5 lower labials, first in contact behind mental, second the widest and fifth the smallest; mental wider than long with suture posterior to rostral and first upper labial. General form of head and details of scalation illustrated in Figure IV.7. Body scales smooth, non-imbricate, homogeneous, and arranged in parallel longitudinal rows; ventral scales only very marginally wider than the adjacent lateral body scales; 3 preanal scales.

Coloration

In life (Figure IV.1B), top of head bluish grey and unpatterned, obscurely variegated with black on sides. Lower labials whitish with black bars, centred on sutures of mental and anterior

two lower labial scales, corner of mouth, than becoming obscure variegations around ear opening and on lateral scales of forebody. There is only very weak ventral extension of black bars on to chin and throat. Dorsal surface bluish grey on forebody gradually merging to reddish brown on body, and slightly pinkish on lower flanks, than light grey on tail. Dorsal surface is uniform, except for some indication of obscure dark spots or variegations, especially on some sutures of body scales. Ventral surface under head and along body whitish, with blackish variegations, becoming less pigmented under tail. In preservative, the reddish brown and grey coloration on dorsal surface becomes light brown. All other aspects of dark bars on lower labials and obscure variegations on body remain.

Details of holotype

Measurements in mm. SVL —57, TL— 131 (229% of SVL), HD— 3.4, HL— 6.9, HW— 4.5, HLL—3.3, ML—4.9, RL— 0.9, RW—1.3, SL—2.6, EW—1.1, LS—2 on both sides, HLS—10, MSR—18, VE—75.

Variation

Scalation: As noted for *D. australis*, variation in the supraloreal contacting the upper labials and interrupting the loreal row, is similarly recorded in *D. australis* S.WA as the more prevalent conditions: supraloreal contacts second upper labial on both sides (as in holotype) in WAMR86666, 91740, 129674, 131899 and 154234; supraloreal contacts second and third upper labial on both sides in WAMR43858, 57742, 86672, 131902 and 144238; supraloreal separated from upper labials by either one large loreal and postnasal or two loreals in WAMR42637, 43860, 46262, 46268, 51772, 75620, 89358, 91089, 91742, 95434, 129003 137203 and 156978. The number of upper labials is variable—but instances of the fifth or third beneath the eye are recorded on the right side only in WAMR43859, 86669 and 129682 and on the left side only in 154234. Equally rare is intraspecific variation in number of midbody scales with 17 in WAMR86666 and 19 in WAMR46262 and WAMR91742. Similar to *D. australis* (Kluge 1974),

the mean number of ventral scales was always greater in females than males; however in *D. australis* S.WA the values are marginally higher.

Coloration and pattern: The paratypes and additional material examined are similarly colored to the holotype in life and in preservative, except in some preserved individuals (e.g., 131902) the dark bars on the lower labials and lateral scales of forebody are more pronounced, and individuals (e.g. WAMR75620, 91089,129003, 137203, 154234) are a very uniform dark grey on head, body and tail. In life, hatchlings of *D. australis* S.WA, have a similar color and head pattern to adults.

Etymology

To be determined.

Distribution and Sympatry

Delma australis S.WA is widespread on the Esperance Plains bioregion and patchily distributed on the Warren and southern Jarrah Forest bioregions in southern Western Australia (Figure IV.2). Records extend east to the vicinity of Thomas River and Cape Arid, west to Canal Rocks and near Busselton and inland to Stirling Range National Park, Ongerup, Ravensthorpe Range, Scaddan and Mount Burdett. The Esperance Plains bioregion is a biogeographically significant area rich in endemic plants, rare ecosystems and vulnerable and specially protected fauna. Approximately 87% of the Esperance Plains bioregion has been largely cleared and developed for intensive agriculture, however much of the remaining vegetation is afforded statutory protection that include many nature reserves and the Cape Arid, Cape Le Grand, Stokes, Fitzgerald River and Stirling Range National Parks where *D. australis* S.WA occurs.

Current records of *australis* S.WA are insufficient to establish if *australis* and *australis* S.WA exhibit sympatry or allopatry (Figure IV.2). Currently the two species are known to occur within 80 km of each other in the east: e.g. 91740 from Cape Arid v. 36229 from Pine Hill and

within 130 km in the west: 42637 from Ongerup v. 12604 from Wagin, and within 20 km near Dundas Nature Resereve. Specimens from these proximate localities do not show any admixture of characters as might be expected if significant levels of gene flow were occurring across a contact zone or step cline. Available information suggests a degree of habitat partitioning between *D. australis* S.WA on the Esperance Plains bioregion and regional *D. australis* occurring more inland on the semiarid Mallee bioregion, however the areas where their ranges interdigitate should be investigated to determine whether sympatry occurs. The only recorded instance of sympatry involving *D. australis* S.WA is with *D. fraseri.*

Habitat

Delma australis S.WA occupies the proteaceous scrub and mallee heaths on sandplain. This habitat preference is exemplified by 65 records of *D. australis* S.WA, recorded as *D. australis*, from 18 sites in which 79% were recorded from mallee heath (Sanders et al., 2012). These diverse vegetation communities provide ample cover for *D. australis* S.WA, where most specimens, including the type series, have been pit-trapped and raked (using a 3-prong cultivator) from leaf litter, spoil-heaps, and mats of dead vegetation and inside abandoned stick-ant nests. It has also been found under logs, mallee roots, rocks and rubbish, especially pieces of corrugated iron in disturbed areas adjacent to uncleared heath, and also occupies the granitic heath, occasionally found under exfoliated granite slabs (B. Maryan, personal observation). There is no habitat data associated with the specimens from the lower southwestern corner of Western Australia (e.g. WAMR129003, 156978, 172507).

Comparison with Other Species

Delma australis S.WA is here compared first with its nearest geographical congener—*D. australis*—the species which it was previously confused with and is most similar to in general

aspects of body size, coloration and scalation Then with the regionally sympatric *D. fraseri*, and finally with the allopatric distant Western Australian species and the closely related *D. torquata*, with which it shares important characters.

Delma australis S.WA is morphologically most similar to regional populations of *D. australis* from the Mallee bioregion (e.g. WAMR30706, 30749, 53461, 57909, 67369, 112666, 112667, 151210, 151218, 151219). These taxa are similar in body size and agree in most details of head and body scalation. However, *D. australis* S.WA differs from *D. australis* in having a more vertically depressed head with mean values expressed for HD and HL being respectively lower and higher, having a higher average number of ventral scales in both sexes, having longer hindlimb flaps in both sexes corresponding with higher hindlimb scale counts.

Differences concerning the coloration and aspects of head patterning are apparent in life: in *D. australis* S.WA the overall appearance is a uniform greyish on the head, forebody and tail with dark variegations (when present) and only dark bars present on the lower labials and lateral scales of forebody with typically weak ventral extension of these on to the chin and throat (IV.1B), while in regional *D. australis* the overall appearance is a brownish body with strong dark variegations or narrow bars present on the head, nape and lateral scales of forebody with typically strong ventral extension of these on to the chin and throat. Additionally, in life *australis* S.WA appears to have a matt-textured (less glossy) body when compared to *australis*. Consistent across live and preserved specimens are patterns of the lower labials: in *australis* S.WA bars are centered over sutures between the mental and anterior two lower labial scales, while in *australis,* bars are typically centered not over the sutures between the mental and anterior two lower labial scales.

Delma australis S.WA differs from *D. fraseri* in having a smaller adult size (SVL up to 93 mm v. up to 140 mm), one pair of supranasals (v. two pairs), typically 18 midbody scale rows

(v. 16), ventral scales not markedly larger than adjacent lateral scales (v. markedly larger) and only dark variegations (when present) on head and neck (v. broad dark bands, often faded in adults).

All other Western Australian species: *D. borea*, *D.butleri*, *D. concinna*, *D. desmosa*, *D. elegans*, *D. grayii*, *D. haroldi*, *D. nasuta*, *D. pax*, *D. tealei* and *D. tincta* are allopatric and differ from *D. australis* S.WA by having a combination of two pairs of supranasals (v. one pair), broad dark bands on head and neck (v. dark variegations (when present) on head and neck) and ventral scales markedly larger than adjacent lateral scales (v. ventral scales not markedly larger than adjacent lateral scales) (Storr *et al.* 1990; Wilson and Swan 2013).

Delma australis S.WA differs from *D. torquata* from southeastern Queensland in having a larger adult size (SVL up to 79 mm v. up to 63 mm), three preanal scales (v. two), typically the fourth upper labial below the eye (v. typically the third), typically 18 midbody scale rows (v. 16) and only dark variegations (when present) on head and neck (v. broad dark bands) (Wilson 2005).

Remarks

Kluge (1974) mentioned in his multivariate analysis of *australis* that number of ventral scales was lower in specimens from the southwestern corner of the state compared to those from more interior regions. This assessment contradicts this study in which we examined a larger sample size from this area and found *australis* S.WA to consistently have a higher number of ventral scales when compared to regional *australis*. This opposing difference is corroborated by Kluge stating he had insufficient samples of females which are longer-bodied correspondingly having a higher number of ventral scales (Maryan et al. 2007).

IV.ii—*Delma australis* N.SA **sp. nov.**
Eyrean Delma (fig. IV.1E, IV.7)

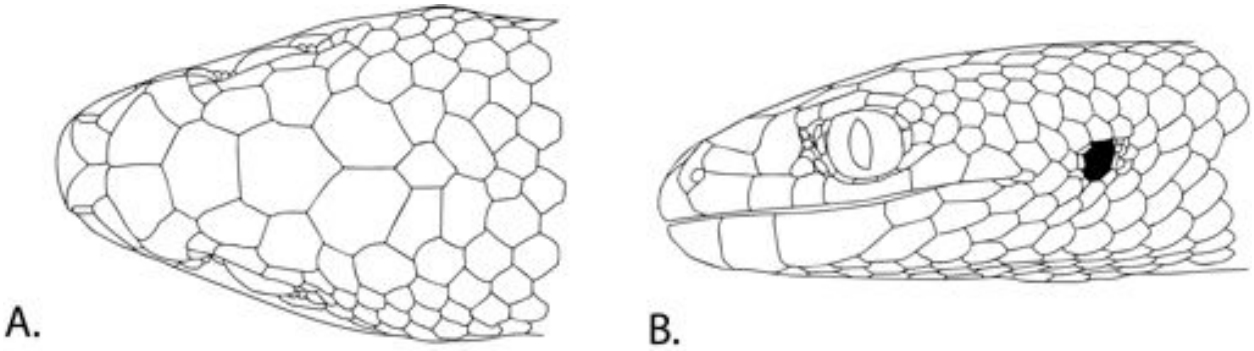

Figure IV.7. Head region of *Delma australis* N.SA (WAM 132470). A. Dorsal view. B. Left lateral view.

Material Examined

Australia: *South Australia* (SAMA): 28138, W of Marree (29 38 00 S, 137 44 00 E); SAMA 28172, Beresford RS (29 14 00 S, 136 39 30 E); 28215, Dalhousie Ruins (26 31 00 S, 135 28 00 E); 44426, 8k NW Mt Kintore (26 30 01 S, 130 26 13 E); 44680, 4k SSW Mt Cuthbert (26 08 09 S, 132 03 00 E); 44720, Todmorden Station (27 39 26 S, 134 39 20 E) ; 46230, Arckaringa Station (27 56 20 S, 134 44 10 E); 46340, 6.5k WNW Johnson Bore (29 30 49 S, 136 09 21 E); 46438, 15k NW Backadinna Hill (29 05 00 S, 135 10 00 E); 46980, 5.6k SSE Mosquito (26 09 28 S, 134 30 49 E); 47178, Peake Station (28 26 10 S, 136 07 41 E); 51992, 4.1k N Warden Hill (30 24 23 S, 139 13 29 E); 2032, Quorn Nature Reserve (32 21 00 S, 138 02 00 E); 53114, 1.9k N Dutchmans Peak (32 18 11 S, 137 57 47 E); 61993, 9.0k SE Moonaree hill (31 58 56 S, 135 40 01 E).

Western Australia (WAMR): 116744, Overlander Roadhouse (26°24`00"S, 114°25`00"E); 117102, ESE Overlander (26°36`00"S, 114°32`00"E); 122450, Hamelin (26°31`21"S, 114°00`09"E); 131015, Hamelin Homestead (26 °31`00"S, 114°00`00"E); 132470, Shothole Canyon (22°03`00"S114°01`00"E); 136283, Muggon (26°46`44"S115°37`40"E).

Holotype

Awaiting assignment.

Additional Material

Australia: *Western Australia*: female, Shothole Canyon, Cape Range National Park (22º03'S, 114º01'E), on 5 May 1998 by B. Bush and B. Maryan (132470).

Australia: *South Australia:* 35854 (X) Krichauff Ranges; SAM 46980 (x) 5.6 km SSE Mostquito (26 09 28 S, 134 30 49 E); SAM 51992 (x) 4.1 km N Warden Hill (30 24 23 S, 139 13 29 E); SAM 52032 (x) Quorn Nature Reserve (32 21 00 S, 138 02 00 E); SAM 53114 (x) 1.9 km N Dutchmans Peak (32 18 11 S, 137 57 47 E); SAM 61993 (x) 9 km SE Moonaree Hill (31 58 56 S, 135 40 01 E); SAM 44720 (x) Todmorden Station (27 39 26 S, 134 39 20 E); SAM 46230 (x) Arckaringa Station (27 56 20 S, 134 44 10 E),; SAM 44426 (x) 8 km NW Mt. Kintore (26 30 01 S, 130 26 13 E); SAM 28215 (x) Dalhousie Ruins (26 31 00 S, 135 28 00 E); SAM 44680 (x) 4 km SSW Mt. Cuthbert (26 08 09 S, 132 03 00 E); SAM 28172 (x) Beresford Station (29 14 00 S, 136 39 30 E); SAM 46438 (x) 15 km NW Backadinna Hill (29 05 00 S, 135 10 00

E); SAM 28138 (x) W of Marree (29 38 00 S, 137 44 00 E); SAM 46340 (x) 6.5 km WNW Johnson Bore (29 30 49 S, 136 09 21 E).

.

Diagnosis

A small species of *Delma* (SVL up to 64 mm) with moderately robust body and relatively short tail (less than 2.5 times length of body), modally 18 midbody scales, 82.3 ventral scales, one pair of supranasals, six upper labials with fourth below eye, supraloreal in contact with second upper labial, ventral scales not markedly larger than adjacent lateral scales, and distinctly weakened facial and throat banding.

Description of Holotype

Awaiting assignment of holotype.

Coloration

Details of holotype

Awaiting assignment.

Etymology

To be determined.

Distribution and Sympatry

The habitat associated with the western Lake Eyre drainage specimens includes gibber plain with *Atriplex*, on watercourses lined with *Eucalyptus* and low, stony hills with drainage channels and *Acacia* (Shea 1991; B. Maryan, personal observation). *Delma australis* N.SA is known broadly from the western Lake Eyre drainage, into extreme southern NT, a single individual (WAMR132470) from the North West Cape peninsula in Western Australia, a heavily dissected limestone plateau sparsely vegetated with *Triodia*, shrubs and low eucalypts. Two individuals (WAMR137675, 137676) from south-central WA, and a Shark Bay population (WAMR 117102, 122450, 136283) were identified by molecular and morphological assessments (Figure IV.2) (Storr and Hanlon 1980). The broad geographic gap between northern South Australia, southern Western Australia, Shark Bay, and Cape Range populations of *australis* N.SA may represent relictual populations isolated by habitat change. Conversely, these

distributional gaps may instead represent collection and sampling gaps. Further surveys of the 47,655 protected hectares of the Cape Range National Park are required to identify the extent of *australis* N.SA's distribution within the Cape Range.

Distributional records suggest the potential for sympatry between *australis* N.SA and *fraseri* in southern WA. Shea (1991) discusses occurrences and sympatry of *Delma* in SA. However, four other species of *Delma* are recorded on the North West Cape peninsula. *Delma nasuta* and *D. tincta* are known from several localities and the regional sample is consistent with other populations of these widespread taxa. The regional endemic species, *D. tealei* has been collected at Shothole Canyon and other localities on the Cape Range. A fourth taxon, currently associated with *D. butleri*, is known from a single specimen (156449) collected at the Learmonth Air Weapons Range, immediately south of the Cape Range National Park.

Habitat

Delma australis is found throughout mallee and *Triodia* habitats throughout the lake Eyre Drainage in eastern South Australia (Shea, 1991). In Western Australia, *D. australis* N.SA has been collected from a single locality in southern WA, in *Eucalyptus* woodland, as well as from the sandy soils and spoils heaps from Shark Bay, north of Kalbarri National Park. A single individual was collected from a limestone plateau of the Cape Range National Park. Scant individuals have been collected from the Northern Territories, and accurate habitat information does not exist for these specimens.

Comparisons with Other Species

Delma australis N.SA is here compared first with *australis* and *australis* S.WA, the two species with which it is most similar to, then with each of the regionally sympatric *butleri*, *nasuta*, *tealei* and *tincta*, and finally with geographically distant congeners with which it shares important characters. In coloration and patterning, *australis* N.SA diverges from true *australis* in

inornate phenotype, most similar to the patterned form of *D. australis* in life, with possibly some subtle differences. The Cape Range and southern Western Australia (WAMR132470, 137675, 137676) individuals does not exhibit the muddied grey dorsal head, and yellow flushed lips and snout of Shark Bay and South Australia conspecifics. Instead, these specimens appear as an patterned intergrade between *australis* sensu stricto and their inornate conspecifics. The nearest regional populations of *D. australis* in the Shark Bay area are markedly different in having a much reduced head pattern with a brownish body, similar to the coloration of SA individuals.

Delma australis N.SA differs from *butleri* in having a smaller adult size (SVL up to 64 mm v. up to 91 mm), one pair of supranasals (v. two pairs), typically 19 midbody scale rows (v. 16) and a reddish body with dark head (v. brownish body without dark head).

Delma nasuta grows to an even larger size (SVL up to 112 mm v. up to 64 mm) and have a more elongate snout, two pairs of supranasals, lower midbody scale rows (typically 16 or 18 v. 19) and a reticulated or spotted body pattern formed by a dark spot or emargination on numerous body scales.

The North West Cape peninsula specimens of *D. tealei* are also larger (SVL up to 88 mm v. up to 64 mm) and have two pairs of supranasals, lower midbody scale rows (typically 14 v. 19), and very different patterning that includes variegated lateral scales on the forebody.

Delma australis N.SA and *tincta* share one pair of supranasals, however *D. tincta* differs in having lower midbody scale rows (typically 14 v. 19) and broad dark bands on head and neck that are especially distinctive on immature specimens but remain visible on most adult specimens.

All other Western Australian species: *borea*, *concinna, desmosa*, *elegans*, *grayii*, *haroldi* and *pax* differ from *australis* N.SA in presence of a combination of two pairs of supranasals (v. one pair), broad dark bands on head and neck (v. dark head with small pale spots), larger SVL

more than 75 mm (v. up to 64 mm) and ventral scales markedly larger than adjacent lateral scales (v. ventral scales not markedly larger than adjacent lateral scales) (Storr *et al.* 1990; Wilson and Swan 2013).

Delma australis N.SA differs from *D. torquata* from southeastern Queensland in having three preanal scales (v. two), typically the fourth upper labial below the eye (v. typically the third), and typically 18 midbody scale rows (v. 16) (Wilson 2005).

IV.viii—Results

Morphological analysis

Using morphology alone, Kluge (1974) recognized and assessed differences between three populations within *australis*; a southwestern Western Australia form (south of 32°30'S, west of 120°E), an Eyre Peninsula form of South Australia (south of 32°S), and a Victoria form. Kluge found significant mean differences in number of preorbital (PRS), preanal (PAS), hindlimb (HLS), and caudal scales (CS); throat pattern (TP); and visceral pigmentation (VP). In agreement with Kluge (1974), Shea (1991) recognized a substantial geographic variation in head patterning. Specimens form the western Lake Eyre drainage (east of 134'E, north of 30'S) exhibited either reduced or absent head markings, in contrast to specimens from the southern reaches of SA, Tomkinson and Musgrave Ranges and northwest SA. Combined, these morphological assessments preliminarily recognized all three major lineages represented in our morphological and molecular results; Kluge's southwestern WA population aligning with *Delma australis* S.WA sp. nov.; Eyre Peninsula and Victoria forms aligning with the southern SA clade of true *australis* found across WA and southern SA; and Shea's inornate inland form representing *australis* N.SA sp. nov.. Distinguishing morphological characteristics and variation within and between newly recognized species are addressed in the diagnosis of each species.

Molecular Analysis

Phylogenetic analyses of mtDNA and nDNA datasets avoid problems of nito-nuclear discordance found elsewhere in the *Delma* tree (see chapter III). Both mtDNA and nDNA support the monophyly of six clades associated with *Delma australis*: *D. torquata* from QLD; *D. concinna* from coastal heaths of central WA; a southwestern WA "*australis*" form—*D. australis* S.WA sp. nov.; a central and northern SA "*australis*" form, the Cape Range individual, a Shark Bay, WA population, and two southern WA individuls (WAMR137675, 137676)—*Delma australis* N.SA sp. nov.; and two clades within *D. australis* sensu stricto a WA and western SA group, and a southern SA (south and east of the Spencer Gulf), VIC, and NSW form.

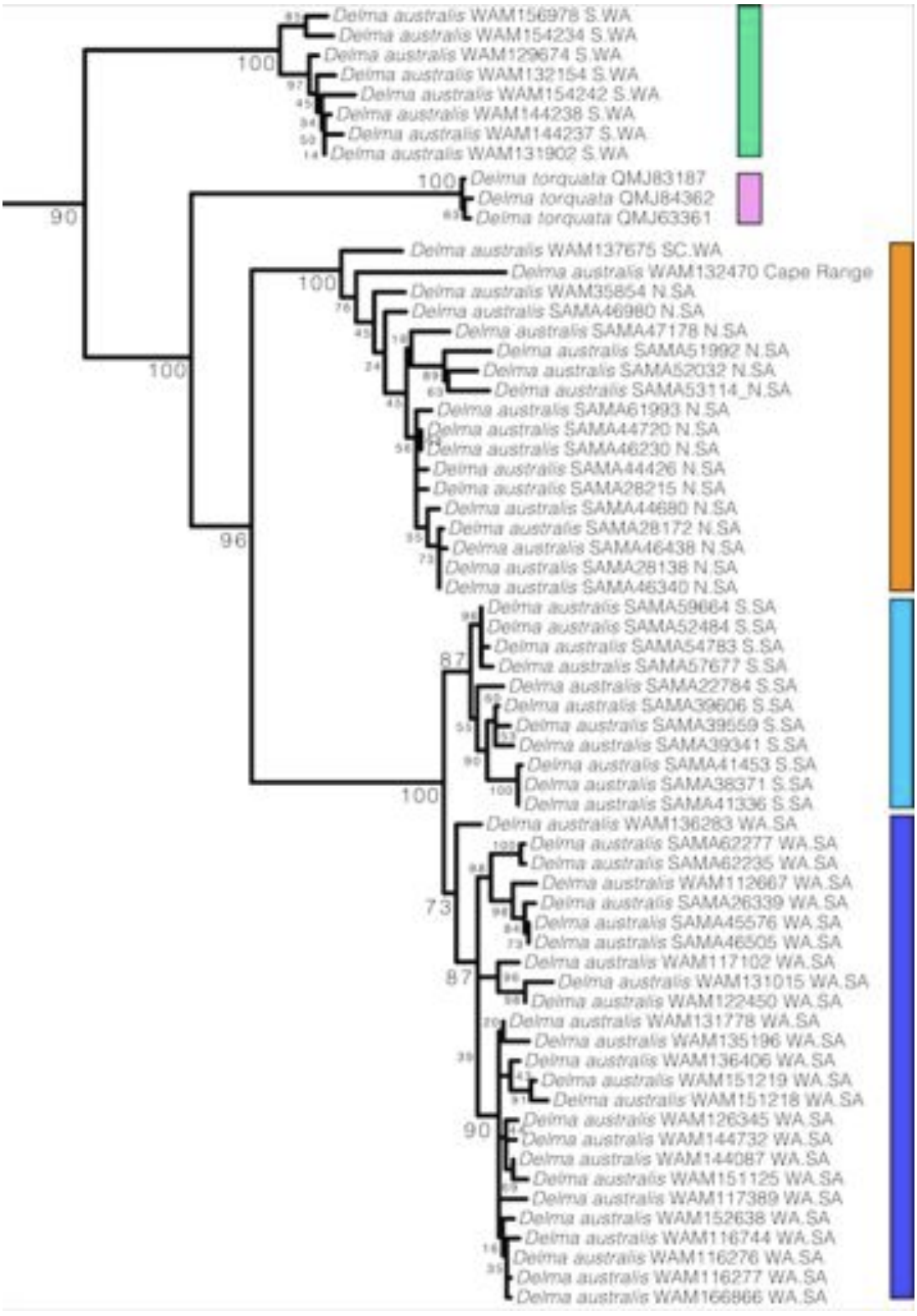

Figure IV.3. Maximum likelihood tree of phylogenetic relationships of the *Delma australis* group, as inferred from ND2. Green indicates the *australis* S.WA clade, pink— *torquata*, orange— *australis* N.SA, and blue designates *australis* sensu stricto. Light blue indicates the southern South Australia (S.SA) clade of *australis* and dark blue, the clade bridging Western Australia-South Australia (WA.SA). Numbers at nodes indicate Bootstrap Support values (BSS).

Run independently, mtDNA and nDNA datasets differ in establishing the position of *concinna* relative to the *australis* group. Mitochondrial (16S+ND2) results moderately support (BPP/BSS 95/63) the placement of *concinna* allied with the remaining *Delma* species, exclusive of *australis* and *torquata*. In contrast, nuclear results strongly ally (100/83) *concinna* with *australis* and *torquata*, as the basal member of clade C (Fig. III.1–C). Both mtDNA and nDNA results render *australis* paraphyletic with regards to *torquata*. Despite conflict in the accurate placement of *concinna*, the concatenated nuclear genealogy mirrors the mitochondrial tree support of five of six mtDNA clades.

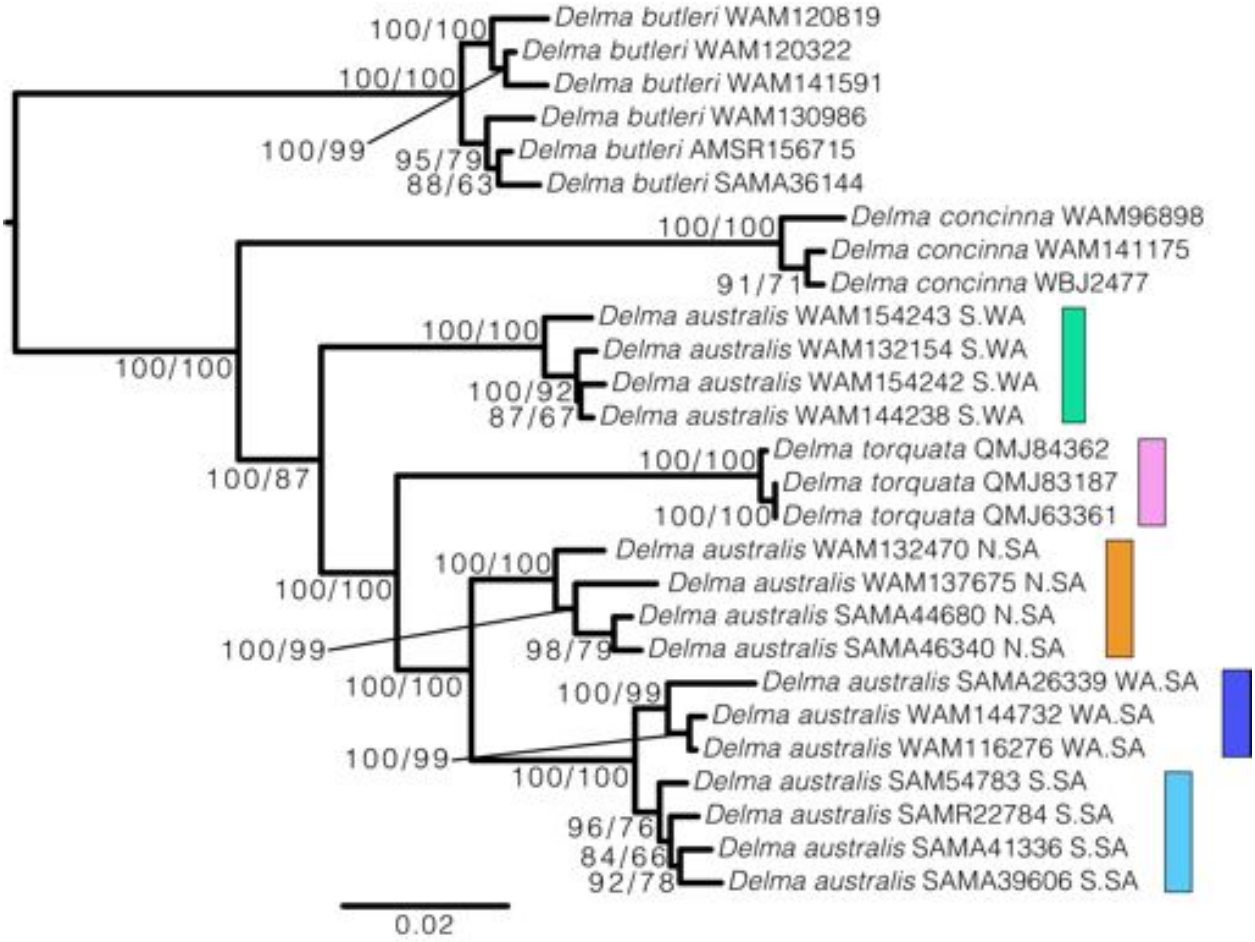

Figure IV.4. Maximum likelihood tree of relationships within the *australis* group as inferred by a mito-nuclear concatenated dataset (16S, ND2, DYNLL1, MXRA5, RAG1, C-mos), numbers indicated at nodes represent Bayesian Posterior Probabilities and Bootstrap Support values (BPP/BSS).

Delma australis sensu stricto comprises two well supported clades from SA and WA with substantial intraspecific divergence, which together form the sister species to *australis* N.SA (Fig. IV.3, IV.4). Within *D. australis* N.SA sp. nov. are three disjunct populations; a northern and central SA inornate form, a Cape Range individual (WAMR132470), and two south-central WA individuals from Balladonia Roadhouse (WAMR137675, 137676). Lineages appear largely geographically distinct, however, areas of near contact or potential zones of sympatry occur between *australis* N.SA*, australis* S.WA and *australis* in WA, and *australis* N.SA and *australis* in SA. Within *D. australis* sensu stricto, mtDNA shows high support (BSS and BPP = 100) for two independently evolving clades. The first (S.SA) is found largely south and east of the Spencer Gulf, SA, across northern VIC and western NSW. The second (WA.SA) is found along coastal and near inland WA from Shark Bay to Esperance, with an apparently disjunct population in western SA. mtDNA suggests genetic isolation between WA.SA and S.SA forms, and again between WA.SA from WA and WA.SA from SA—which appear disrupted by the Nullarbor Plain. nDNA analysed independently however shows poor support for the independence of WA.SA and S.SA clades of *australis*, suggesting the genetic split is relatively young, and nDNA has not yet adequately sorted these lineages.

Both mtDNA and nDNA analyses support the monophyly (BSS and BPP = 100) of *D. australis* N.SA sp. nov. from central and northern SA, and two disjunct populations; a single individual from Shothole Canyon, Cape Range, WA (WAMR132470), and two individuals collected several km northeast of Dundas Nature Reserve, WA (WAMR137675, 137676). Due to the cryptic nature of *australis* N.SA in WA, and rugged landscape of the Cape Range, genetic samples of these isolated populations are scarce. However, with increased sampling, we hope to address the biogeographic pattern of these genetic divergences further.

Our results support the monophyly of *concinna* and *torquata,* and their independent temporal affiliations with the *australis* complex. Paraphyly of *australis* with respect to *torquata* aids us in identifying the otherwise cryptic lineage *australis* N.SA. As the result of only recent specific recognition, genetic sampling of *australis* S.WA remains limited, and intraspecific diversity is not well supported. However, habitat heterogeneity along the southern coast of WA may encourage further discrete populational structuring within *australis* S.WA.

A Bayesian time-tree produced by the program BEAST 1.8.0 allowed an estimation of divergence dates within the *australis* group based on the nuclear dataset (fig. III.5). All species of this complex (including *concinna* and *torquata*) are returned in similar topological fashion as our BI and ML analyses. The crown *Delma* split between *torquata* and all other delmas appears to have occurred approximately 38 Mya, while *australis*+*concinna* diverged from remaining *Delma* ca. 35 Mya, and the speciation even between *australis* and *australis* N.SA appears approximately 16 million years old.

IV.ix—Discussion

Despite substantial morphological divergence between *concinna* and the remaining *australis* clade, mtDNA and nDNA datasets remain concordant across all *australis* complex lineages, and *torquata*, strongly supporting the monophyly of all recognized species and clades. Although *concinna* and *australis* may be found sympatrically, *torquata* exists widely geographically separated from remaining *australis* group members by the Mulga Lands, Darling Riverine Plains, and Nandewar bioregions (Fig. IV.8). Historical contact between these species would suggest some semblance of habitat homongeneity between these populations at a point in recent Australian biogeography, potentially within the past 20 Mya. The divergence of *australis* S.WA prior to the divergence of *torquata*, and potentially within a zone of sympatry with

australis, suggests a mode of speciation apart from allopatry as the cause. However, the preference of *australis* S.WA for more mesic refugia may be an indicator of habitat preference and partitioning.

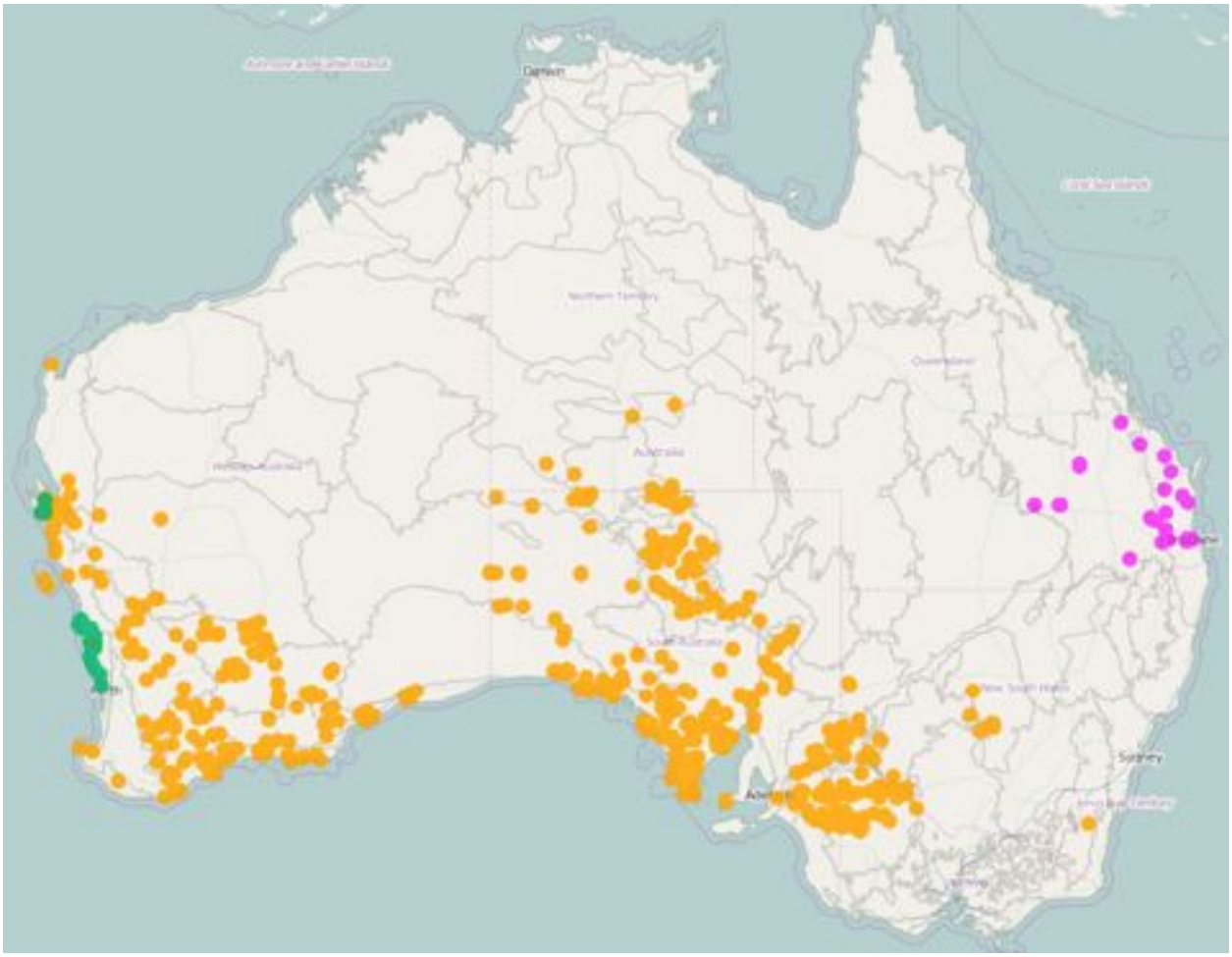

Figure IV.8. Geographic distribution of *Delma torquata* (pink) and *Delma australis* group species, including: *concinna* (green), *australis* S.WA (orange), *australis* N.SA (orange), and *australis* (orange). This map highlights current geographic isolation between *australis* and *torquata* by the Darling Riverine Plains, Mulga Lands, and Nandewar bioregions. The Nullarbor and Hampton bioregions disrupt populations and gene flow between Western Australia WA.SA *australis* and South Australia WA.SA *australis*. The Flinders Lofty Block just south of the Spencer Gulf separates S.SA *australis* present in the Murray Darling Depression from WA.SA *australis* on the Eyre Peninsula, and from *australis* N.SA to the north. Allopatry of WA.SA *australis* and *concinna* in WA is apparent by partitioning in the Swan Coastal Plain to the south, and Geraldton Sandplains region to the north.

Morphological similarity between *australis* s.s. and *australis* N.SA belies considerable molecular divergence and millions of years of genetic isolation. Although mtDNA suggests a significant divergence between WA.SA and S.SA populations of *australis*, nDNA analyzed independently shows only moderate support for the independence of these clades. This finding

suggests the genetic split between these forms is relatively young, and nDNA has not yet adequately resolved lineage sorting. Limited by a slower mutational rate, nuclear data fails to parse fine-scale population-level relationships as successfully as mitochondrial data. Incomplete sorting as the result of a recent divergence does allow us to infer the common ancestor of *australis* and *australis* N.SA split prior to the extreme aridification of south coastal WA and SA, allowing further divergence within WA.SA *australis* to become isolated east and west of the Nullarbor Plain, and S.SA south of the Spencer Gulf. The Flinders Range, and elevational impediment to admixture between WA.SA and S.SA *australis* separates populations north and south of the Spencer Gulf. Estimates for the Flinders Range range between 480–360 Mya, establishing these mountains far preceded pygopodids (Richards and Singleton, 1981). As such, the current distribution of *australis* both east and west is likely the result of shrinking plant cover in the Broken Hill Complex, Stony Plains, and Simpson Strzelecki Dunefields bioregions—during Australia's aridification—which border the Flinders Range to the east and north.

The success of pygopodids, and particularly *Delma* in arid regions of Australia suggests a close relationship between this genus and family and the aridification of continental Australia. Species richness in *Delma* experienced a surge in the Late Miocene between 20–6 Mya, as Australia rapidly dried out. *Delma*, and particularly members of the *australis* group, are strongly associated with *Triodia* spinifex, tussock grass, and related dense, low vegetation, and groundcover which provide suitable habitat (Fig. IV.9). In contrast, a paucity of *Delma* records from hyper-arid regions such as Channel Country, Gibson Desert, Little Simpson Desert, Nullarbor Plain, and the Simpson Strzelecki Dunefields, suggest *Delma* are limited in the scope of their drought-tolerance (Pianka, 1969, 2010; Wilson and Swan, 2013). Desertification of the landscape resulted in the creation of less-arid corridors of habitat between preferential biomes, which have been shown as biogeographic alleyways for fairy-wrens (Driskell et al., 2003; Ford,

1987; Schodde and Weatherly, 1982) as well as squamates *Ctenophorous scutulatus, Egernia depressa, Ctenotus leonhardii*, *Eremiascincus richardsonii,* and *Tympanocryptis* spp. (Pianka, 1972; Shoo et al., 2008). The temporal nature of these corridors, 4–2.5 Mya may have resulted in allopatric speciation events. While species of the *australis* group appear broadly distributed along the southern portion of the continent, dispersal of WA.SA *australis* in WA and subsequent splitting of this population, may be the result of use of the Nullarbor Plain Corridor (Fig. III.6), followed by its collapse as the result of continued aridification 2.5–0 Mya.

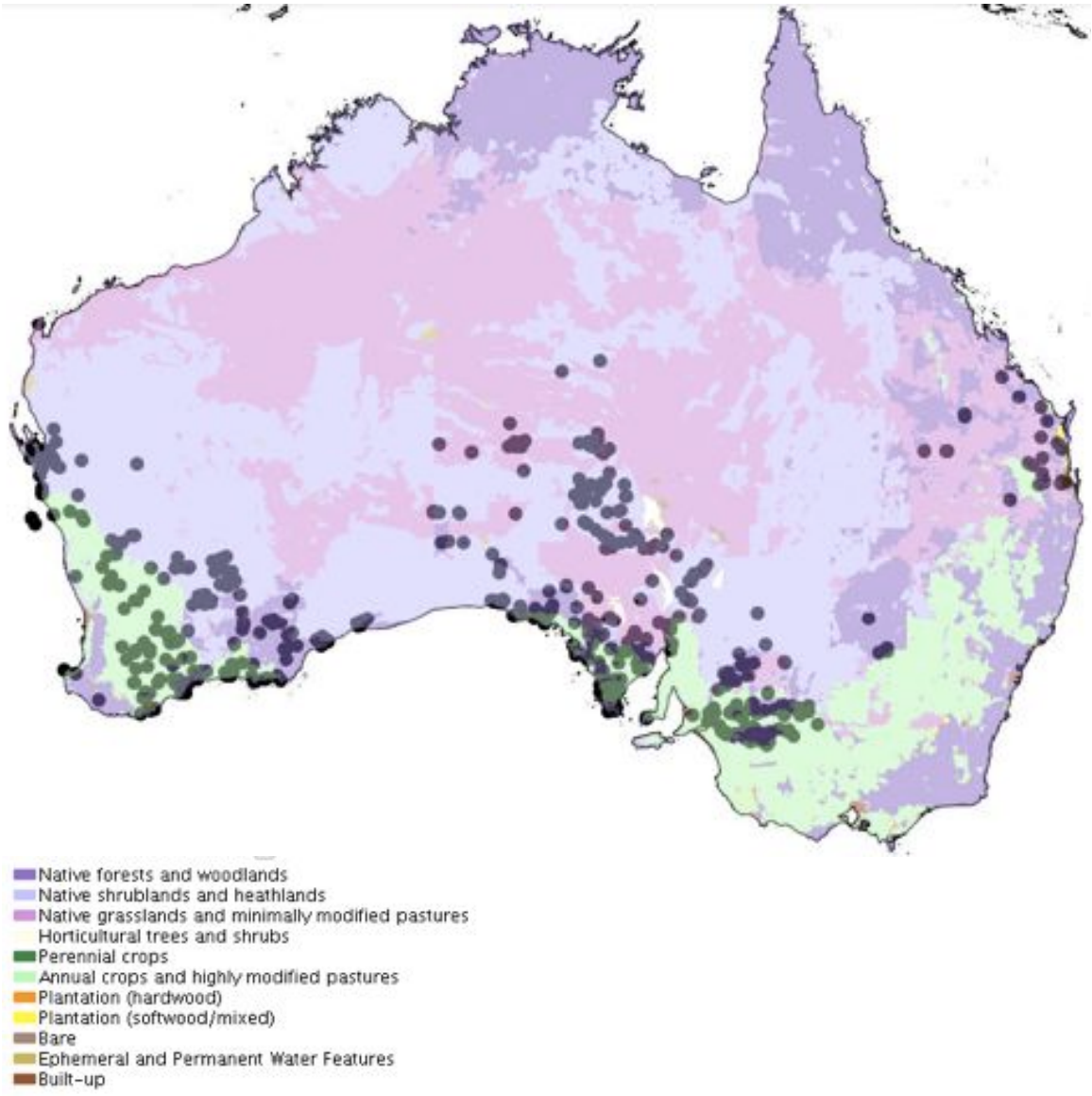

Figure IV.9. Distributional map of *australis, australis* S.WA, *australis* N.SA, and *torquata* records mapped atop contemporary landcover assessment of continental Australia.

Because of the generalist habits—both dietary and habitat preferences—of most delmas, identifying direct causes of speciation events is difficult. The rapid radiation of species richness within this group is most likely the result of considerable expansion of xeric biomes, but may also be attributable to rapid growth and subsequent shrink of mesic and rainforest habitats 6–2.5 Mya. Proliferation of temperate biomes and closed forest systems in this period may have reduced or fractured available habitat, resulting in allopatric divergence events. Upon succeeding reduction of this mesic Pleistocene expansion, the potential for secondary contact between previously separated species may have caused the mitochondrial reticulations we see in *Delma* today.

Study of hemipenial condition has discovered the inscribed phylogenetic signal of reproductive organs, beginning with Cope (1896) (Arnold, 1986a, b; Böhme, 1971; Branch, 1982, 1986; Dowling, 1967; Dowling and Savage, 1960; Keogh, 1999; Klaver and Böhme, 1986; Köhler et al., 2012; McCann, 1946). The benefits of studying the squamate copulatory organs lies in their diverse morphology, the various characters which can be described, counted, and scored, including size, shape, and ornamentation (Dowling and Savage, 1960; Keogh, 1999). The hemipenial conditions of pygopodids are covered in the subsequent chapter, however general hemipenial morphology unites the *australis* species complex, separate from the remaining *Delma* species. All three species currently confused under *australis* exhibit a single-lobed hemipene, described colloquially as boxing-mitt in shape, and covered completely (save the sulcus spermaticus) in fine micro-ornamentation. Assessment of the hemipenial condition of *D. concinna* and *torquata* is currently unavailable, but may add to synapomorphic characters of this group.

The present study has clarified the taxonomic status of *Delma australis*, and identified two new species well differentiated genetically but only subtly distinct morphologically. Our

evidence demonstrates the remaining WA.SA and S.SA populations of *australis* to be monophyletic representing a widespread polymorphic species with discrete phenotypic forms. The detection of the new species— *australis* S.WA from the Esperance Plains and adjacent humid southwestern corner of Western Australia was initially investigated owing to the strong evidence of reproductive isolation provided by the molecular data. Otherwise, the subtle morphological differences may have been ascribed to polymorphism and local phenotypic variation. The geographic ranges of *D. australis* and *D. australis* S.WA appear to be allopatric, with current records suggesting gaps of 80–130 km between populations that seems to coincide with an abrupt boundary over a very large distance between the cooler southerly Esperance Plains and drier northern Mallee bioregions. Gene flow between the populations, if it occurs at all, is clearly limited and insufficient to influence the genetic or morphological characteristics of the spatially adjacent populations. However, considering the proximity of the two bioregions and their corresponding transition in differing vegetation communities and soil structures (Beard 1990), contact zones between *D. australis* and *D. australis* S.WA should be looked at to investigate the nature and extent of genetic interactions between these species.

Southwestern Australia is recognized globally as one of the world's top 25 biodiversity hotspots (Myers et al. 2000), based largely on its highly diverse and endemic flora (Beard et al. 2000). The entire area is effectively a relatively damp 'island' refuge surrounded by oceans and desert (Hopper and Gioia, 2004). Despite the overall regional herpetofaunal diversity being considered impoverished due to the cooler climatic conditions (How et al. 1987; Chapman 1995), the area supports exceptional endemism with several monotypic genera including frogs (*Metacrinia*, *Myobatrachus* and *Spicospina*), turtles (*Pseudemydura*), lizards (*Pletholax*) and snakes (*Paroplocephalus* and *Rhinoplocephalus*) and species with very restricted distributions (Kay and Keogh 2012; Doughty and Oliver 2013). Southern WA reigns as one of the fastest

growing urban and agricultural regions in Australia (Kennedy 1990). Our assessment of *D. australis* adds yet another vertebrate species *D. australis* S.WA, to the growing number of regional endemics. Although not immediately threatened, the establishment of protected areas on the Esperance Plains understates the importance as core habitat for this species. The continual documentation of endemic species resulting from the re-evaluation of previously known taxa demonstrates that we are still far from completing the inventory of the vertebrates from the most highly disturbed southwestern Western Australia.

V. Notes on hemipenial morphology of the Pygopodidae Boulenger 1884: a phylogenetic tool

Ian G. Brennan, Aaron M. Bauer

V.i—Abstract

The Pygopodidae is a near-endemic Australian Family of limb-reduced, imbricately scaled gekkotans, currently composed of 44 species (43 in Australia, 2 in New Guinea). Phylogenetic studies of the Pygopodidae have enlisted molecular, morphometric, and osteological methods to resolve intergeneric and interspecific relationships, however, Böhme (1988) presented the only detailed morphological description of the hemipenes of pygopodids—a pair of pages concerning four species from three genera. Here, we contribute to Böhme's initial observations, by describing hemipenial condition in an additional 19 species across four genera, bringing current totals to 23 pygopodid species across five of seven currently recognized genera. Focused sampling of the genus *Delma* allows us to identify species groups based on hemipenial shape and ornamentation, and general morphology of cloacal spurs. We identify the presence of a singly lobed hemipenis in both *Aprasia* and *Delma*, and hypothesize this reduction in reproductive anatomy has occurred twice independently in pygopodid evolution.

V.ii—Introduction: Diversity within a Divergent Lineage

Near-limbless geckos of the Family Pygopodidae represent a unique radiation in Australian biogeographic history. The snake-like pygopodids are characterized by an absence of forelimbs, imbricate body scales, and a severe reduction of hindlimbs (Wilson and Swan, 2013; Cogger, 2014). Current taxonomy recognizes 44 species across seven genera; *Aprasia* Gray 1839 (14 spp.), *Delma* Gray 1831 (21 spp.), *Lialis* Gray 1835 (2 spp.), *Ophidiocephalus* Lucas & Frost 1897 (1 sp.), *Paradelma* Kinghorn 1926 (1 sp.), *Pletholax* Cope 1864 (1 sp.), and *Pygopus* Merrem 1820 (6 spp.). Although limblessness is not a novel adaptation in squamate evolutionary

history (Anniellidae, Anguidae, Cordylidae, Dibamidae, Gymnopthalmidae, Serpentes), pygopodids have become the most ecologically diverse limbless squamates save Serpentes. Current phylogenetic understanding suggests two independent burrowing lineages—*Aprasia* and *Ophidiocephalus*; shrub-swimmers—*Delma concinna*, *Pletholax*; squamate-specialist ambush predators—*Lialis*; a morphologically conservative genus of arthropod generalists—*Delma*; arachnid-specialists—*Pygopus*; and an insectivore with nectarivorous habits—*Paradelma*.

Despite morphometric, molecular, and osteological assessments of the Pygopodidae, intergeneric and many interspecific relationships remain poorly understood (Underwood, 1957; Kluge, 1974; 1976; Shea, 1987; 1991; Hutchinson, 1997; Jennings, et al., 2003; Maryan, et al., 2007; Oliver, et al., 2010), and no phylogenetic study has included hemipenial characters. Böhme's (1988) description of the hemipenes remains an invaluable contribution to the understanding of hemipenial condition in squamates as well as Gekkotans, but with coverage of just four pygopodid species across three genera, it remains too incomplete for any phylogenetic use. Here, we present a more inclusive look at the hemipenial morphology of the pygopodid family as a whole, with heavy sampling for the genus *Delma*, and aim to elucidate the synapomorphies shared by monophyletic groups within the family. The addition of Böhme's descriptions to our dataset prove extremely valuable, contributing observations on species which were inaccessible for this study.

V.iii—Monophyly of the Pygopodidae and Previous Phylogenetic Study

Although externally, pygopodids are substantially morphologically divergent from other gekkotans, evidence for the close relationship between these groups has been recognized and supported for a considerable period of time (Boulenger, 1885; Shute and Bellairs, 1953; Mcdowell and Bogert, 1954; Underwood, 1957; Miller, 1966; Wever, 1974; Greer, 1989).

Recent molecular studies have solidified the position of pygopodids within the Gekkota, as well as within the Pygopodoidea, further validating conclusions made in Böhme's (1988) preliminary hemipenial assessment of the Pygopodidae. While recent molecular studies have elucidated the sister relationship between pygopodids and carphodactylids, intergeneric relationships within the Pygopodidae have varied greatly, with no single topology receiving overwhelming support (Jennings, et al., 2003; Jackman, et al., 2008; Oliver and Sanders, 2009; Oliver and Bauer, 2011; Daza and Bauer, 2012). Morphological methods for phylogenetic analysis have also failed to create a single, favored tree, and have conflicted strongly with molecular trees. As a result of the great phenotypic diversification between pygopodid genera, and conservatism within genera, previously assessed morphological characters are largely uninformative at the intergeneric level, and highly susceptible to homoplasy at the interspecific level.

While flap-footed geckos have remained a monophyletic group, the Pygopodidae itself has been variously split on a number of occasions, generally as a result of the diminutive nature of *Aprasia*: Gray (1845)—Aprasiadae and Pygopodidae; Jensen (1901)—Ophiopsisepsidae (*Aprasia* as *Ophiopsiseps*) and Pygopodidae; Wells (2007)—Aprasiadae (*Abiliniea, Aprasia, Ophidiocephalus*) and Pygopodidae (*Delma, Lialis, Paradelma, Pletholax, Pygopus*). Additionally, Kluge (1976) recognized two subfamilies: the Pygopodinae (*Delma* and *Pygopus*) and Lialisinae (all remaining genera), and revisited this topic once again (Kluge, 1987) to reduce the flap-footed geckos to a subfamily—Pygopodinae, alongside the Diplodactylinae (Tribes Carphodactylini and Diplodactylini) within a greater Pygopodidae. Subsequently, Jennings et al.'s (2003) combined molecular-morphological results confidently supported a united Pygopodidae, and dispensed with subfamilial distinctions, instead recognizing a basal split between a group comprising *Delma* and *Lialis*, and all remaining pygopodid genera. More complete molecular sampling (Lee et al., 2009; Oliver, 2009) has strongly contradicted Jennings

et al.'s (2003) and previous findings, instead recognizing *Delma* as sister to all other pygopodid genera, and continues to confidently support the monophyly of this unique family.

V.iv—Hemipenial Morphology and Systematics

Morphological characters of male intromittent organs, particularly in squamates, provide sufficient systematic characteristics for inferring correct phylogenetic relationships (Branch, 1982; Arnold, 1986; Branch, 1986; Böhme, 1988; Köhler, et al., 2012).

Historically, many studies have discussed and relied upon the phylogenetic signal of hemipenial morphology, beginning with Cope (1896) (Mccann, 1946; Dowling and Savage, 1960; Dowling, 1967; Böhme, 1971; Branch, 1982; Arnold, 1986; 1986; Branch, 1986; Klaver and Böhme, 1986; Keogh, 1999; Köhler, et al., 2012). Distinct morphological characters and ornamentation, low intraspecific variation, and the rapid evolutionary trend of male genital morphology in relation to other morphological characters, make the study of hemipenial morphology a particularly valuable tool for systematists (Eberhard, 1985; Böhme, 1988; Keogh, 1999). Copulatory organs are diverse in their morphology, with various characters which can be described, counted, and scored, including size, shape, and ornamentation (Dowling and Savage, 1960; Keogh, 1999). Despite lack of resolution at deeper taxonomic levels, comparative phylogenetic study of the hemipenes is a great tool for specific and generic levels due to extremely low intraspecific variation. Ontogenetic and seasonal variation tied to reproductive activity may constitute some intraspecific variation, and has been recorded from some lacertids, iguanids, and chameleons (Böhme, 1988), and more recently in the gecko genus *Uroplatus* (Glaw, et al., 2006). However, ontogenetic change generally influences size, and not shape or ornamentation. While various other morphological characters or systems may be artificially influenced by homoplasy via factors of natural history; ecology, diet, or locomotion, hemipenial morphology appears

distanced from these pitfalls (Dowling, 1967; Böhme, 1971; Arnold, 1986; Branch, 1986; Klaver and Böhme, 1986; Böhme, 1988; Keogh, 1999).

Hemipenial diagnosis within the Gekkota began with Cope (1896), in the description of hemipenes from five currently recognized genera— *Cyrtodactylus, Eublepharus, Phyllodactylus, Tarentola*, and *Thecadactylus*. Since then, several studies have included observations and assessments of gekkotan hemipenes with phylogenetic implications. Standardly, gekkotan intromittent organs are bi-lobed, and often asymmetrical, with varying arrays of ornamentation. The new-world spaerodactylid genus *Aristelliger*, unique among gekkotans, poses a baculum-like structure, described and illustrated first by Kluge (1982), as a spiny ossification with a serrated edge, which extends distally from the apex of each lobe (Rösler and Böhme, 2006). Exclusive of Böhme (1988) however, descriptions of the genital morphology of pygopodids is absent. Additionally, cloacal spurs, and post-cloacal bones and sacs are often associated with reproductive morphology, and their presence in gekkotans is reviewed extensively by Kluge (1982).

To date, Böhme (1988) remains the only description and discussion of pygopodid hemipenes. In his description of *Aprasia*, *Delma*, and *Pygopus* genitals, Böhme interprets the position and state of calyces of *Pygopus* as a plesiomorphic character, supporting Kluge's (1974, 1976) placement of this genus as the basal-most member of the family. Using Kluge's (1976) subfamilial groups, the Pygopodinae (*Delma* and *Pygopus*) and Lialisinae (*Aprasia, Lialis, Ophidiocephalus, Pletholax*), Böhme identifies conflict within this ranking by way of similarity in ornamentation—or lack thereof—in *Aprasia* and *Delma*. He suggests the nude nature of *Aprasia* and *Delma* hemipenes may reflect a close evolutionary history, or instead be the result of an ornamental-reversal, or hemipenial simplification, as also seen in *Brookesia* (Klaver and Böhme, 1986). Current understanding of intergeneric relationships based on molecular results

however refute a sister taxa relationship between *Aprasia* and *Delma*, and phylogenetic conclusions regarding intergeneric relationships within the Pygopodidae by Böhme (1988) should be viewed as an artifact of insufficient sampling. Despite deep external morphological divergence from a tetrapodal ancestor, Böhme does identify pygopodid hemipenes as uniquely gekkotan, and a strong unifying character of the group. In order to continue in the same vein of Böhme's discovery, here we diagnose and describe the hemipenial morphology of a number of Australian pygopodids, particularly of the genus *Delma*, adding to current documentation of pygopodid hemipenes. Images, descriptions, and preparation of these organs may aid in future phylogenetic assessments of the Pygopodidae and future work in this area will provide additional discernible characteristics for recognizing, delimiting, and describing new species.

V.v—Methods and Materials: Hemipenial Preparation

The hemipenial condition is a complicated one, and paired hemipenes represent a synapomorphy of squamate reptiles (Greer, 1989). Hemipenes themselves are paired tubular organs, which when not in use are retracted and stored within the body in "inside-out" fashion (Dowling and Savage, 1960). When tucked inside the body, they are inverted like a glove, and upon stimulation, are engorged and pushed outside of the body—the inside in the stored state becoming the outer wall upon eversion. Upon being everted, hemipenes may protrude laterally, anteriorly, or posteriorly from the cloaca, and may be decorated with a number of ornaments including calyces (calyculi), flounces, spikes, hooks, and lobes. We generally follow terminology as proposed by (Dowling and Savage, 1960), however refer to Keogh (1999) for moderate adjustments. Accurate morphological hemipenial assessment—particularly of apical lobes—requires a fully everted hemipenis, either preserved in situ, or manually everted as described by Pesantes (1994). We acquired specimens on loan from the Western Australian Museum with

completely everted organs, and only in the absence of such specimens, did we select individuals with incompletely everted hemipenes. We abstained from destructive practices by excluding species for which entirely or partially everted organs could not be obtained. Incompletely everted hemipenes were injected to capacity with 1% KOH solution and left for one hour to soften tissue for manual eversion. After an hour, KOH was removed from organs, and liquid 1.5% agarose gel dyed with alizarin red was injected via 30 gauge hypodermic syringe, to complete volume. Dyed agarose gel set inside the hemipenes instantly, and red coloration allowed for increased contrast of structures, aiding observation and imaging.

Morphology of pygopodid hemipenes is severely reduced in complexity as well as physical size, when compared to other squamate taxa (Dowling, 1967; Arnold, 1986; Branch, 1986; Hoskin, 2011; Köhler, et al., 2012). Lack of calcareous spines and spicules present in other squamates makes staining structures difficult, and imaging of pygopodid hemipenes a challenge. As a result, we have reduced the number of characters addressed by Keogh (1998), and provide brief overall descriptions of organs of each species.

V.vi—Characters and Hemipenial Descriptions

Shape: Single (S), bi-lobed symmetrical (BS), bi-lobed asymmetrical (BA), or bi-lobed with additional median lobe (T).

Ornamentation: Nude (N), undifferentiated (UD) ornamentation is homogeneous and uniform over the entire surface of the hemipenis (e.g. spines only). Differentiated (D) ornamentation is defined as two or more differing types of ornaments (spines and micro-ornamentation).

Base: Ornamented (O) or nude (N).

Terminal sulcus: Sulcus spermaticus terminates at apex of lobe (TSA), at lateral edge of lobe (TSL), or medially as a sulcal pad (TSP). In asymmetrical conditions, the smaller lobe is listed first/followed by the larger lobe.

Spurs: General shape of the spur is rounded (R), pointed (P), flattened (F) or terminates in comb-like projections (C). Direction in which the spur projects is either posteriorly (P), dorsally (D) or posteriodorsally (U). A rounded spur which points dorsally would be marked RD.

As a result of low intraspecific variation in hemipenial morphology, the small sample sizes of this study should provide sufficient for our interest (Arnold, 1986; Böhme, 1988; Keogh, 1999). The relatively small breadth of this study however, (22 spp., 5 genera—Table V.1) allows us to describe each species independently. Closely related species, or those similar in hemipenial morphology may refer to one another. Several species (*Aprasia parapulchella*, *Delma pax*, *Lialis burtonis)*, are included despite incompletely everted hemipenes. These cases were not everted when fixed, and could not be manually everted, however still provide some phylogenetic utility. Characters which could not be scored for these taxa are symbolized by—in Table V.2.

Table V.1. Taxa, locality data, and sources of specimens examined in this study.

Taxon	Collection no.*	State	Locality	Latitude	Longitude
Aprasia haroldi	WAM 163615	Western Australia	Dirk Hartog Island	25°41'60"S	113°0'0"E
Aprasia parapulchella	WAM 144181	Western Australia	4 km S Collie	33°22'03"S	116°13'49"E
Aprasia parapulchella	WAM 153920	Western Australia	Bindoon Military Training Area	31°20'31"S	116°15'39"E
Aprasia pulchella	UMMZ 131241	Western Australia	Canning Dam	NA	NA
Aprasia repens	WAM 144255	Western Australia	Burns Beach	31°43'04"S	115°45'59"E
Aprasia repens	WAM 153978	Western Australia	Bindoon Military Training Area	31°11'42"S	116°18'26"E
Aprasia smithi	WAM 120652	Western Australia	8 km NW Mardathuna Homestead	24°25'44"S	114°30'00"E
Delma australis	WAM 112667	Western Australia	Ponier Rock	32°56'00"S	123°30'00"E
Delma australis	WAM 116279	Western Australia	Kalbarri	27°51'00"S	114°10'00"E
Delma australis	WAM 135108	Western Australia	Bullabulling	30°51'59"S	120°54'24"E
Delma australis	WAM 140395	Western Australia	90 km NE Wubin	29°31'23"S	117°10'10"E
Delma 'australis' sp. nov.	WAM 144236	Western Australia	Bandalup Hill	33°40'29"S	120°23'54"E
Delma 'australis' sp. nov.	WAM 172285	Western Australia	Scaddan	33°26'27"S	121°43'17"E
Delma borea	WAM 154148	Western Australia	Barrow Island	20°47'18"S	115°27'43"E
Delma borea	WAM 158010	Western Australia	Koolan Island	16°08'45"S	123°44'57"E
Delma butleri	WAM 120322	Western Australia	7 km E Cape Cuvier	24°13'26"S	113°27'41"E
Delma butleri	WAM 120819	Western Australia	25 km SSE Peron Homestead	26°03'00"S	113°37'00"E
Delma butleri	WAM 123911	Western Australia	Bulong	30°45'00"S	121°48'00"E
Delma desmosa	WAM 134414	Western Australia	Lake MacKay	22°26'47"S	128°17'33"E
Delma elegans	WAM 135462	Western Australia	Mount Brockman	22°28'00"S	117°18'00"E
Delma fraseri	WAM 115138	Western Australia	Ken Hearst Park	32°04'60"S	115°52'60"E
Delma fraseri	WAM 135503	Western Australia	Redcliffe, Perth Suburb	31°56'00"S	115°57'00"E
Delma fraseri	WAM 141191	Western Australia	15 Km NNE Lancelin	30°59'31"S	115°23'43"E
Delma fraseri	WAM 154039	Western Australia	Muchea Air Weapons Range	31°38'16"S	115°55'31"E
Delma grayii	WAM 154364	Western Australia	Hindmarsh Nature Reserve	31°17'00"S	117°02'00"E
Delma grayii	WAM 156220	Western Australia	Ballajura	31°51'11"S	115°55'11"E
Delma haroldi	WAM 138951	Western Australia	West Angelas	23°11'42"S	118°36'54"E
Delma haroldi	WAM 154831	Western Australia	Goldsworthy, Shay Gap Road	20°25'45"S	120°11'11"E
Delma inornata	UMMZ 131156	Victoria	Numurkah	NA	NA
Delma inornata	UMMZ 131186	New South Wales	Finley	NA	NA
Delma nasuta	WAM 154288	Western Australia	Fortescue Marsh	21°48'09"S	118°54'39"E
Delma nasuta	WAM 157568	Western Australia	Robe River	21°40'26"S	115°53'21"E
Delma pax	WAM 135337	Western Australia	Cape Lambert	20°48'36"S	116°56'31"E
Delma pax	WAM 166212	Western Australia	Mount Whaleback	23°19'41"S	120°01'07"E
Delma tincta	WAM 135487	Western Australia	Urala Station	21°46'58"S	114°52'11"E
Delma tincta	WAM 141584	Western Australia	1 km N Quobba Homestead	24°22'24"S	113°24'19"E
Delma tincta	WAM 146589	Western Australia	228 km SSW Port Hedland	22°20'24"S	119°00'00"E
Lialis burtonis	WAM 110652	Western Australia	Shay Gap Road, Goldsworthy	21°43'00"S	122°14'00"E
Lialis burtonis	WAM 154003	Western Australia	Muchea Air Weapons Range	31°38'32"S	115°55'03"E
Lialis burtonis	WAM 154007	Western Australia	Muchea Air Weapons Range	31°38'32"S	115°55'03"E
Pletholax g. gracilis	WAM 106172	Western Australia	Marangaroo	31°48'00"S	115°50'00"E
Pletholax g. gracilis	WAM 137463	Western Australia	Cervantes	30°45'03"S	115°12'11"E
Pygopus lepidopodus	ZFMK 21290	New South Wales	Sydney	NA	NA
Pygopus nigriceps	UMMZ 131174	South Australia	Innaminka	NA	NA

*UMMZ = University of Michigan Museum of Zoology; WAM = Western Australian Museum; ZFMK = Zoologisches Forschungsmuseum Alexander Koenig.

Aprasia haroldi

Fully everted—extremely minute, single lobe covered entirely in micro-ornamental stippling—save the sulcus. Base nude until constriction at bottom of lobe, sulcus broad and shallow. Hemipenis boxing glove shaped.

Aprasia parapulchella

Incompletely everted—bi-lobed. Sulcus narrow at base, until constriction at base of fork, sulcus becomes broad and shallow along lengths of lobes. Light micro-ornamentation of asulcal side, with sulcus nude.

*Aprasia pulchella**

Fully everted—bi-lobed and asymmetrical, inner lobe (as prepared in-situ) larger. Sulcus spermaticus forked, with much longer branch on inner lobe. Little ornamentation can be observed beside the presence of a pustular epithelium, and absence of calyx bearing surfaces.

Aprasia repens (Fig.V.1—1a,b)

Fully everted—single lobe. Asulcal and lateral faces completely covered with micro-ornamental stippling, including base. Slipper-shaped hemipenis, recurving posteriorly, elf-shoe in appearance, similar in jai alai shape to *A. smithi*. Sulcus narrow and deep until reaching lobe, becomes deep and wide, transitioning into sulcal pad, pad strongly surrounded by deep suclal lips. Distinct nub at posterior facing edge of asulcal face—potential remnant of secondary lobe.

Aprasia smithi

Fully everted—single lobe. Hemipenis is long, thin, and curves dorsally and against body wall after exiting cloaca. Stippled with micro-ornamentation laterally, with stronger spines along asulcal ridge. The sulcus is wide and shallow, and reaches apex. Hemipenis resembles Jai alai mit.

Delma australis (Fig.V.1—2a,b)

Fully everted—single lobe, boxing glove shape, extends laterally from cloaca and curls back towards midline. Both sulcate and asulcate surfaces covered in fine micro-ornamentation, with the exclusion of broad, shallow sulcus which does not reach apex.

Delma sp. nov. (*australis* group)

Fully everted—single lobe, apex appears more truncate and lobe more bulbous than *australis*. Strongly ornamented on both sulcal and asulcal faces, with the exclusion of the sulcus. Sulcus sharply edged by lips, and deep, terminating prior to apex. Apex projects posteriorly substantially, but does not reach point found in *australis*.

Delma borea

Fully everted—bi-lobed and strongly asymmetrical. Posterior/ventral lobe elongate with truncate, nude apex, which is reached by sulcus. Dorsal/anterior lobe hammer shaped, with sulcus reaching lateral face before opening onto sulcal pad. Base and lower quarter of lobes nude, but finely micro-ornamented across asulcal face. Terminus of longer lobe ends in flat disc, with sulcal lips strongly folding over, nearly closing over sulcus.

Delma butleri

Carnarvon (WAM 120322, 120819)—Fully everted—bi-lobed. Lobes appear approximately equal in size, shallowly forked compared to other delmas, disctinctly Y-shaped in comparison to T shape of *butleri* WAM 123911. Base nude until just prior to cleft, with micro-ornamentation covering asulcal face, becoming stronger laterally. Sulcus, buffered by deep sulcal lips, extends laterally beyond split of lobes, opening onto sulcal pad, facing dorsally.

WAM 123911—Fully everted—bi-lobed, with distinct “whale-tail” shape, T split between lobes, with apex of lobes terminating more in points than the lobular end of Carnarvon *butleri* samples. Sulcus is deep and narrow, forks at cleft of lobes, and extends laterally. Medial

lateral faces of lobes (closest to one another) nude. Sulcus terminates laterally, opening out onto nude sulcal pad.

Delma desmosa

Fully everted—bi-lobed and highly asymmetrical, similar in general shape to *tincta, elegans, pax*, and *borea*. Anterior/dorsal lobe much shorter, with hammerhead shape. Posterior/ventral lobe elongate, with truncate, nude tip, and strongly folded sulcal lips. Both sulcal and asulcal faces are ornamented.

Delma elegans (Fig.V.1—3a,b)

Fully everted—bi-lobed. Asulcal face strongly stippled and micro-ornamented, but restricted to the lobes, base nude, and lateral sides of lobes stippled. Anterior lobe much smaller and broader, but unlike the hammerhead shape of *pax*. Sulcus very deep and narrow on both lobes, extending laterally away from midline and not directly towards apex, becoming shallow at most distal edge of sulcal pad—sulcal pad nude.

Delma fraseri

Fully everted—bi-lobed. Smaller lobe approximately one-third size of larger, however similar in shape—broad and spatulate, clover leaf shaped. Entire hemipenis bare, no strong stippling as in others. Sulcus narrow and deep, until reaching cleft of lobes, then becomes extremely shallow channel which diverts laterally away from the midline, and opens up into a shallow pad-like surface on each lobe.

Delma grayii

Fully everted—bi-lobed, both lobes approximately same size; asulcal side only lightly stippled, following around to lateral edges; sulcus deep and narrow, deepest at cleft between lobes, and becomes extremely narrow and channel-like as bifurcates and diverts away from midline; lobe-sulcus-channel opens up onto broad, flat, pad covering most of sulcal side of lobe.

Delma haroldi (Fig.V.1—4a,b)

Fully everted—bi-lobed and only slightly asymmetrical, with posterior lobe smaller, but of similar overall shape. Sulcus is deep and narrow, and terminates laterally on each lobe, after splitting at lobe-fork. Sulcus opens up onto nude sulcal pad. Asulcal face only lightly ornamented, extending onto base. Spur projects posteriorly, and distal tip covered in several projects, giving it a comb-like appearance.

*Delma inornata**

Fully everted—bi-lobed, hemipenis is bulb-shaped, with poorly differentiated apical lobes. The inner (in-situ) lobe is larger than outer lobe. Sulcus is forked, and surface epithelium is covered by strongly pustulous features, absent of calyces.

Delma nasuta (Fig.V.1—5a,b)

Fully everted—bi-lobed, with strong asymmetry between lobes. Anterior/dorsal lobe (generally smaller in asymmetrical-hemipened delmas) strongly cleft at distal end of sulcus, opening onto laterally-facing sulcal pad. Smaller lobe clover-leaf shaped. Posterior/ventral lobe larger, and truncate at terminus, with sulcus reaching apex. Sulcal lips on larger lobe strongly overlap sulcus. Asulcal face only lightly ornamented, base nude. Spurs project dorsally and posteriorly, and terminate in comb-like tips, not as pronounced as *haroldi*.

Delma pax (Fig.V.1—7a,b)

Fully everted—bi-lobed, with dorsal lobe shorter and broader, hammerhead in shape, truncate, with sulcus reaching apex; ventral lobe elongate, narrow, end truncate, covered in micro-ornamentation; asulcal surface micro-ornamented laterally, nude medially; sulcus deep and narrow; both lobes nude until beyond fork, with finely stippled tips.

Delma petersoni (Fig.V.1—6a,b)

Fully everted—strongly bi-lobed, with deep cleft between approximately similar sized lobes; almost entirely nude, similar to *fraseri*; deep, narrow sulcus bisects at lobe-cleft, becomes narrow channels diverting away from midline and opening out into broad flat surface on sulcal side.

Delma tincta

Fully everted—bi-lobed and asymmetrical, with hammerhead shape of smaller lobe. Both lobes, including asulcal faces, but excluding sulcal pads, are covered in fine micro-ornamentation which is strongest on asulcal face of large lobe. Sulcus narrow and deep, continues laterally from lobe-fork, to lateral edge of sulcal pad of shorter lobe, and to apex of elongate lobe. Smaller, hammer-shaped lobe broad and flattened, creating large sulcal face large composed of sulcal pad. Spur rounded posteriorly and small, covered partially by first postcloacal scale.

Lialis burtonis

Incompletely everted—distinctly bi-lobed, deep sulcus, and base nude. Asulcal and sulcal faces, excluding sulcus, covered in fine ornamentation.

Pletholax gracilis (Fig.V.1—8a,b)

Fully everted—bi-lobed, and mitten shaped, dorsal lobe substantially reduced, ventral lobe larger and elongate; asulcal surface partially nude, but densely covered in micro-spines and ornamentation laterally, base nude until constriction at base of lobe division; sulcus is narrow, but deep, and widens towards apices, sulcus reaches apex of each lobe. (106172, 137463)

*Pygopus lepidopodus**

Incompletely everted—specimen preserved in 1864. Median lobe can be made out—reminiscent of *P. nigriceps*. Basal calyces on base are small and end prior to apex of lateral lobes.

*Pygopus nigriceps**

Fully everted—tri-lobed, short and broad. Sulcus spermaticus divided into two long forks along the length of larger, divided lobes. Sulcus is a deep depression. A small, pear-shaped, undivided lobe sits between larger lateral main lobes. Asulcal face covered in small calyces, base covered in transverse calyces with beaded edges. The outer lateral lobes are covered with small deep calyces with prickly edges. Asulcal face of lobes smooth.

*Denotes taxa examined by Böhme (1988), and included in this study.

Table V.2. Summary of hemipenial morphology of pygopodid geckos. *denote taxa examined by Böhme (1988).

Taxon	No.	Shape	Ornamentation	Base	Terminal Sulcus	Spurs
Aprasia haroldi	1	S	UD	N	TSA	—
Aprasia parapulchella	1	BA	UD	N	TSA/TSP	—
**Aprasia pulchella*	1	BA	UD	—	TSA	—
Aprasia repens	2	S	UD	O	TSA/TSP	—
Aprasia smithi	1	S	D	N	TSA/TSP	—
Delma australis	4	S	UD	N	TSP	FU
Delma australis S.WA	2	S	UD	N	TSP	FU
Delma borea	2	BA	UD	N	TSP/TSA	RP
Delma butleri	3	BS	UD	N	TSL/TSP	CP
Delma desmosa	1	BA	UD	N	TSL/TSA	RP
Delma elegans	1	BA	UD	N	TSL/TSP	RP
Delma fraseri	2	BA	N	N	TSL/TSP	PU
Delma grayii	2	BS	UD	N	TSL/TSP	PP
Delma haroldi	1	BA	UD	N	TSL/TSP	CP
**Delma inornata*	3	BA	UD	N	—	—
Delma nasuta	2	BA	UD	N	TSL/TSA	CP
Delma pax	2	BA	UD	N	TSL/TSA	RP
Delma petersoni	2	BS	N	N	TSL/TSP	PU
Delma tincta	3	BA	UD	N	TSL/TSA	RP
Lialis burtonis	4	B–	D-micro and calyces	N	—	—
Pletholax gracilis	2	BA	D–micro and spines	N	TSA	—
**Pygopus lepidopodus*	1	T	D-micro and calyces	O	TSA	—
**Pygopus nigriceps*	1	T	D-micro and calyces	O	TSA	—

Symbols as follows: S=Single lobe, BA=Bi-lobed asymmetrical, BS=Bi-lobed symmetrical, UD=Undifferentiated ornamentation, D=Differentiated ornamentation, N=Nude of ornamentation, TSA=Sulcus terminates at apex of lobe, TSL=Sulcus terminates at lateral edge of lobe, TSP=Sulcus terminates medially into broad sulcal pad. See materials and methods for descriptions of characters, and Table V.1 for material examined.

V.vii.—Phylogenetic Discussion of Hemipenes in Pygopodidae

Relative to other squamate groups, and even other gekkotans, pygopodid hemipenes are markedly reduced in their overall morphology (Böhme, 1988). Morphological reduction in hemipenial characters may be the result of an ancestral miniaturization event at the base of the

pygopodid tree, as seen in *Brookesia* chameleons (Klaver and Böhme, 1986). While in contrast, similarly small squamates such as gymnopthalmids have not seen this simplification in hemipenial morphology, pygopodid hemipenial size (length from cloaca to apex) relative to body length (SVL) is substantially smaller than that of the gymnopthalmid *Iphisa elegans* (Nunes, et al., 2012). This morphological simplification is most pronounced in the three species of *Aprasia* (*A. haroldi, A. repens, A. smithi*) and two *Delma* species (*D. australis*, *D.* sp. nov.) which exhibit single-lobed hemipenes. These species are among the smallest members of their respective genera, and the disjunct nature of this characteristic in the pygopodid tree suggests two independent evolutionary events. Presence of bi-lobed hemipenes in all five examined pygopodid genera, as well as the exclusive condition in carphodactylid and diplodactylid geckos, supports the pygopodid and Pygopodoidean ancestral hemipenial conditions as bi-lobed.

Mitochondrial history suggests a basal split within *Aprasia* which finds the examined *haroldi, pulchella, repens*, and *smithi* members of a single monophyletic group, and *parapulchella* a member of the remaining deep divergence. *Aprasia haroldi, repens*, and *smithi* all occur as closely related taxa within a single clade, closely related to *Aprasia fusca* and *A. rostrata*, as well as the recently described *clairae* (Maryan, et al., 2013) and *litorea* (Maryan, et al., 2013)—for which no hemipenial assessment has been made. *Aprasia pulchella*—closely related to the singly-lobed group, exhibits the bi-lobed hemipenial condition, similar to the asymmetrically bi-lobed hemipenes of *Aprasia parapulchella*, despite only distant relatedness within *Aprasia*. Only moderate current molecular and hemipenial sampling of this genus requires additional assessment of *Aprasia* species to determine if the ancestral condition is an asymmetrically bi-lobed hemipenis, and the single lobe hemipenis occurs as a synapomorphy of the *fusca* group (*smithi, litorea, haroldi, clairae, repens, rostrata, fusca*). Reduction in hemipenial characters as a result of miniaturization in fossorial limbless squamates has been

observed in the morphologically and ecologically similar typhlopids (Khan, 1999; Thomas and Hedges, 2007).

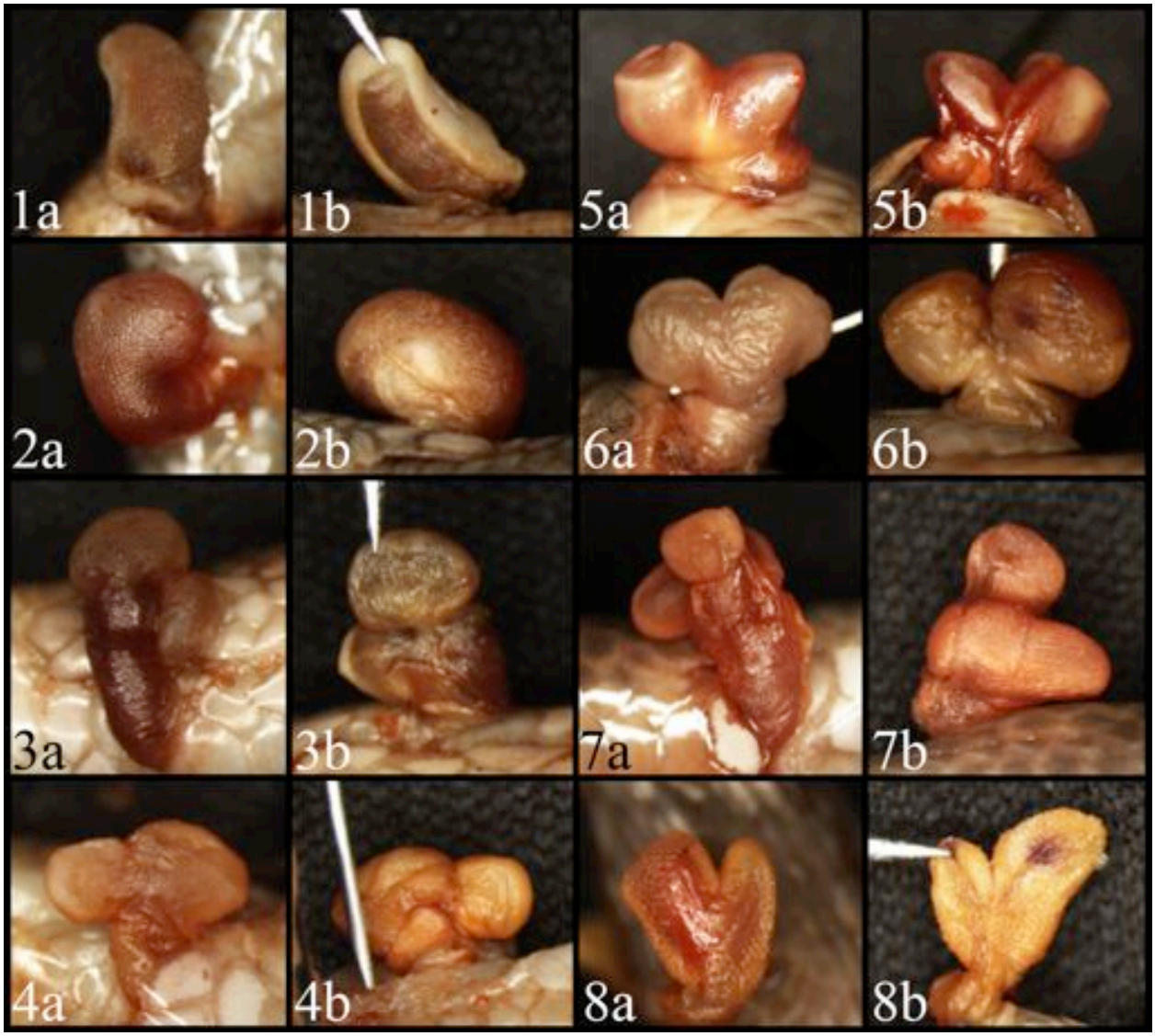

Figure V.1. Asulcal (a) and sulcal (b) views hemipenes of eight species of Pygopodids: 1–*Aprasia repens* WAMR144255; 2–*Delma australis* WAMR112667; 3–*Delma elegans* WAMR135462; 4–*Delma haroldi* WAMR163615; 5–*Delma nasuta* WAMR154288; 6– *Delma petersoni* WAMR165873; 7– *Delma pax* WAMR135337; 8–*Pletholax gracilis* WAMR106172.

Perhaps more surprising than morphological reduction in the diminutive fossorial *Aprasia*, is the occurrence of singly-lobed hemipenes in the *Delma australis* group. Here, hemipenial reduction is noted in *D. australis* and the newly described *D. australis* S.WA, however remaining members of the group *D. concinna* and *D. torquata* await assessment.

Concordance between mtDNA and nDNA topologies may indicate a similar hemipenial condition between *australis* sensu lato and *torquata*. Assessment of hemipenial morphology of *concinna* and *torquata* would contribute to the understanding of this group. Observation of singly-lobed hemipenes in *D. concinna* or *D. torquata* would strongly support inclusion of these species in the *D. australis* clade, establishing a synapomorphy of this group. In contrast, identification of a bi-lobed hemipenis in *D. torquata* would hint at a potential past introgression event.

Within the bi-lobed pygopodids, there remains considerable distinction between genera, species groups, and individual species. Although members of *Aprasia* may exhibit either singly- or bi-lobed hemipenes, regardless of overall shape, the sulcus spermaticus appears as a broad sulcal pad, comprising most of the sulcal face of the hemipenis. The sulcal lips in *Aprasia* also strongly delineate the sulcus spermaticus, and the entirety of the asulcal and sulcal faces, including even the sulcal lips, are covered in fine micro-ornamentation. The sulcal pad terminates at the apex in both singly- and bi-lobed species of *Aprasia*, and remains unornamented in all observed species.

The moderate to small sized, heavily nuchal banded *Delma* species of northern and northwestern portions of Australia: *D. borea, D. desmosa, D. elegans, D. pax, D. tincta*, can be distinguished by asymmetry not only in size, but in general shape of the bi-lobed hemipenes. In *D. borea, D. desmosa*, *D. pax*, and *D. tincta* a hammer shaped lobe extends anteriorly or proximally, while the second lobe, elongate, with a truncate apex and strongly folded sulcal lips, extends dorsally or distally. *D. elegans* also exhibits a strongly asymmetrical design, however the disparity in shape between the anterior/medial and dorsal/distal lobes are less pronounced, and the dorsally projecting lobe is not elongate, nor truncate in apex. Based on similarity in shape, asymmetry, and ornamentation, we suggest a close affinity between the *D. borea, D. desmosa,*

D. pax, and *D. tincta*, but are unable to further hypothesize systematics based on hemipenial morphology alone. *D. elegans* appears to show a much simplified asymmetrical condition, potentially embodying the ancestral condition for this group.

Delma fraseri and *D. petersoni*, previously confused under a single species, display a nearly identical hemipenial condition, most likely the result of recent ancestry. Hemipenes of these two species are either narrowly asymmetrical, or symmetrical in size and shape, both nude of ornamentation, with sulci that terminate laterally on sulcal pads. Based on mitochondrial data (Jennings et al., 2003), *D. grayii* has been recognized as sister taxon to *D. fraseri*, and despite similar hemipenial morphology—narrowly asymmetrical bulb-shaped lobes, sulcus terminating laterally in pads—preliminary nuclear DNA data (Brennan, 2014) suggests this sister relationship may instead be an artifact of a historical introgression event. In light of these preliminary findings, external appearance, and the extreme hemipenial similarity between *D. fraseri* and *D. petersoni*, we suggest a sister taxa relationship between these two species. We identify hemipenial similarity with *D. grayii* may be the result of aforementioned introgression event, the cause of such an event, or a bi-lobed, narrowly asymmetrical, bulb-shaped, largely unornamented hemipenis may represent the ancestral *Delma* hemipenial condition.

Moderate asulcal ornamentation, alongside a narrowly asymmetrical bi-lobed design unites *Delma grayii* with *D. inornata* and the *D. butleri* group (*D. butleri, D. haroldi, D. nasuta*). Save *D. nausta*, this group is typified by micro-ornamentation restricted to the lobes, distal to the point of bifurcation of the sulcus. The sulcus terminates laterally onto shallow broad sulcal pads, which are also devoid of ornamentation. Within *D. butleri* we recognize two differing hemipenial conditions: large-bodied and lightly patterned *D. butleri* from the Carnarvon region (WAM120322, WAM 120819) display hemipenes similar to that of *D. haroldi*, whereas the more northern and inland *D. butleri* (WAM123911) shows a distinct shape and lack of

ornamentation which highlights the necessity of further study within this broadly distributed morphologically variable species. *D. nasuta* also exhibits an enigmatic hemipenial condition in which the strongly asymmetrical lobes are both truncate, and the sulcus remains deep and narrow as it terminates at the apex of each lobe. Despite disparate hemipenial morphology, *D. nasuta* has been associated with *D. butleri* and *D. haroldi* based on general morphology (Kluge, 1974), osteology (Kluge, 1976), and mitochondrial (Jennings et al., 2003) and nuclear (Brennan, 2014) DNA results. Here, we also recognize as a synapomorphy of the *D. butleri* clade, the comb-like serrated edge of the cloacal spurs. The spurs are oriented posteriorly, and small projections of the distal spur edge are most pronounced in *D. haroldi*, weaker in *D. butleri*, and less developed but still observable in *D. nasuta*. The generalized morphology of the hemipenes in this *D. inornata*, *D. grayii*, and *D. butleri* group, as well as in *D. fraseri* and *D. petersoni*, despite a non sister-taxa relationship may suggest that an approximately symmetrical bi-lobed, and relatively unornamented hemipenis may constitute the ancestral *Delma* hemipenial design. While hemipenial sampling for this genus remains incomplete, this hypothesis would suggest the strongly asymmetrical hemipenis of the northwest Australian group (*D. borea, D. desmosa, D. elegans, D. pax, D. tincta*), and the singly-lobed hemipenis of the *D. australis* group represent significant morphological divergences.

The monotypic genus *Pletholax* displays a strongly asymmetrical bi-lobed hemipenis which is covered by coarse, dense spines along the lateral and apical portions of the asulcal face, and the sulcal lips. Hemipenes of *Pletholax gracilis* are unlike any other pygopodid hemipenis in ornamentation, as well as general shape. The morphology of *Pygopus* hemipenes are also unique to pygopodids in the presence of a third, undivided, medial lobe. Both observed species—*Pygopus lepidopodus* and *P. nigriceps*—display this medial lobe, as well as differentiated ornamentation of the sulcal and asulcal faces, and ornamented hemipenial bases. Assessment of

Lialis burtonis is limited to incompletely everted specimens, and as such, makes phylogenetic inference difficult, however, we observe that this species shows a bi-lobed condition, and lobes appear covered in differentiated ornamentation similar to that of *Pygopus*. Similarity in ornamentation may suggest systematic relatedness between *Pygopus* and *Lialis*, or may be an artifact of the much larger adult size of species of these genera, relative to that of other pygopodids.

V.viii.—Cloacal Spurs and Reproductive Behavior

Morphology of the cloacal spurs and post-cloacal bones and sacs are often mentioned in the context of reproductive biology. In Gekkotans, post-cloacal bones and sacs have been heavily reviewed by Kluge (1982), however little attention has been paid to cloacal spurs of geckos. Due to the paucity of behavioral data regarding pygopodids, we draw on the observations of other gekkotans and squamates to address the implication of cloacal spurs and postcloacal bones in reproductive success (Kluge, 1982; Kluge, 1987). The occurrence of post-cloacal bones is a synapomorphy of gekkotans, uniting the pygopodids with other members of this group (Greer, 1989). While cloacal bones were identified by Kluge (1982) in all examined pygopodid species, cloacal sacs were absent in all *Delma* and *Lialis*; present in both sexes of *Paradelma* and *Pygopus*; present in males of *Aprasia* and *Pletholax*, absent in female *Pletholax*, and inter- and intraspecifically variable in *Aprasia* females.

In the eublepharid gecko *Coleonyx variegatus*, the presence and use of spurs are important for successful mating (Greenberg, 1943). Here, after positioning himself alongside the female, and contorting himself to face vent-to-vent, the male slides the closer spur longitudinally along the female's body axis, and across her cloacal opening, in an attempt to gain purchase among the loose skin below the vent. In doing so, the pull of the male's spur draws back the

lower lip of the female's cloaca, causing her cloaca to gape, creating an opportunity for the male to evert and insert his hemipenis. Although pygopodid and eublepharid geckos differ morphologically, specifically in the presence or absence of loose post-cloacal skin, spurs may still serve a similar purpose.

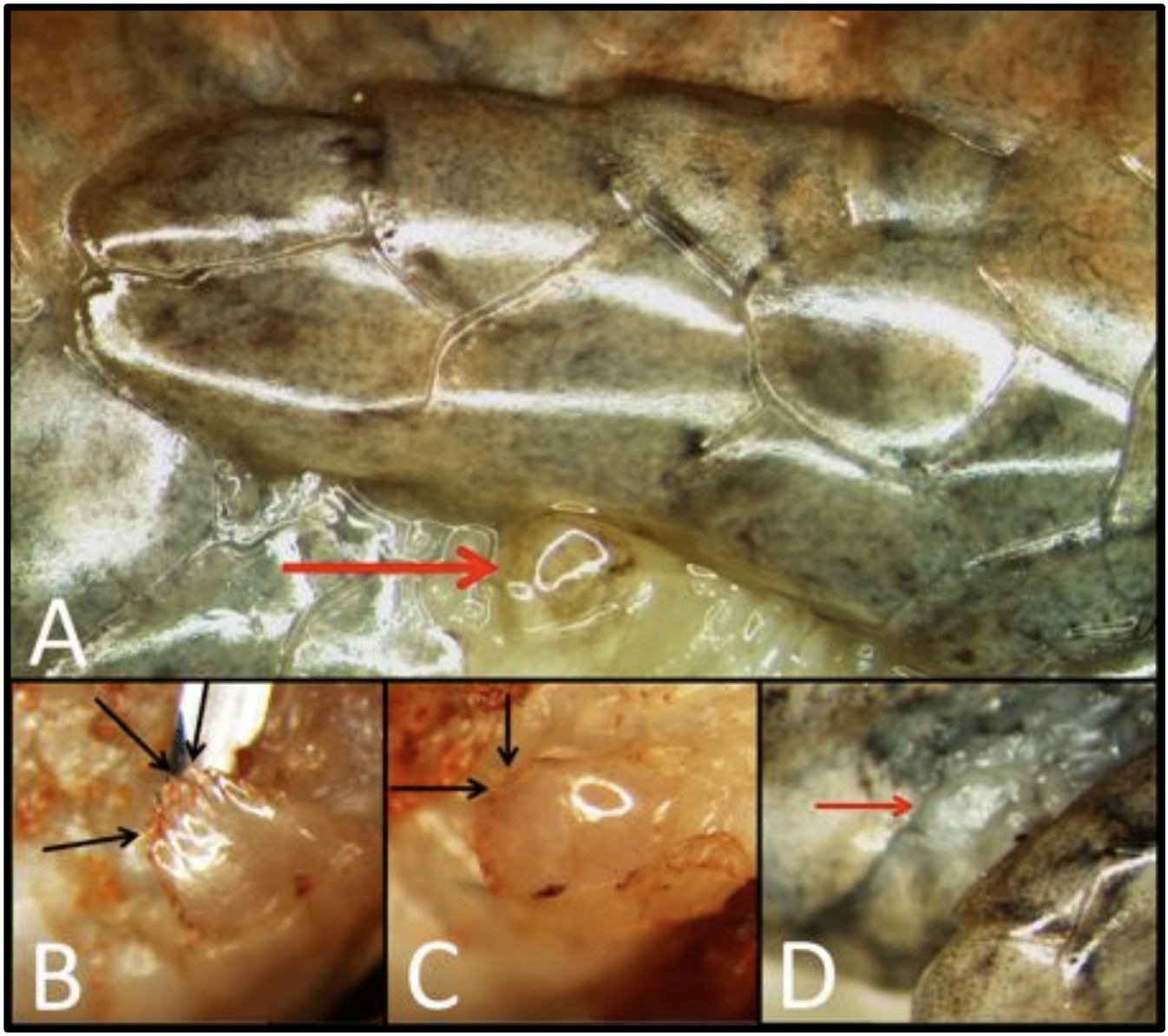

Figure V.2 Lateral view of right cloacal spur of : A—*Delma fraseri* WAMR141191; B—*Delma haroldi* WAMR163615; C–*Delma nasuta* WAMR154288; D—*Delma australis* WAMR140395. Red arrows indicate position of the spur, and black arrows indicate fine projections on posterior-facing distal tip of the spur, a synapomorphy of the *D. butleri* group.

In other limb reduced squamates, such as pythonid snakes—whose imbricate scales and tighter skin more accurately resemble the pygopodid condition—cloacal spurs appear as the only external vestige of the hind limbs, where they tip the distal portion of the femur (Greer, 1997). Here, males may use the spur to stroke and stimulate the female during courtship, gauge and encourage her receptivity, and as in eublepharids tactily align the cloaca and expedite mating (Murphy, et al., 1981; Hoser, 1985; Schouten, 1985; Walsh, 1985; Slip and Shine, 1988; Greer, 1997). Additionally, spurs may be used in male–male combat, to gain purchase and scratch the opposition (Barker, et al., 1979; Van Der Heijden, 1986). It is important to note the association between spurs and femoral remnants in pythonids, and the presence of external hindlimbs in pygopodids acknowledges the non-homology of spurs across these squamate families. This however, does not require their use to differ.

Cloacal spurs in pygopodids are small structures hidden behind the hindlimb flap, just dorsal and posterior to the cloaca. Spurs are indistinguishable from hindlimb scales in *Aprasia*, but in the comparatively speciose *Delma*, spurs represent another morphological character capable of identifying species groups. As mentioned, the large, comb-like spur of *D. haroldi* (Fig.V.2B), is visible to a much reduced degree in the closely related *D. butleri* and *D. nasuta* (Fig.V.2C). In *D. australis* and *D.'australis*' sp. nov., the spur (Fig.V.2D) is much less pronounced, rounded, and wider than it is long. In contrast, members of the *D. fraseri* and northwest Australia groups display moderate sized spurs which are rounded in the smaller members of the northwest group *D. borea, D. desmosa, D. elegans, D. pax, D. tincta,* and are pointed in *D. fraseri* (Fig.V.2A) and *D. petersoni*.

While this study adds to the current knowledge of hemipenial structure and spur morphology and their phylogenetic affinities within Pygopodidae, we present this data as a work in progress. Continued hemipenial assessment of *Delma* species and other pygopodid genera will

contribute substantially to our understanding of reproductive evolution and isolation within the flap-footed geckos. The remarkable morphological divergence of pygopodids when compared to their gekkotan ancestors, represents an immense leap, which may present itself in other aspects of anatomy not yet assessed. Complete descriptions of the hemipenes of monotypic *Ophidiocephalus* and *Paradelma*, and more complete description of *Lialis* species may further provide insight into intergeneric relationships within this unique family.

VI.—Literature Cited

Arnold, E.N., 1986a. The hemipenis of lacertid lizards (Reptilia: Lacertidae): Structure, variation, and systematic implications. Journal of Natural History 20, 1221-1257.

Arnold, E.N., 1986b. Why copulatory organs provide so many useful taxonomic characters: the origin and maintenance of hemipenial differences in lacertid lizards (Reptilia: Lacertidae). Biological Journal of the Linnean Society 29, 263-281.

Ballard, J.W.O., Whitlock, M.C., 2004. The incomplete natural history of mitochondria. Molecular Ecology 13, 729-744.

Barker, D.G., Murphy, J.B., Smith, K.W., 1979. Social behavior in a captive group of Indian pythons, *Python molurus* (Serpentes: Boidae) with formation of a linear social heirarchy. Copeia 1979, 466-471.

Barker, W.R., Greenslade, P.J.M., 1982. Evolution of the flora and fauna of arid Australia. Peacock Publications, Frewville, South Australia.

Bauer, A.M., 1986. Saltation in the pygopodid lizard, *Delma tincta*. Journal of Herpetology 20, 462-463.

Bauer, A.M., 2013. Geckos: The Animal Answer Guide. JHU Press.

Bauer, A.M., de Silva, A., Greenbaum, E., Jackman, T., 2007. A new species of day gecko from high elevation in Sri Lanka, with a preliminary phylogeny of Sri Lankan Cnemaspis (Reptilia, Squamata, Gekkonidae). Zoosystematics and Evolution 83, 22-32.

Beck, R.M.D., 2008. A dated phylogeny of marsupials using a molecular supermatrix and multiple fossil constraints. Journal of Mammalogy 89, 175-189.

Belfiore, N.M., Liu, L., Moritz, C., 2008. Multilocus phylogenetics of a rapid radiation in the genus *Thomomys* (Rodentia: Geomyidae). Systematic Biology 57, 294-310.

Böhme, W., 1971. Über das Stachelepithel am Hemipenis lacertider Eidechsen und seine systematische Bedeutung. Zeitschrift fur zoologische Systematik und Evolutionsforschung, 187-223.

Böhme, W., 1988. Zur Genitalmorphologie der Sauria: Funktionelle und stammesgeschichtliche Aspekte. Zoologisches Forschungsinstitut und Museum Alexander Koenig, Bonn, Germany. 27.

Boulenger, G.A., 1885. Catalogue of the lizards in the British Museum of Natural History. British Museum of Natural History, London. 1.

Branch, W.R., 1982. Hemipeneal morphology of platynotan lizards. Journal of Herpetology 16, 16-38.

Branch, W.R., 1986. Hemipenial morphology of African snakes: a taxonomic review Part 1. Scolecophidia and Boidae. Journal of Herpetology 20, 285-299.

Brown, W.M., George, M., Wilson, A.C., 1979. Rapid evolution of animal mitochondrial DNA. Proceedings of the National Academy of Sciences, USA 76, 1967-1971.

Byrne, M., Steane, D.A., Joseph, L., Yeates, D.K., Jordan, G.J., Crayn, D., Aplin, K., Cantrill, D.J., Cook, L.G., Crisp, M.D., Keogh, J.S., Melville, J., Moritz, C., Porch, N., Sniderman, J.M.K., Sunnucks,

P., Weston, P.H., 2011. Decline of a biome: evolution, contraction, fragmentation, extinction and invasion of the Australian mesic zone biota. Journal of Biogeography 38, 1635-1656.

Byrne, M., Yeates, D.K., Joseph, L., Kearney, M., Bowler, J., Williams, M.A.J., Cooper, S., Donnellan, S.C., Keogh, J.S., Leys, R., Melville, J., Murphy, D.J., Porch, N., Wyrwoll, K.H., 2008. Birth of a biome: insights into the assembly and maintenance of the Australian arid zone biota. Molecular Ecology 17, 4398-4417.

Carranza, S., Arnold, E.N., 2006. Systematics, biogeography, and evolution of Hemidactylus geckos (Reptilia: Gekkonidae) elucidated using mitochondrial DNA sequences. Molecular Phylogenetics and Evolution 38, 531-545.

Chapman, A., Dell, J., 1985. Biology and zoogeography of the amphibians and reptiles of the Western Australian wheatbelt. Records of the Western Australian Museum 12, 1-46.

Cliburn, J.W., 1957. Leaping ability of the glass lizard. Herpetologica 1957, 24.

Cogger, H., 2014. Reptiles and Amphibians of Australia. CSIRO Publishing, Collingwood, Victoria, xxx, 1033.

Cope, E.D., 1896. On the hemipenes of the Sauria. Proceedings of the Academy of Natural Sciences of Philadelphia, 461-467.

Cracraft, J., 1986. Origin and evolution of continental biotas speciation and historical congruence within the Australasian avifauna. Evolution 40, 977-996.

Cunningham, C.W., Zhu, H., Hillis, D.M., 1998. Best-fit maximum-likelihood models for phylogenetic inference: empirical tests with known phylogenies. Evolution 52, 978-987.

Darriba, D., Taboada, G.L., Doallo, R., Posada, D., 2012. jModelTest 2: more models, new heuristics, and parallel computing. Nature Methods 9, 772.

Daza, J.D., Bauer, A.M., 2012. Temporal bones of the Gekkota support molecular relationships within the Pygopodoidea. Journal of Herpetology 46, 381-386.

Daza, J.D., Bauer, A.M., In press. Cranial anatomy of the pygopodid lizard *Aprasia repens*, a Gekkotan masquerading as a Scolecophidian.

Donnellan, S.C., Hutchinson, M.N., Saint, K.M., 1999. Molecular evidence for the phylogeny of Australian gekkonoid lizards. Biological Journal of the Linnean Society 67, 97-118.

Dowling, H.G., 1967. Hemipenes and other characters in colubrid classifications. Herpetologica 23, 138-142.

Dowling, H.G., Savage, J.M., 1960. A guide to the snake hemipenis: a survey of basic structure and systematic characteristics. Zoologica 45, 17-28.

Driskell, A.C., Pruett-Jones, S., Tarvin, K.A., Hagevik, S., 2003. Evolutionary relationships among blue- and black-plumaged populations of the white-winged fairy-wren (*Malurus leucopterus*). Australian journal of zoology 50, 581-595.

Drummond, A.J., Rambaut, A., 2007. BEAST: Bayesian evolutionary analysis by sampling trees. BMC Evolutionary Biology 7, 214.

Eberhard, W.G., 1985. Sexual Selection and Animal Genitalia. Harvard University Press, Cambridge, Massachusetts.

Ehmann, H., 1981. The natural history and conservation of the bronzeback (*Ophidiocephalus taeniatus* Lucas and Frost)(Lacertilia, Pygopodidae). Proceedings of the Melbourne Herpetological Symposium. C.B. Banks and A.A. Martin, pp. 7-13.

Estes, R., de Queiroz, K., Gautheir, J., 1988. Phylogenetic relationships within Squamata. Phylogenetic Relationships of the Lizard Families, Essays Commemorating Charles L. Camp. Stanford University Press, Palo Alto, California, p. 119-281.

Felsenstein, J., 1978. Cases in which parsimony or compatibility methods will be positively misleading. Systematic Biology 27, 401-410.

Fenwick, A.M., Gutberlet Jr, R.L., Evans, J.A., Parkinson, C.L., 2009. Morphological and molecular evidence for phylogeny and classification of South American pitvipers, genera *Bothrops*, *Bothriopsis*, and *Bothrocophias* (Serpentes: Viperidae). Zoological Journal of the Linnean Society 156, 617-640.

Fisher-Reid, M.C., Wiens, J., 2011. What are the consequences of combining nuclear and mitochondrial data for phylogenetic analysis? Lessons from *Plethodon* salamanders and 13 other vertebrate clades. BMC Evolutionary Biology 11, 300.

Fitzsimons, J.A., 2011. Southward range expansion of the Mourning Gecko *Lepidodactylus lugubris* on mainland Australia and nearshore islands. Australian Zoologist 35, 619-621.

Ford, J., 1987. Minor isolates and minor geographical barriers in avian speciation in continental Australia. Emu 87, 90-102.

Frost, D.R., Hillis, D.M., 1990. Species in concept and practice: herpetological applications. Herpetologica 46, 86-104.

Fujita, M.K., McGuire, J.A., Donnellan, S.C., Moritz, C., 2010. Diversification and persistence at the arid-monsoonal interface: Australia-wide biogeography of the Bynoe's gecko (*Heteronotia binoei*; Gekkonidae). Evolution 64, 2293-2314.

Gamble, T., Bauer, A.M., Greenbaum, E., Jackman, T.R., 2008. Evidence for Gondwanan vicariance in an ancient clade of gecko lizards. Journal of Biogeography 35, 88-104.

Gans, C., 1974. Biomechanics: An approach to vertebrate biology. Lippincott, Philadelphia.

Gans, C., Mendelssohn, H., 1972. Sidewinding and jumping progression of vipers. Toxins of animal and plant origin, 17-38.

Garcia‐Porta, J., Ord, T., 2013. Key innovations and island colonization as engines of evolutionary diversification: a comparative test with the Australasian diplodactyloid geckos. Journal of evolutionary biology 26, 2662-2680.

Glaw, F., Kosuch, J., Henkel, F.-W., Sound, P., Böhme, W., 2006. Genetic and morphological variation of the leaf-tailed gecko *Uroplatus fimbriatus* from Madagascar, with description of a new giant species. Salamandria 42, 129-144.

Gorman, G.C., Gress, F., 1970. Sex chromosomes of a pygopodid lizard *Lialis burtonis*. Experientia, 206-207.

Gray, J.E., 1845. Catalogue of the Specimens of Lizards in the Collection of the British Museum. Edward Newman, by order of the Trustees of the British Museum, London, UK.

Greenberg, B., 1943. Social behavior of the western banded gecko, *Coleonyx variegatus* Baird. Physiological Zoology 16, 110-122.

Greer, A.E., 1989. Pygopodidae - Flap-footed Lizards. The Biology and Evolution of Australian Lizards. Surrey Beatty & Sons Pty Limited, 43 Rickard Road, Chipping Norton, New South Wales, p. 97-116.

Greer, A.E., 1997. Pythonidae - Pythons. The Biology and Evolution of Australian Snakes. Surrey Beatty & Sons Pty Limited, 43 Rickard Road, Chipping Norton, NSW, p. 358.

Groth, J.G., Barrowclough, G.F., 1999. Basal divergences in birds and the phylogenetic utility of the nuclear RAG-1 gene. Molecular Phylogenetics and Evolution 12, 115-123.

Guindon, S., Gascuel, O., 2003. A simple, fast, and accurate method to estimate large phylogenies by maximum-likelihood. Systematic Biology, 696-704.

Han, D., Zhou, K., Bauer, A.M., 2004. Phylogenetic relationships among gekkotan lizards inferred from C-mos nuclear DNA sequences and a new classification of the Gekkota. Biological Journal of the Linnean Society 83, 353-368.

Heinicke, M.P., Greenbaum, E., Jackman, T.R., Bauer, A.M., 2010. Molecular phylogenetics of Pacific *Nactus* (Squamata: Gekkota: Gekkonidae) and the diphyly of Australian species. Proceedings of the California Academy of Sciences 61, 633-646.

Heinicke, M.P., Greenbaum, E., Jackman, T.R., Bauer, A.M., 2011. Phylogeny of a trans-Wallacean radiation (Squamata, Gekkonidae, *Gehyra*) supports a single early colonization of Australia. Zoologica Scripta 40, 584-602.

Hoser, R.T., 1985. The role of pelvic spurs. Herptile 10, 95.

Hoskin, C.J., 2011. The invasion and potential impact of the Asian House Gecko (*Hemidactylus frenatus*) in Australia. Austral Ecology 36, 240-251.

How, R., Dell, J., Humphreys, W., 1987. The ground vertebrate fauna of coastal areas between Busselton and Albany, Western Australia. Records of the Western Australian Museum 13, 553-574.

Huelsenbeck, J.P., Larget, B., Miller, R.E., Ronquist, F., 2002. Potential applications and pitfalls of Bayesian inference of phylogeny. Systematic Biology 51, 673-688.

Huelsenbeck, J.P., Ronquist, F., 2001a. MrBayes: Bayesian inference of phylogenetic trees. Bioinformatics 17, 754-755.

Huelsenbeck, J.P., Ronquist, F., 2001b. MRBAYES: Bayesian inference of phylogeny. Bioinformatics, 754-755.

Huelsenbeck, J.P., Ronquist, F., Nielsen, R., Bollback, J.P., 2001. Bayesian inference of phylogeny and its impact on evolutionary biology. Science 294, 2310-2314.

Hutchinson, M.N., 1997. The first fossil pygopod (Squamata: Gekkota), and a review of mandibular variation in living species. Memoirs of the Queensland Museum 41, 355-366.

Igea, J., Juste, J., Castresana, J., 2010. Novel intron markers to study the phylogeny of closely related mammalian species. BMC Evolutionary Biology 10, 369.

Jackman, T.R., Bauer, A.M., Greenbaum, E., 2008. Molecular phylogenetic relationships of the geckos of the genus *Nactus* and their relatives (Squamata : Gekkonidae). Acta Herpetologica 3, 1-18.

Jamieson, B., Oliver, S., Scheltinga, D., 1996. The Ultrastructure of the Spermatozoa of Squamata—I. Scincidae, Gekkonidae and Pygopodidae (Reptilia). Acta Zoologica 77, 85-100.

Jennings, W.B., Pianka, E.R., Donnellan, S., 2003. Systematics of the lizard Family Pygopodidae with implications for the diversification of Australian temperate biotas. Systematic Biology 52, 757-780.

Jensen, A.S., 1901. Om Ophiopsiseps nasutus du Bocage og dens stilling i reptiliernes system. Videnskabelige Meddelelser Naturhistorisk Forening i København. 2.

Kelly, C.M.R., Barker, N.P., Villet, M.H., Broadley, D.G., 2009. Phylogeny, biogeography and classification of the snake superfamily Elapoidea: a rapid radiation in the late Eocene. Cladistics 25, 38-63.

Keogh, J.S., 1999. Evolutionary implications of hemipenial morphology in the terrestrial Australian elapid snakes. Zoological Journal of the Linnean Society 1999, 239-278.

Khan, M.S., 1999. Two new species and a subspecies of blind snakes of genus *Typhlops* from Azad Kashmir and Punjab, Pakistan (Serpentes: Typhlopidae). Russian Journal of Herpetology 6, 231-240.

King, M., Horner, P., 1993. Family Gekkonidae. Fauna of Australia. Australian Government Publishing Service, Canberra, Australia, p. 9-15.

King, M., King, D., 1977. The evolution of sex chromosomes in lizards. In: Calaby, J.H., Tyndale-Biscoe, C.G. (Eds.), Reproduction and evolution: Proceedings of the fourth symposium on comparative biology of reproduction. Australian Academy of Sciences, Canberra, Australia, p. 55-60.

Klaver, C., Böhme, W., 1986. Phylogeny and classification of the Chamaeleonidae (Sauria) with special reference to hemipenis morphology. Bonner Zoologische Monographien 22, 1-64.

Kluge, A.G., 1974. A taxonomic revision of the lizard family Pygopodidae. Miscellaneous Publications Museum of Zoology University of Michigan 147, 1-221.

Kluge, A.G., 1976. Phylogenetic relationsihps in the lizard family Pygopodidae an evaluation of theory methods and data. Miscellaneous Publications Museum of Zoology University of Michigan 152, 1-71.

Kluge, A.G., 1982. Cloacal bones and sacs as evidence of gekkonoid lizard relationships. Herpetologica, 348-355.

Kluge, A.G., 1987. Cladistic relationships in the Gekkonoidea (Squamata; Sauria). Miscellaneous Publications of the Museum of Zoology, University of Michigan 173, 1-54.

Köhler, J., Hahn, M., Köhler, G., 2012. Divergent evolution of hemipenial morphology in two cryptic species of mainland anoles related to *Anolis polylepis*. Salamandria 48, 1-11.

Kubatko, L.S., Gibbs, H.L., Bloomquist, E.W., 2011. Inferring species-level phylogenies and taxonomic distinctiveness using multilocus data in *Sistrurus* rattlesnakes. Systematic Biology 60, 393-409.

Lanfear, R., Calcott, B., Ho, S.Y.W., Guindon, S., 2012. PartitionFinder: Combined Selection of Partitioning Schemes and Substitution Models for Phylogenetic Analyses. Molecular Biology and Evolution 29, 1695-1701.

Leaché, A.D., 2009. Species tree discordance traces to phylogeographic clade boundaries in North American fence lizards (*Sceloporus*). Systematic Biology 58, 547-559.

Leaché, A.D., 2010. Species trees for spiny lizards (Genus *Sceloporus*): Identifying points of concordance and conflict between nuclear and mitochondrial data. Molecular Phylogenetics and Evolution 54, 162-171.

Leaché, A.D., Koo, M.S., Spencer, C.L., Papenfuss, T.J., Fisher, R.N., McGuire, J.A., 2009. Quantifying ecological, morphological, and genetic variation to delimit species in the coast horned lizard species complex (*Phrynosoma*). Proceedings of the National Academy of Sciences, USA 106, 12418-12423.

Leaché, A.D., McGuire, J.A., 2006. Phylogenetic relationships of horned lizards (*Phrynosoma*) based on nuclear and mitochondrial data: Evidence for a misleading mitochondrial gene tree. Molecular Phylogenetics and Evolution 39, 628-644.

Lee, M.S.Y., Oliver, P.M., Hutchinson, M.N., 2009. Phylogenetic uncertainty and molecular clock calibrations: A case study of legless lizards (Pygopodidae, Gekkota). Molecular Phylogenetics and Evolution 50, 661-666.

Lemmon, A.R., Moriarty, E.C., 2004. The Importance of Proper Model Assumption in Bayesian Phylogenetics. Systematic Biology 53, 265-277.

Macey, J.R., Ananjeva, N.B., Wang, Y., Papenfuss, T.J., 2000. Phylogenetic relationships among Asian gekkonid lizards formerly of the genus Cyrtodactylus based on cladistic analyses of allozymic data: monophyly of Cyrtopodion and Mediodactylus. Journal of Herpetology, 258-265.

Maddison, W.P., 1997. Gene Trees in Species Trees. Systematic Biology 46, 523-536.

Maryan, B., Aplin, K.P., Adams, M., 2007. Two new species of the *Delma tincta* group (Squamata : Pygopodidae) from northwestern Australia. Records of the Western Australian Museum 23, 273-305.

Maryan, B., Bush, B.G., Adams, M., 2013a. Morphological and molecular assessment of *Aprasia fusca* and *A. rostrata* (Squamata: Pygopodidae), with a description of a new species from the Lake MacLeod region, Western Australia. Records of the Western Australian Museum 144, 28.

Maryan, B., How, R.A., Adams, M., 2013b. A new species of the *Aprasia repens* species-group (Squamata: Pygopodidae) from Western Australia. Records of the Western Australian Museum 30, 28.

McCann, C., 1946. The hemipenis in reptiles. Journal of the Bombay Natural History Society 46, 348-373.

McDonald, S., 2014. Australian Online Reptile Database.

McDowell, S.B., Bogert, C.M., 1954. The systematic position of *Lanthanotus* and the affinities of the anguinomorphan lizards. Bulletin of the American Museum of Natural History 105, 1-142.

McGowran, B., Holdgate, G.R., Li, Q., Gallagher, S.J., 2004. Cenozoic stratigraphic succession in southeastern Australia. Australian Journal of Earth Sciences 51, 459-496.

McGuire, J.A., Linkem, C.W., Koo, M.S., Hutchison, D.W., Lappin, A.K., Orange, D.I., Lemos-Espinal, J., Riddle, B.R., Jaeger, J.R., 2007. Mitochondrial introgression and incomplete lineage sorting through space and time: Phylogenetics of Crotaphytid lizards. Evolution 61, 2879-2897.

Mead, J., Hollenshead, M., Swift, S., Bell, C., Baynes, A., 2008. Pygopus (Squamata: Pygopodidae) from mid-Holocene cave deposits, Western and South Australia. Records of the Western Australian Museum 25, 87-93.

Miller, M.R., 1966. The cochlear ducts of lizards. Proceedings of the California Academy of Sciences 33, 255-359.

Moriyama, E.N., Powell, J.R., 1997. Synonymous substitution rates in *Drosophila*: Mitochondrial versus nuclear genes. Journal of Molecular Evolution 45, 378-391.

Murphy, J.B., Lamoreaux, W.E., Barker, D.G., 1981. Miscellaneous notes on the reproductive biology of reptiles. Eight species of the family Boidae, genera *Acranthophis*, *Aspidites*, *Candoia*, *Liasis*, and *Python*. Kansas Academy of Science 84, 39-49.

O'Neill, E.M., Schwartz, R., Bullock, C.T., Williams, J.S., Shaffer, H.B., Aguilar-Miguel, X., Parra-Olea, G., Weisrock, D.W., 2013. Parallel tagged amplicon sequencing reveals major lineages and phylogenetic structure in the North American tiger salamander (*Ambystoma tigrinum*) species complex. Molecular Ecology 22, 111-129.

Oliver, P.M., 2009. Systematics and diversity of Australian Pygopodoid geckos (Pygopodoidea; Gekkota; Squamata). School of Earth and Environmental Sciences. University of Adelaide, Adelaide, South Australia, p. 227.

Oliver, P.M., Bauer, A.M., 2011. Systematics and evolution of the Australian knob-tail geckos (*Nephrurus*, Carphodactylidae, Gekkota): Plesiomorphic grades and biome shifts through the Miocene. Molecular Phylogenetics and Evolution 59, 664-674.

Oliver, P.M., Couper, P., Amey, A., 2010. A new species of *Pygopus* (Pygopodidae; Gekkota; Squamata) from north-eastern Queensland. Zootaxa 27, 47-61.

Oliver, P.M., Sanders, K.L., 2009. Molecular evidence for Gondwanan origins of multiple lineages within a diverse Australasian gecko radiation. Journal of Biogeography 36, 2044-2055.

Panhuis, T.M., Butlin, R., Zuk, M., Tregenza, T., 2001. Sexual selection and speciation. Trends in Ecology & Evolution 16, 364-371.

Patchell, F.C., Shine, R., 1986. Food habits and reproductive biology of the Australian legless lizards (Pygopodidae). Copeia 1986, 30-39.

Pesantes, O.S., 1994. A method for preparing the hemipenis of preserved snakes. Journal of Herpetology 28, 93-95.

Pianka, E.R., 1969. Habitat specificity, speciation, and species density in Australian desert lizards. Ecology 50, 498-502.

Pianka, E.R., 1972. Zoogeography and speciation of Australian desert lizards: an ecological perspective. Copeia 1972, 127-145.

Pianka, E.R., 2010. Notes on the ecology of four species of pygopodid lizards in the Great Victoria Desert. Western Australian Naturalist 27, 175-181.

Poe, S., Chubb, A.L., 2004. Birds in a bush: Five genes indicate explosive evolution of Avian Orders. Evolution 58, 404-415.

Portik, D.M., Bauer, A.M., Jackman, T.R., 2011. Bridging the gap: western rock skinks (*Trachylepis sulcata*) have a short history in South Africa. Molecular Ecology 20, 1744-1758.

Portik, D.M., Wood Jr, P.L., Grismer, J.L., Stanley, E.L., Jackman, T.R., 2012. Identification of 104 rapidly-evolving nuclear protein-coding markers for amplification across scaled reptiles using genomic resources. Conservation Genetics Resources 4, 1-10.

Pyron, R., Burbrink, F., Wiens, J., 2013. A phylogeny and revised classification of Squamata, including 4161 species of lizards and snakes. BMC Evolutionary Biology 13, 1-54.

Rato, C., Carranza, S., Harris, D.J., 2011. When selection deceives phylogeographic interpretation: The case of the Mediterranean house gecko, *Hemidactylus turcicus* (Linnaeus, 1758). Molecular Phylogenetics and Evolution 58, 365-373.

Rato, C., Carranza, S., Perera, A., Carretero, M.A., Harris, D.J., 2010. Conflicting patterns of nucleotide diversity between mtDNA and nDNA in the Moorish gecko, *Tarentola mauritanica*. Molecular Phylogenetics and Evolution 56, 962-971.

Reeder, T.W., 1995. Phylogenetic relationships among phrynosomatid lizards as inferred from mitochondrial ribosomal DNA sequences: substitutional bias and information content of transitions relative to transversions. Molecular Phylogenetics and Evolution 4, 203-222.

Richards, J., Singleton, O., 1981. Palaeozoic Victoria, Australia: igneous rocks, ages and their interpretation. Journal of the Geological Society of Australia 28, 395-421.

Rindal, E., Brower, A.V.Z., 2011. Do model-based phylogenetic analyses perform better than parsimony? A test with empirical data. Cladistics 27, 331-334.

Roelants, K., Gower, D.J., Wilkinson, M., Loader, S.P., Biju, S.D., Guillaume, K., Moriau, L., Bossuyt, F., 2007. Global patterns of diversification in the history of modern amphibians. Proceedings of the National Academy of Sciences, USA 104, 887-892.

Röll, B., 2000. Gecko vision—visual cells, evolution, and ecological constraints. Journal of neurocytology 29, 471-484.

Röll, B., 2001. Multiple origin of diurnality in geckos: evidence from eye lens crystallins. Naturwissenschaften 88, 293-296.

Romer, A.S., 1956. Osteology of the Reptiles. The University of Chicago Press, Chicago, Illinois.

Ronquist, F., Teslenko, M., van der Mark, P., Ayres, D.L., Darling, A., Höhna, S., Larget, B., Liu, L., Suchard, M.A., Huelsenbeck, J.P., 2012. MrBayes 3.2: Efficient Bayesian phylogenetic inference and model choice across a large model space. Systematic Biology 61, 539-542.

Rösler, H., Böhme, W., 2006. Peculiarities of the hemipenes of the gekkonid lizard genera Aristelliger Cope, 1861 and Uroplatus Duméril, 1806. Herpetologia Bonnensis II. Proceedings of the 13th Congress of the Societas Europaea Herpetologica, pp. 121-124.

Saint, K.M., Austin, C.C., Donnellan, S.C., Hutchinson, M.N., 1998. C- mos a nuclear marker useful for squamate phylogenetic analysis. Molecular Phylogenetics and Evolution 10, 259-263.

Sanders, K.L., Lee, M.S.Y., Leys, R., Foster, R., Scott Keogh, J., 2008. Molecular phylogeny and divergence dates for Australasian elapids and sea snakes (Hydrophiinae): evidence from seven genes for rapid evolutionary radiations. Journal of evolutionary biology 21, 682-695.

Savitzky, A.H., 1983. Coadapted character complexes among snakes: fossoriality, piscivory, and durophagy. American Zoologist 23, 397-409.

Schodde, R., Weatherly, R., 1982. The Fairy-wrens: a monograph of the Maluridae. Lansdowne Editions, 203.

Schouten, J.R., 1985. Experiences in keeping and breeding of the green tree python, *Chondropython viridis* (Schlegel 1872), negative and positive results. Litteratura Serpentium 5, 122-156.

Shea, G.M., 1987. Two new species of *Delma* (Lacertilia : Pygopodidae) from Northeastern Queensland and Australia and a note on the status of the genus *Aclys*. Proceedings of the Linnean Society of New South Wales 109, 203-212.

Shea, G.M., 1991. Revisionary notes on the Genus *Delma* (Squamata: Pygopodidae) in South Australia and the Northern Territory. Records of the South Australian Museum (Adelaide) 25, 71-90.

Shea, G.M., 1993. Family Pygopodidae. Fauna of Australia: Amphibia and Reptilia, p.

Shoo, L., Rose, R., Doughty, P., Austin, J.J., Melville, J., 2008. Diversification patterns of pebble-mimic dragons are consistent with historical disruption of important habitat corridors in arid Australia. Molecular Phylogenetics and Evolution 48, 528-542.

Shute, C.C.D., Bellairs, A.d.A., 1953. The cochlear apparatus of Gekkonidae and Pygopodidae and its bearing on the affinities of these groups of lizards. Proceedings of the Zoological Society of London 123, 695-709.

Sites Jr, J.W., Marshall, J.C., 2003. Delimiting species: a renaissance issue in systematic biology. Trends in Ecology; Evolution 18, 462-470.

Sites Jr, J.W., Marshall, J.C., 2004. Operational criteria for delimiting species. Annual Review of Ecology, Evolution, and Systematics 35, 199-227.

Slip, D.J., Shine, R., 1988. The reproductive biology and mating system of diamond pythons, *Morelia spilota* (Serpentes: Boidae). Herpetologica 44, 396-404.

Stamatakis, A., 2014. RAxML Version 8: A tool for phylogenetic analysis and post-analysis of large phylogenies. Bioinformatics, 1093.

Stanley, E.L., Bauer, A.M., Jackman, T.R., Branch, W.R., Mouton, P.L.F.N., 2011. Between a rock and a hard polytomy: Rapid radiation in the rupicolous girdled lizards (Squamata: Cordylidae). Molecular Phylogenetics and Evolution 58, 53-70.

Storr, G., Smith, L., Johnstone, R., 1990. Lizards of Western Australia. III. Geckos and Pygopods. Western Australian Museum, Perth.

Strutzenberger, P., Brehm, G., Fiedler, K., 2011. DNA barcoding-based species delimitation increases species count of *Eois* (Geometridae) moths in a well-studied tropical mountain forest by up to 50%. Insect Science 18, 349-362.

Swofford, D.L., 2003. PAUP*. Phylogenetic Analysis Using Parsimony (*and Other Methods). Version 4. Sinauer Associates, Sunderland, Massachusetts. .

Thomas, R., Hedges, S.B., 2007. Eleven new species of snakes of the genus *Typhlops* (Serpentes: Typhlopidae) from Hispaniola and Cuba. Zootaxa 1400, 1-26.

Toews, D.P.L., Brelsford, A., 2012. The biogeography of mitochondrial and nuclear discordance in animals. Molecular Ecology 21, 3907-3930.

Uetz, P., Hošek, J., 2014. The Reptile Database. In: Uetz, P., Hošek, J. (Eds.). http://www.reptile-database.reptarium.cz/.

Underwood, G., 1957. On lizards of the family pygopodidae. A contribution to the morphology and phylogeny of the squamata. Journal of Morphology 100, 207-268.

van der Heijden, B., 1986. The husbandry and breeding of *Chondropython viridis*. Litteratura Serpentium 6, 4-12.

Vidal, N., Hedges, S.B., 2009. The molecular evolutionary tree of lizards, snakes, and amphisbaenians. Comptes Rendus Biologies 332, 129-139.

Walsh, T., 1985. Husbandry and breeding of *Chondropython viridis*. Newsletter of the Reptile Keepers' Association 8, 4-11.

Wells, R.W., 2007. Some taxonomic and nomenclatural considerations on the Class Reptilia. A review of species of the genus *Aprasia* Gray 1839 (Aprasiaidae). Australian Biodiversity Records, 1-17.

Wever, E.G., 1974. The ear of *Lialis burtonis* (Sauria: Pygopodidae), its structure and function. Copeia 1974, 297-305.

Wiens, J.J., 2005. Can incomplete taxa rescue phylogenetic analyses from long-branch attraction? Systematic Biology 54, 731-742.

Williams, M.A.J., 2001. Quaternary Australia: extremes in the last glacial-interglacial cycle. In: Veevers, J.J. (Ed.), Billion-Year Earth History of Australia and Neighbours in Gondwanaland. GEMOC Press, Sydney, Australia, p. 55-59.

Wilson, S., 2005. Field Guide to Reptiles of Queensland, Frenchs Forest, New South Wales.

Wilson, S., Swan, G., 2013. A complete guide to Reptiles of Australia. New Holland Publishers, Chatswood, New South Wales, 592.

Wood Jr, P.L., Heinicke, M.P., Jackman, T.R., Bauer, A.M., 2012. Phylogeny of bent-toed geckos (*Cyrtodactylus*) reveals a west to east pattern of diversification. Molecular Phylogenetics and Evolution 65, 992-1003.

Appendix 1

Table I.1. Synapoorphies of the Gekkota, Pygopodidae, and *Delma*, adapted from Cogger (1989) and Kluge (1974).

	Derived character states within		
	Gekkota	Pygopodidae (in combination)	*Delma* (in combination)
External Morphology	Dorsal crest absent	Forelimbs absent Hindlimbs severly reduced, individual digits not visible externally Pupil vertical, oval, or slit-like Body scales imbricate	One pair of enlarged scales over parietal region Anteriormost nasal scales always meet on midline Nostril bordered by more than two scales (*D. impa*r exceptional) 18 or less midbody scale rows Scales smooth (*D. concinna* exceptional) 13 or less caudal scale rows Almost always 3 subcaudal scale rows External auditory meatus large
Behavior	Ability to vocalize Wiping of face, jaws, and eyes with tongue		
Skull	Palpebral absent Frontals encircle forebrain Parietal foramen absent Parietals posteromedially convex Parietals lack fossa for ascending process of occipital tectum Septomaxilla with posterolateral wing Lacrimal absent Recessus scalae tympani with two medial apertures Pterygoid teeth absent Jugal lacks dorsal process Postorbital absent Supratemporal arch incomplete Epipterygoid abuts underside of prootic's alar process Stapeslacks dorsal process Ectopterygoid extends along anterolateral side of infraorbital vacuity Parasphenoid process unossified Dentary overlaps Meckel's groove	Premaxilla single Median ventral process of premaxilla absent Osteoderms absent	
Postcranial Skeleton	Intermedium absent Postcloacal bones present	Vertebrae procoelous Vertebrae with prominent subcentral foramina Vertebrae with median constriction	
Soft Anatomy	Parietal eye absent Extracolumellar muscle present Cochlear Limbus of inner ear with spindle body Rectus superficialis muscle absent Postcloacal pockets present	Rectus superficialis present Postcloacal bones present	Preanal pores absent
Reprod-uction	Brood size reduced, usually a constant 2		

Appendix 2

Species	**Collection ID**	**State**	**Locality**	**Latitude**	**Longitude**
Aprasia aurita	SAMA 43054	Victoria	Wathe Fauna Reserve	35°33'00"S	142°25'00"E
Aprasia fusca	SAMA 52288	Western Australia	1 km NW Bullara Homestead	NA	NA
Aprasia inaurita	SAMA 47087	South Australia	St. Peter Island	32°15'00"S	133°35'00"E
Aprasia parapulchella	AMS 127439	New South Wales	20 km N Tarcutta	35°9'58"S	147°52'59"E
Aprasia parapulchella	MVD 66569	Victoria	Bendigo Whipstick	36°45'00"S	144°15'00"E
Aprasia picturata	WAM 131647	Western Australia	35 km E Leonora	28°57'00"S	121°48'00"E
Aprasia pseudopulchella	SAMA 40729	South Australia	2 km E Burra	33°40'00"S	138°57'00"E
Aprasia pulchella	WAM 80000	Western Australia	Jarrahdale	32°20'00"S	116°04'00"E
Aprasia repens	WAM 172989	Western Australia	Jandakot Regional Park at King Rd.	32˚13'37"S	115˚53'53"E
Aprasia repens	WAM 106018	Western Australia	Booragoon	32°02'30"S	115°51'00"E
Aprasia smithi	SAMA 106018	Western Australia	NA	NA	NA
Aprasia striolata	ABTC 6575	South Australia	Flinders Island 10 km NW Port Lincoln	NA	NA
Delma australis	SAMA 22784	South Australia	Mt. Remarkable NP, 2.1 km E Sugargum Lookout	32°50'00"S	138°5'00"E
Delma australis	SAMA 26339	South Australia	Yalata Roadhouse	31°28'10"S	131°35'30"E
Delma australis	SAMA 28138	South Australia	W of Marree	29°38'00"S	137°44'00"E
Delma australis	SAMA 28172	South Australia	Beresford RS	29°14'00"S	136°39'30"E
Delma australis	SAMA 28215	South Australia	Dalhousie Ruins	26°31'00"S	135°28'00"E
Delma australis	SAMA 38371	South Australia	Pooginook CP, 3 km N	34°07'00"S	140°06'00"E
Delma australis	SAMA 39341	South Australia	1 km SE Alawoona	34°44'27"S	140°30'43"E
Delma australis	SAMA 39559	South Australia	4 km SE Quandong Bore	35°32'20"S	140°46'12"E
Delma australis	SAMA 39606	South Australia	3 km S Buccleuch	35°21'54"S	139°52'51"E
Delma australis	SAMA 41336	South Australia	Oakbank Outstation	33°07'40"S	140°36'20"E
Delma australis	SAMA 41453	South Australia	Atkindale HS	34°03'30"S	140°08'00"E
Delma australis	SAMA 44426	South Australia	8 km NW Mt Kintore	26°30'01"S	130°26'13"E
Delma australis	SAMA 44680	South Australia	4 km SSW Mt Cuthbert	26°08'09"S	132°03'00"E
Delma australis	SAMA 44720	South Australia	Todmorden Station	27°39'26"S	134°39'20"E
Delma australis	SAMA 45576	South Australia	5 km NNE Inila Rockwater	31°43'50"S	133°27'02"E
Delma australis	SAMA 46230	South Australia	Arckaringa Station	27°56'20"S	134°44'10"E
Delma australis	SAMA 46340	South Australia	6.5 km WNW JohnsonBore	29°30'49"S	136°09'21"E
Delma australis	SAMA 46438	South Australia	15 km NW Backadinna Hill	29°05'00"S	135°10'00"E
Delma australis	SAMA 46505	South Australia	3.8 km SSE Mungutana m	29°22'49"S	135°40'55"E
Delma australis	SAMA 46980	South Australia	5.6 km SSE Mosquito	26°09'28"S	134°30'49"E
Delma australis	SAMA 47178	South Australia	Peake Station	28°26'10"S	136°07'41"E
Delma australis	SAMA 51992	South Australia	4.1 km N Warden Hill	30°24'23"S	139°13'29"E
Delma australis	SAMA 52032	South Australia	Quorn Nature Reserve	32°21'00"S	138°02'00"E
Delma australis	SAMA 52484	South Australia	20.1 km SSE Port Lincoln	34°54'16"S	135°55'08"E
Delma australis	SAMA 53079	South Australia	1 km E Mt Elm	31°54'27"S	138°19'43"E
Delma australis	SAMA 53114	South Australia	1.9 km N Dutchmans Peak	32°18'11"S	137°57'47"E
Delma australis	SAMA 54783	South Australia	Port Lincoln	34°54'16"S	135°55'08"E
Delma australis	SAMA 57677	South Australia	2.4 km ESE Sheoak Hill	33°24'44"S	136°45'21"E
Delma australis	SAMA 59664	South Australia	Yorke Peninsula	35°09'44"S	137°05'16"E
Delma australis	SAMA 60395	South Australia	113.9 km W Oak Valley	29°26'58"S	129°33'57"E
Delma australis	SAMA 61993	South Australia	9.0 km SE Moonaree hill	31°58'56"S	135°40'01"E
Delma australis	SAMA 62235	South Australia	184 km SSW Watarru	28°30'28"S	132°07'29"E
Delma australis	SAMA 62277	South Australia	180 km SSW Watarru	28°30'09"S	129°04'49"E
Delma australis	WAM 35854	Western Australia	Krichauff Ranges	24°00'00"S	132°00'00"E

Delma australis	WAM 112666	Western Australia	Ponier Rock	32°56'00"S	123°30'00"E
Delma australis	WAM 112667	Western Australia	Ponier Rock	32°56'00"S	123°30'00"E
Delma australis	WAM 116276	Western Australia	Kalbarri	27°51'00"S	114°10'00"E
Delma australis	WAM 116277	Western Australia	Kalbarri	27°51'00"S	114°10'00"E
Species	Collection ID	State	Locality	Latitude	Longitude
Delma australis	WAM 116744	Western Australia	Overlander Roadhouse	26°24'00"S	114°25'00"E
Delma australis	WAM 117102	Western Australia	ESE Overlander	26°36'00"S	114°32'00"E
Delma australis	WAM 117389	Western Australia	Toomey Hills	31°33'26"S	119°51'38"E
Delma australis	WAM 122450	Western Australia	Hamelin	26°31'21"S	114°00'09"E
Delma australis	WAM 126345	Western Australia	Aurora Range	30°21'16"S	119°42'09"E
Delma australis	WAM 129674	Western Australia	Kundip	33°41'00"S	120°09'00"E
Delma australis	WAM 131015	Western Australia	Hamelin Homestead	26°31'00"S	114°00'00"E
Delma australis	WAM 131778	Western Australia	Wandina Homestead	27°56'00"S	115°32'00"E
Delma australis	WAM 131902	Western Australia	Hellfire Bay	34°00'15"S	122°10'20"E
Delma australis	WAM 132154	Western Australia	Duke of Orleans Bay	33°56'00"S	122°33'00"E
Delma australis	WAM 132470	Western Australia	Shothole Canyon	22°03'00"S	114°01'00"E
Delma australis	WAM 135196	Western Australia	Perenjori	29°26'00"S	116°48'00"E
Delma australis	WAM 136283	Western Australia	Muggon	26°46'44"S	115°37'40"E
Delma australis	WAM 136406	Western Australia	Norseman	32°12'00"S	121°47'00"E
Delma australis	WAM 137675	Western Australia	Balladonia Roadhouse	32°02'00"S	122°55'00"E
Delma australis	WAM 137676	Western Australia	Coolgardie	32°1'60"S	122°55'00"E
Delma australis	WAM 144087	Western Australia	Cunderdin	31°39'00"S	117°17'00"E
Delma australis	WAM 144237	Western Australia	Bandalup Hill	33°40'29"S	120°23'54"E
Delma australis	WAM 144238	Western Australia	Bandalup Hill	33°40'29"S	120°23'54"E
Delma australis	WAM 144732	Western Australia	Bungalbin Hill	30°19'00"S	119°29'00"E
Delma australis	WAM 151125	Western Australia	Eyre Bird Observatory	32°13'28"S	126°18'10"E
Delma australis	WAM 151218	Western Australia	Salmon Gums	32°49'59"S	121°24'50"E
Delma australis	WAM 151219	Western Australia	Salmon Gums	32°49'59"S	121°24'50"E
Delma australis	WAM 152638	Western Australia	Middle Island	28°54'35"S	113°54'53"E
Delma australis	WAM 154234	Western Australia	Kundip	33°40'26"S	120°11'45"E
Delma australis	WAM 154242	Western Australia	Kundip	33°40'01"S	120°12'03"E
Delma australis	WAM 154243	Western Australis	Kundip	33°40'01"S	120°12'03"E
Delma australis	WAM 156978	Western Australia	Canal Rocks	33°39'46"S	115°00'45"E
Delma australis	WAM 166866	Western Australia	Oakajee	28°34'25"S	114°35'04"E
Delma australis	WAM 77765	Western Australia	Toolinna Rockhole	32°45'05"S	124°58'50"E
Delma australis	AMS 149844	Western Australia	15 km SW Kulin	32°45'00"S	118°1'59"E
Delma australis	WAM 132470	Western Australia	Shothole Canyon, Cape Range NP	22°3'3"S	114°1'00"E
Delma borea	WAM 110606	Western Australia	Tanami Desert	19°34'47"S	128°51'53"E
Delma borea	WAM 141530	Western Australia	Quanbun Downs Station	18°21'27"S	125°13'10"E
Delma borea	WAM 172694	Western Australia	Irvine Island	16°19'21"S	124°02'48"E
Delma borea	WAM 171015	Western Australia	Adolphus Island	15°04'59"S	128°08'25"E
Delma borea	WAM 97093	Western Australia	Mount Daglish	16°16'46"S	124°57'32"E
Delma borea	WAM 96944	Western Australia	Dromedaries	16°34'20"S	124°56'40"E
Delma borea	WAM 108737	Western Australia	Sturt Creek	18°40'00"S	128°34'60"E
Delma borea	WAM 108815	Western Australia	Banana Springs	18°56'26"S	128°47'4"E
Delma borea	WAM 110606	Western Australia	Tanami Desert	19°34'47"S	128°51'53"E
Delma borea	WAM 112725	Western Australia	Mandora	19°44'01"S	120°50'16"E
Delma borea	WAM 169993	Western Australia	Yampi Peninsula	16°10'36"S	123°38'22"E
Delma borea	WAM 157426	Western Australia	Tanami Desert	19°53'59"S	128°49'37"E
Delma borea	WAM 157430	Western Australia	Tanami Desert	19°53'59"S	128°49'37"E
Delma borea	WAM 157937	Western Australia	Barrow Island	20°46'59"S	115°24'11"E
Delma borea	WAM 157938	Western Australia	Barrow Island	20°46'59"S	115°24'11"E
Delma borea	WAM 167769	Western Australia	Mitchell Plateau	14°49'13"S	125°43'16"E
Delma borea	WAM 168033	Western Australia	Prince Regent River	15°44'46"S	125°22'24"E

Delma borea	WAM 168664	Western Australia	Katers Island	14°28'00"S	125°31'60"E
Delma borea	WAM 168790	Western Australia	Middle Osborn Island	14°19'00"S	126°00'00"E
Delma borea	WAM 168813	Western Australia	Middle Osborn Island	14°19'00"S	126°00'00"E
Delma borea	WAM 169989	Western Australia	Yampi Peninsula	16°10'36"S	123°38'22"E
Species	Collection ID	State	Locality	Latitude	Longitude
Delma borea	WAM 158589	Western Australia	East Montalivet Island	14°16'46"S	125°18'22"E
Delma borea	WAM 165969	Western Australia	North Maret Island	14°24'02"S	124°58'40"E
Delma borea	WAM 171025	Western Australia	Saint Andrew Island	15°21'20"S	125°00'45"E
Delma borea	WAM B00679	Western Australia	Coronation Island	14°59'19"S	124°55'23"E
Delma borea	NTM R29687	Northern Territories	Bustard Island, Groote Eylandt Area	13°38'26"S	136°23'22"E
Delma borea	NTM R28954	Northern Territories	Bulldog Pass, Nr Cox Peninsula Road	12°25'35"S	130°38'26"E
Delma borea	NTM R36349	Northern Territories	Victoria River Region, Kalkarindji	17°26'45"S	130°50'11"E
Delma borea	WAM 114462	Western Australia	King Hall Island	16°04'41"S	123°24'33"E
Delma borea	WAM 139058	Western Australia	Mandora	19°44'01"S	120°50'16"E
Delma borea	WAM 141530	Western Australia	Quanbun Downs Station	18°10'12"S	125°16'15"E
Delma borea	WAM 158963	Western Australia	Koolan Island	16°07'29"S	123°45'28"E
Delma borea	WAM 158999	Western Australia	Koolan Island	16°07'29"S	123°45'28"E
Delma borea	WAM 163561	Western Australia	Anjo Peninsula	13°59'59"S	126°28'11"E
Delma borea	WAM 168386	Western Australia	Gibbings Island	16°09'03"S	123°30'51"E
Delma borea	WAM 168439	Western Australia	Margaret Island	16°22'24"S	123°23'42"E
Delma borea	WAM 168458	Western Australia	Sir Graham Moore Island	13°53'00"S	126°33'00"E
Delma borea	WAM 168702	Western Australia	Katers Island	14°28'00"S	125°31'60"E
Delma borea	WAM 171018	Western Australia	Darcy Island	15°20'28"S	124°23'37"E
Delma borea	WAM 171019	Western Australia	Augustus Island	15°20'46"S	124°33'47"E
Delma borea	WAM 171020	Western Australia	Coronation Island	14°59'19"S	124°55'23"E
Delma borea	WAM 171024	Western Australia	Byam Martin Island	15°22'20"S	124°21'32"E
Delma borea	WAM 171026	Western Australia	Uwins Island	15°16'00"S	124°48'27"E
Delma borea	WAM 171027	Western Australia	Coronation Island	14°59'19"S	124°55'23"E
Delma borea	WAM 171627	Western Australia	Storr Island	15°56'34"S	124°34'09"E
Delma borea	WAM 171628	Western Australia	Nw Molema Island	16°14'52"S	123°52'56"E
Delma borea	WAM 171633	Western Australia	Kingfisher Island	16°05'42"S	124°04'42"E
Delma borea	WAM 171634	Western Australia	Wulalam Island	16°22'57"S	124°14'03"E
Delma borea	WAM 171636	Western Australia	Long Island	16°33'33"S	123°21'18"E
Delma borea	WAM 171638	Western Australia	Lachlan Island	16°36'06"S	123°29'19"E
Delma borea	WAM 171719	Western Australia	Wargul Wargul Island	13°56'15"S	126°10'28"E
Delma borea	WAM B01168	Western Australia	Adolphus Island	15°06'27"S	128°08'45"E
Delma borea	WAM B01183	Western Australia	Adolphus Island	15°06'27"S	128°08'45"E
Delma borea	WAM B01811	Western Australia	Hidden Island	16°13'12"S	123°27'59"E
Delma butleri	AMS 156715	New South Wales	35 km From Mt. Hope On Euabalong Rd	32°56'48"S	146°11'32"E
Delma butleri	WAM 120322	Western Australia	7 km E Cape Cuvier	24°13'26"S	113°27'41"E
Delma butleri	WAM 120349	Western Australia	6 km NNE Cape Cuvier	24°11'35"S	113°27'19"E
Delma butleri	WAM 120401	Western Australia	Cape Cuvier	24°08'18"S	113°26'45"E
Delma butleri	WAM 120819	Western Australia	25 km SSE Peron Homestead	26°03'03"S	113°37'00"E
Delma butleri	WAM 123625	Western Australia	7 km SSE Denham	25°58'32"S	113°34'15"E
Delma butleri	WAM 141591	Western Australia	5 km WSW Boolathana Homestead	24°35'21"S	113°32'10"E
Delma butleri	WAM 141592	Western Australia	5 km WSW Boolathana Homestead	24°35'21"S	113°32'10"E
Delma butleri	WAM 156449	Western Australia	Learmonth Air Weapons Range	22°25'04"S	113°45'50"E
Delma butleri	WAM 156840	Western Australia	Old Yamarna Homestead	28°09'58"S	123°40'23"E
Delma butleri	WAM 172191	Western Australia	Ilkurlka Roadhouse	28°22'21"S	127°32'19"E
Delma butleri	WAM 114298	Western Australia	Boolathana Homestead	25°35'00"S	118°22'00"E
Delma bulteri	WAM 130986	New South Wales	19.7 Km N Coombah Roadhouse, Silver City Hwy	32°48'58"S	141°36'58"E
Delma bulteri	SAM 36144	New South Wales	Coombah	32°48'58"S	141°36'58"E
Delma concinna	WAM 96898	Western Australia	Tamala	26°40'00"S	113°47'00"E

Delma concinna	WAM 141175	Western Australia	Lancelin	30°57'43"S	115°21'53"E
Delma concinna	WBJ 2477	Western Australia	Lesueur NP	NA	NA
Delma desmosa	WAM 114555	Western Australia	Sandfire Roadhouse	19°46'00"S	121°05'00"E
Delma desmosa	WAM 163287	Western Australia	Neale Junction	28°17'23"S	125°49'20"E
Species	Collection ID	State	Locality	Latitude	Longitude
Delma desmosa	WAM 166043	Western Australia	Neale Junction	28°17'23"S	125°49'20"E
Delma elegans	WAM 110872	Western Australia	Pannawonica	21°40'00"S	115°50'07"E
Delma elegans	WAM 146640	Western Australia	Pouyouwuncubban	22°08'58"S	119°01'07"E
Delma elegans	WAM 110900	Western Australia	Pannawonica	21°40'00"S	115°50'07"E
Delma elegans	WAM 139247	Western Australia	Meentheena	21°15'20"S	120°27'18"E
Delma fraseri	WAM 96701	Western Australia	Dryandra	32°46'60"S	116°55'00"E
Delma fraseri	WAM 106203	Western Australia	Nukarni (Presumably)	31°18'03"S	118°12'01"E
Delma fraseri	WAM 114162	Western Australia	Mount Mcmahon, Ravensthorpe Range	33°32'60"S	120°05'60"E
Delma fraseri	WAM 114578	Western Australia	Spalding Park, Geraldton	28°45'60"S	114°37'00"E
Delma fraseri	WAM 114927	Western Australia	Dongara	29°15'00"S	114°55'60"E
Delma fraseri	WAM 115101	Western Australia	Ken Hearst Park	32°04'60"S	115°52'60"E
Delma fraseri	WAM 115102	Western Australia	Ken Hearst Park	32°04'60"S	115°52'60"E
Delma fraseri	WAM 115115	Western Australia	Ken Hearst Park	32°04'60"S	115°52'60"E
Delma fraseri	WAM 115138	Western Australia	Ken Hearst Park	32°04'60"S	115°52'60"E
Delma fraseri	WAM 115139	Western Australia	Ken Hearst Park	32°04'60"S	115°52'60"E
Delma fraseri	WAM 115140	Western Australia	Ken Hearst Park	32°04'60"S	115°52'60"E
Delma fraseri	WAM 115141	Western Australia	Ken Hearst Park	32°04'60"S	115°52'60"E
Delma fraseri	WAM 115227	Western Australia	Spalding Park, Geraldton	28°38'60"S	114°37'60"E
Delma fraseri	WAM 116093	Western Australia	Buller River	28°37'60"S	114°35'60"E
Delma fraseri	WAM 116845	Western Australia	Ellendale Pool, Greenough River	28°51'60"S	114°58'00"E
Delma fraseri	WAM 116846	Western Australia	Ellendale Pool, Greenough River	28°51'60"S	114°58'00"E
Delma fraseri	WAM 116847	Western Australia	Ellendale Pool, Greenough River	28°51'60"S	114°58'00"E
Delma fraseri	WAM 116877	Western Australia	4 km SE Carrollgouda Well	27°24'60"S	114°16'00"E
Delma fraseri	WAM 119061	Western Australia	Spalding Park, Geraldton	28°38'60"S	114°37'60"E
Delma fraseri	WAM 119240	Western Australia	2 km NE Cape Burney	28°51'05"S	114°37'60"E
Delma fraseri	WAM 119420	Western Australia	18 km SSW Ravensthorpe	33°44'22"S	119°59'27"E
Delma fraseri	WAM 120662	Western Australia	Between Lancelin And Ledge Point	31°04'54"S	115°22'16"E
Delma fraseri	WAM 125962	Western Australia	Narngulu, Geraldton	28°48'60"S	114°40'60"E
Delma fraseri	WAM 126099	Western Australia	Neerabup NP	31°40'60"S	115°45'00"E
Delma fraseri	WAM 127540	Western Australia	Esperance	33°51'05"S	121°52'60"E
Delma fraseri	WAM 127609	Western Australia	Mcdermid Rock	31°42'60"S	121°34'00"E
Delma fraseri	WAM 129670	Western Australia	10 km S Quairading	32°06'60"S	117°24'02"E
Delma fraseri	WAM 129686	Western Australia	Lort River	33°45'00"S	121°13'60"E
Delma fraseri	WAM 129687	Western Australia	Lort River	33°45'00"S	121°13'60"E
Delma fraseri	WAM 131927	Western Australia	6.5 km S Condingup	33°48'60"S	122°31'60"E
Delma fraseri	WAM 132811	Western Australia	Yorkrakine Hill	31°25'60"S	117°31'00"E
Delma fraseri	WAM 132826	Western Australia	10 km Ne Bindoon	31°18'06"S	116°09'02"E
Delma fraseri	WAM 132842	Western Australia	10 km Sse Wongan Hills	31°58'18"S	116°45'24"E
Delma fraseri	WAM 134755	Western Australia	Jilakin Lake	32°40'29"S	118°20'09"E
Delma fraseri	WAM 135222	Western Australia	Dundas Rock	32°21'60"S	121°45'00"E
Delma fraseri	WAM 135242	Western Australia	Dundas Rock	32°21'60"S	121°45'00"E
Delma fraseri	WAM 135503	Western Australia	Redcliffe, Perth Suburb	31°55'60"S	115°57'01"E
Delma fraseri	WAM 135697	Western Australia	North Bannister, Albany Highway	32°34'60"S	116°27'01"E
Delma fraseri	WAM 140507	Western Australia	Ca 15 km WNW Cataby	30°42'54"S	115°25'12"E
Delma fraseri	WAM 140778	Western Australia	Lancelin	31°00'60"S	115°19'60"E
Delma fraseri	WAM 141191	Western Australia	Ca 15 km NNE Lancelin	30°59'31"S	115°23'43"E
Delma fraseri	WAM 141195	Western Australia	Ca 15 km NNE Lancelin	31°01'35"S	115°21'42"E
Delma fraseri	WAM 146908	Western Australia	Marchagee Track	30°12'18"S	115°32'27"E
Delma fraseri	WAM 151706	Western Australia	Muchea Air Weapons Range	31°38'39"S	115°55'26"E

Delma fraseri	WAM 153976	Western Australia	Bindoon Military Training Area	31°09'41"S	116°15'38"E
Delma fraseri	WAM 153976	Western Australia	Bindoon Military Training Area	31°09'41"S	116°15'38"E
Delma fraseri	WAM 153977	Western Australia	Bindoon Military Training Area	31°10'18"S	116°15'48"E
Delma fraseri	WAM 153998	Western Australia	Bindoon Military Training Area	31°38'39"S	115°55'26"E
Species	Collection ID	State	Locality	Latitude	Longitude
Delma fraseri	WAM 154008	Western Australia	Muchea Air Weapons Range	31°38'32"S	115°550'3"E
Delma fraseri	WAM 154021	Western Australia	Muchea Air Weapons Range	31°38'32"S	115°55'03"E
Delma fraseri	WAM 154039	Western Australia	Muchea Air Weapons Range	31°38'16"S	115°55'31"E
Delma fraseri	WAM 154052	Western Australia	Muchea Air Weapons Range	31°38'16"S	115°55'31"E
Delma fraseri	WAM 154194	Western Australia	Near Kundip	33°40'55"S	120°11'56"E
Delma fraseri	WAM 154435	Western Australia	Near Kundip	33°40'01"S	120°12'03"E
Delma fraseri	WAM 156219	Western Australia	Pingrup Area	33°34'04"S	118°49'12"E
Delma fraseri	WAM 156277	Western Australia	42.6 km Ne Holt Rock	32°24'33"S	119°43'41"E
Delma fraseri	WAM 157863	Western Australia	Eyre Highway	32°18'52"S	123°32'33"E
Delma fraseri	WAM 165300	Western Australia	Cape Burney	28°51'06"S	114°38'24"E
Delma fraseri	WAM 166865	Western Australia	Oakajee	28°34'25"S	114°35'04"E
Delma fraseri	WAM 169903	Western Australia	Dirk Hartog Island	25°54'07"S	125°06'34"E
Delma fraseri	WAM 169904	Western Australia	Dirk Hartog Island	25°44'39"S	124°58'60"E
Delma fraseri	WAM 172980	Western Australia	Borracoppin	31˚23'49"S	118˚28'14"E
Delma fraseri	WAM 172994	Western Australia	SE Of Dongara	29˚19'02"S	115˚59'24"E
Delma grayii	WAM 115749	Western Australia	Geraldton	28°45'60"S	114°37'00"E
Delma grayii	WAM 119065	Western Australia	Yetna	28°36'05"S	114°42'01"E
Delma grayii	WAM 119655	Western Australia	Wicherina Reserve	28°43'60"S	115°00'00"E
Delma grayii	WAM 120086	Western Australia	Wicherina Reserve	28°43'60"S	115°00'00"E
Delma grayii	WAM 120665	Western Australia	Unknown	NA	NA
Delma grayii	WAM 127635	Western Australia	Unknown	NA	NA
Delma grayii	WAM 127639	Western Australia	Neerabup	31°41'00"S	115°46'00"E
Delma grayii	WAM 127664	Western Australia	Unknown	NA	NA
Delma grayii	WAM 130146	Western Australia	Preston Beach	32°53'24"S	115°39'32"E
Delma grayii	WAM 131871	Western Australia	8 km S Eneabba	29°52'60"S	115°16'60"E
Delma grayii	WAM 146399	Western Australia	Kalbarri	28°00'08"S	114°12'30"E
Delma grayii	WAM 154064	Western Australia	Muchea	31°39'19"S	115°55'48"E
Delma grayii	WAM 172986	Western Australia	Brand HWY 2.5 km S of Waddi Rd	30˚37'38"S	115˚27'54"E
Delma haroldi	WAM 108987	Western Australia	Beebingarra Creek	20°25'00"S	118°42'00"E
Delma haroldi	WAM 116425	Western Australia	Lake Hancock	24°45'08"S	124°44'01"E
Delma haroldi	WAM 102710	Western Australia	Little Sandy Desert	23°53'52"S	120°36'15"E
Delma haroldi	WAM 116425	Western Australia	Lake Hancock	24°45'08"S	124°44'01"E
Delma haroldi	WAM 135925	Western Australia	Port Hedland	20°31'00"S	118°21'00"E
Delma inornata	AMS 142790	New South Wales	Ironmines Rd, 6.4 km S Yass, Goulburn Rd	34°42'00"S	149°03'00"E
Delma inornata	AMS 141999	New South Wales	Nevertire, between Nyngan and Nevertire	31°38'00"S	147°20'00"E
Delma inornata	SAMA 23530	South Australia	Lake Alexandrina	35°19'00"S	139°13'00"E
Delma impar	SAMAR 43328	Australian Capital Territory	Gungahlin Town Centre	35°13'00"S	149°8'00"E
Delma impar	SAMAR 43325	Australian Capital Territory	Gungahlin Town	35°13'00"S	149°08'00"E
Delma impar	SAMAR 43973	Victoria	Sunshine	37°48'00"S	144°50'00"E
Delma impar	SAMAR 51504	South Australia	Hacks Lagoon CP	37°06'15"S	140°43'45"E
Delma impar	SAMAR 52585	South Australia	Lake Omerod near Naracoorte	36°58'41"S	140°40'07"E
Delma labialis	QMJ 89155	Queensland	Nebo	21°37'27"S	148°07'08"E
Delma labialis	QMJ 89591	Queensland	Cook	11°43'59"S	142°36'20"E
Delma mitella	ABTC 58998	Queensland	7.8 km W Paluma	NA	NA
Delma mitella	QMJ 80846	Queensland	Tolga, 1.5 W, Atherton	17°12'42"S	145°27'10"E
Delma molleri	SAMAR 23137	South Australia	2.6 km from Scarfes Hut, Mt. Remarkable NP	32°50'00"S	138°05'00"E
Delma molleri	SAMAR 30311	South Australia	Rochester Historic Site	33°42'00"S	138°28'00"E
Delma molleri	SAMAR 36233	South Australia	Clare	33°42'00"S	138°28'00"E
Delma molleri	SAMAR 64965	South Australia	5.96 km S Orroroo	32°40'45"S	138°37'18"E

Delma nasuta	WAM 164761	Western Australia	Warmun	16°57'26"S	128°14'15"E
Delma nasuta	WAM 154362	Western Australia	Barrow Island	20°46'35"S	115°26'53"E
Delma nasuta	WAM 158415	Western Australia	Giralia Station	22°41'38"S	114°23'28"E
Delma nasuta	WAM 169366	Western Australia	Point Salvation	28°12'00"S	123°36'00"E
Species	Collection ID	State	Locality	Latitude	Longitude
Delma nasuta	WAM 172192	Western Australia	Ilkurlka Roadhouse	28°20'01"S	127°23'50"E
Delma nasuta	WAM 140343	Western Australia	Millstream-Chichester Np	22°23'00"S	117°53'00"E
Delma nasuta	WAM 154170	Western Australia	Barrow Island	20°47'12"S	115°27'22"E
Delma nasuta	NTM 35899	Queensland	Camooweal	NA	NA
Delma nasuta	NTM 35901	Queensland	Camooweal	NA	NA
Delma pax	WAM 134068	Western Australia	Newman	23°05'45"S	118°52'21"E
Delma pax	WAM 172570	Western Australia	Cummins Range	19°16'56"S	127°06'51"E
Delma pax	WAM 110079	Western Australia	Karratha	20°51'07"S	116°56'40"E
Delma pax	WAM 164314	Western Australia	Dixon Island	20°37`00"S	117°05`00"E
Delma pax	WAM 106278	Western Australia	South Hedland, Port Hedland	20°23'60"S	118°35'60"E
Delma petersoni	WAM 165873	Western Australia	Queen Victoria Spring	29°19'11"S	124°31'28"E
Delma petersoni	WAM 165874	Western Australia	Queen Victoria Spring	29°14'04"S	124°31'08"E
Delma petersoni	SAMA 20804	South Australia	N End Stock Route	32°51'00"S	135°57'00"E
Delma plebeia	QMJ 80132	Queensland	Bungil	26°34'41"S	148°54'26"E
Delma plebeia	QMJ 89574	Queensland	Stanthorpe	28°56'46"S	151°23'37"E
Delma tealei	WAM 153811	Western Australia	Cape Range NP	22°07'08"S	114°03'44"E
Delma tealei	WAM 153813	Western Australia	Yardie Homestead Caravan	21°53'37"S	114°00'34"E
Delma tealei	WAM 153819	Western Australia	Cape Range NP	22°03'49"S	114°00'42"E
Delma tincta	AMS 118978	New South Wales	Manilla Rubbish Tip	30°45'00"S	150°43'00"E
Delma tincta	AMS 151607	New South Wales	14.8 km S Olive Downs Homestead, Sturt Np	29°9'58"S	141°52'18"E
Delma tincta	WAM 102401	Western Australia	Barlee Range Nature Reserve	23°04'47"S	115°47'14"E
Delma tincta	WAM 137953	Western Australia	Kununurra	15°35'20"S	128°59'00"E
Delma tincta	WAM 116545	Western Australia	Irwin River	29°08'00"S	115°21'00"E
Delma tincta	WAM 164218	Western Australia	Mount Percy	17°40'51"S	124°56'20"E
Delma tincta	WAM 139648	Western Australia	Depot Hill, Giralia	29°08'00"S	115°21'00"E
Delma tincta	WAM 153820	Western Australia	Charles Knife Road, Cape Range NP	22°07'08"S	114°03'44"E
Delma tincta	WAM 164218	Western Australia	Mount Percy	22°07'08"S	114°03'44"E
Delma tincta	WAM 102815	Western Australia	Burrup Peninsula	20°40'39"S	116°45'11"E
Delma tincta	WAM 114391	Western Australia	Broome	17°55'00"S	122°15'00"E
Delma tincta	WAM 114490	Western Australia	Wicherina Dam	28°43'60"S	115°00'00"E
Delma tincta	WAM 129587	Western Australia	Newman	22°55'00"S	118°54'02"E
Delma tincta	WAM 137953	Western Australia	Kununurra	15°35'20"S	128°58'60"E
Delma tincta	WAM 153814	Western Australia	Yardie Homestead Caravan	21°53'37"S	114°00'34"E
Delma tincta	WAM 157704	Western Australia	Newman	22°56'03"S	118°53'15"E
Delma tincta	WAM 158202	Western Australia	Roy Hill	22°44'19"S	120°47'30"E
Delma tincta	WAM 165261	Western Australia	Karratha	20°45'58"S	116°37'25"E
Delma tincta	WAM 168506	Western Australia	Coulomb Point	17°36'12"S	122°11'30"E
Delma tincta	WAM 168507	Western Australia	Coulomb Point	17°36'12"S	122°11'30"E
Delma tincta	WAM 170055	Western Australia	Wodgina	21°03'46"S	118°54'40"E
Delma tincta	ANWC R05405	Queensland	Shoalwater Bay Army Reserve, N Rockhampton	22°33'30"S	150°46'55"E
Delma tincta	ANWC R05368	Queensland	Shoalwater Bay Army Reserve, N Rockhampton	22°33'30"S	150°46'55"E
Delma tincta	SAM 90213	Queensland	63 Km W of Winton, Boulia Rd.	22°15'58"S	142°27'58"E
Delma torquata	WMJ 63361	Queensland	Kilkivan	25°58'02"S	152°05'17"E
Delma torquata	QMJ 83187	Queensland	Wongi State Forest, 45 km WNW Maryborough	25°25'60"S	152°16'04"E
Delma torquata	QMJ 84362	Queensland	Tanduringie Creek, W Cooyar Mt.	26°55'53"S	151°45'01"E
Lialis burtonis	AMS 141027	New South Wales	Beulah Station, 90 km NE Bourke	29°21'23"S	146°13'14"E
Lialis burtonis	AMS 151574	New South Wales	Sturt NP, Olive Downs Homestead	29°03'05"S	141°51'34"E
Lialis burtonis	ERP 30061	Western Australia	Laverton	NA	NA

Lialis jicari	JAM	Irian Jaya	NA	NA	NA
Ophidiocephalus taeniatus	SAMA 44653	South Australia	6.5 km SW of Gypsum Bore, Todmorden Station	27°39'26"S	134°39'20"E
Pletholax gracilis	WBJ 2483	Western Australia	Leseur NP	NA	NA
Species	Collection ID	State	Locality	Latitude	Longitude
Pygopus lepidopodus	SAMH 35	Western Australia	NA	NA	NA
Pygopus lepidopodus	WBJ 1206	Western Australia	Leseur NP	NA	NA
Pygopus nigriceps	ERP 29509	Western Australia	Laverton	NA	NA
Pygopus orientalis	QMJ 56089	Queensland	Peak Downs	23°01'00"S	147°52'60"E